UNIVERSITY OF OKLAHOMA

GRADUATE COLLEGE

Identification and Analysis of the Response Regulator Binding Site on the Surface of the Histidine-Containing Phosphotransfer Protein YPD1 from *Saccharomyces cerevisiae*

A Dissertation

SUBMITTED TO THE GRADUATE FACULTY
in partial fulfillment of the requirements for the
Degree of
Doctor of Philosophy

By

Stace Wayne Porter
Norman, Oklahoma
2003

Downloaded from SHAREOK. Persistent Handle URL: https://hdl.handle.net/11244/661

UMI Number: 3109056

INFORMATION TO USERS

The quality of this reproduction is dependent upon the quality of the copy submitted. Broken or indistinct print, colored or poor quality illustrations and photographs, print bleed-through, substandard margins, and improper alignment can adversely affect reproduction.

In the unlikely event that the author did not send a complete manuscript and there are missing pages, these will be noted. Also, if unauthorized copyright material had to be removed, a note will indicate the deletion.

UMI®

UMI Microform 3109056

Copyright 2004 by ProQuest Information and Learning Company.

All rights reserved. This microform edition is protected against unauthorized copying under Title 17, United States Code.

ProQuest Information and Learning Company
300 North Zeeb Road
P.O. Box 1346
Ann Arbor, MI 48106-1346

© Copyright by Stace Wayne Porter 2003
All Rights Reserved.

Identification and Analysis of the Response Regulator Binding Site on the Surface of the Histidine-Containing Phosphotransfer Protein YPD1 from *Saccharomyces cerevisiae*

A Dissertation APPROVED FOR THE
DEPARTMENT OF CHEMISTRY AND BIOCHEMISTRY

BY

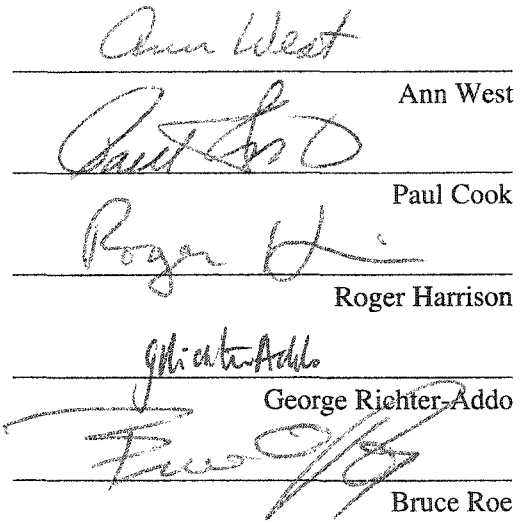

Acknowledgements

I must first give appreciation to my major professor Dr. Ann West who has guided me throughout my graduate career. Dr. West has continuously supported me in all the projects that I have been involved in and without her support I would not have been able to perform the work presented in this dissertation. I would like to thank her for providing insightful feedback as well as giving me the opportunity learn and explore the subtleties of two-component signal transduction.

I would also like to acknowledge the members of my Graduate Advisory Committee, Dr. Paul Cook, Dr. Bruce Roe, Dr. Roger Harrison, Dr. Phil Klebba, and Dr. George Richter-Addo. Their feedback and guidance has been greatly appreciated, and as a result I have benefited from my interactions with them.

It has been wonderful working with my colleagues who have provided insightful discussions about all aspects of science. In particular I would like to thank Dr. Fabiola Janiak-Spens, Dan Copeland, Hui Tan, David Sparling, and Qingping Xu for making the environment in our laboratory such a pleasure to work in. Fabiola deserves special appreciation for teaching me the basic tools needed for research, for critical reading of manuscripts, and for devoting the time and energy it takes to answer questions. Without Qingping Xu's work on the structural determination of YPD1 I could not have identified the response regulator binding site on the surface of YPD1. Without the contributions of all the members of the laboratory it would have been impossible for me to finish my work in a reasonable amount of time.

This dissertation would not have been possible without the love and support of my wife Laurinda to whom I owe considerable gratitude. It has not always been easy juggling experiments, a wife, and two daughters, but through love and patience we have made it work. Her support and encouragement has helped me throughout my graduate career and for that I cannot say thank you enough. Finally, I would like to acknowledge my parents who have provided me with unconditional support in everything that I do. Without their loving encouragement I would have never had the opportunity to present this body of work.

Table of Contents

ACKNOWLEDGEMENTS iv

TABLE OF CONTENTS vi

LIST OF TABLES viii

LIST OF FIGURES ix

LIST OF ABBREVIATIONS x

General Abbreviations x
Gene Designations x
Protein Designations x

ABSTRACT xi

1. INTRODUCTION 1

1.1. Signal Transduction 1
1.2. Two-Component Signal Transduction 3
1.3. Histidine Kinases 5
1.4. Response Regulators 9
1.5. Multi-step Phosphorelay Signal Transduction Systems 11
1.6. Osmoregulation in *Saccharomyces cerevisiae* 12
1.7. Crystal structure of YPD1 16
1.8. Significance of Studies Involving Two-Component Systems 18
1.9. Research Focus 19

2. MATERIALS AND METHODS 21

2.1. Materials 21
2.2. Construction of Vectors 21
2.3. QuikChange Mutagenesis 23
2.4. Megaprimer Mutagenesis 26
2.5. Yeast Two-Hybrid Assay 29
2.6. Western Blots 31
2.7. Pull down assay 31
2.8. Native Gel-Shift Assay 33

3. IDENTIFICATION OF THE SSK1-R2 BINDING SITE ON YPD1 34

3.1. Introduction 34
3.2. Results 35
3.3. Discussion 43
3.3.1 SSK1-R2 Binding Site on YPD1 43

4. YPD1-RESPONSE REGULATOR INTERACTIONS: A COMPARATIVE STUDY 48

4.1. Introduction 48
4.2. Results 49
4.2.1 SLN1-R1 and SKN7-R3 Interaction Screen with YPD1 49
4.2.2 Analysis of YPD1 Q34 Mutants 56
4.2.3 Analysis of YPD1 E58 Mutants 60
4.3. Discussion 63
4.3.1 Comparison of Wild-Type YPD1/Response Regulator Interactions 63
4.3.2 Comparison of YPD1/Response Regulator Binding Interfaces 64
4.3.3 Site-Specific Enhanced Interaction Mutants. 65
4.3.4 Summary 67

5. STRUCTURAL ANALYSIS OF THE YPD1/SLN1-R1 COMPLEX 68

5.1. INTRODUCTION 68
5.2. RESULTS 69
5.2.1 Structure of the Complex 69
5.2.2 Analysis of the Protein-Protein Interface 72
5.3. DISCUSSION 78
5.3.1 Comparison of the YPD1/SLN1-R1 Co-Crystal Structure to Yeast Two-Hybrid Results 78
5.3.2 Specificity Determinants of Protein-Protein Interactions. 80
5.3.3 Summary 81

6. DISCUSSION OF PROTEIN-PROTEIN INTERACTIONS 83

6.1. INTRODUCTION 83
6.2. DISCUSSION 84
6.2.1 Survey of Protein-Protein Interfaces 84
6.2.2 Comparison to the Spo0B/Spo0F Complex 87
6.2.3 Comparison of Yeast Two-Hybrid Results to *in vitro* Assays 92
6.2.4 Specificity of HPt Protein/Response Regulator Protein Interactions 95
6.2.5 Conclusions 97

REFERENCES 102

List of Tables

CHAPTER 2 21

TABLE 2-1: PRIMERS USED FOR SITE-DIRECTED MUTAGENESIS OF YPD1 25
TABLE 2-2: PLASMIDS USED IN THE YPD1-REPONSE REGULATOR YEAST TWO-HYBRID SCREEN 27
TABLE 2-3: PRIMERS USED FOR Q34 AND E58 YPD1 MUTAGENESIS 28
TABLE 2-4: PLASMIDS USED IN THE YPD1 Q34 AND E58 MUTANT YEAST TWO-HYBRID SYSTEM 30

CHAPTER 3 34

TABLE 3-1: YPD1/SSK1-R2 YEAST TWO-HYBRID INTERACTIONS 40

CHAPTER 4 48

TABLE 4-1: YPD1/RESPONSE REGULATOR YEAST TWO-HYBRID INTERACTIONS 53
TABLE 4-2: YPD1 SURFACE RESIDUES INVOLVED IN SPECIFIC INTERACTIONS 54
TABLE 4-3: YPD1 Q34X/RESPONSE REGULATOR YEAST TWO-HYBRID INTERACTIONS 57
TABLE 4-4: YPD1 E58X/RESPONSE REGULATOR YEAST TWO-HYBRID INTERACTIONS 62

CHAPTER 5 68

TABLE 5-1: YPD1/SLN1-R1 INTERMOLECULARCONTACTS 74

CHAPTER 6 83

TABLE 6-1: KINETIC DATA FOR SLN1-R1/YPD1 PHOSPHORYL TRANSFER 95

List of Figures

CHAPTER 1 1

FIGURE 1-1: FLOW OF A PHOSPHORYL GROUP THROUGH A TWO-COMPONENT SYSTEM 4
FIGURE 1-2: CLASS I VERSUS CLASS II HISTIDINE KINASES 6
FIGURE 1-3: STRUCTURES OF A CLASS I AND CLASS II HISTIDINE KINASE 8
FIGURE 1-4: STRUCTURES OF RESPONSE REGULATOR PROTEINS 10
FIGURE 1-5: EXAMPLES OF MULTI-STEP PHOSPHORELAY SYSTEMS 12
FIGURE 1-6: THE MULTI-STEP PHOSPHORELAY IN *S. CEREVISIAE* 14
FIGURE 1-7: THE CRYSTAL STRUCTURE OF THE YEAST HPT PROTEIN YPD1 17

CHAPTER 2 21

FIGURE 2-1: YEAST TWO-HYBRID VECTORS 22
FIGURE 2-2: SELECTION OF SURFACE RESIDUES FOR MUTATION 23
FIGURE 2-3: OVERVIEW OF THE QUIKCHANGE MUTAGENESIS SYSTEM 24

CHAPTER 3 34

FIGURE 3-1: OVERVIEW OF THE YEAST TWO-HYBRID SYSTEM 37
FIGURE 3-2: IN VIVO PROTEIN-PROTEIN INTERACTION SCREEN BETWEEN YPD1 AND SSK1-R2 39
FIGURE 3-3: PROTEIN EXPRESSION PROFILE OF DBD-YPD1 FUSION PROTEINS IN STRAIN MAV203 41
FIGURE 3-4: RIBBON DIAGRAM AND MOLECULAR SURFACE REPRESENTATION OF YPD1 42
FIGURE 3-5: HYDROPHOBIC SURFACE MAP AND HPT SEQUENCE ALIGNMENT 45

CHAPTER 4 48

FIGURE 4-1: YEAST TWO-HYBRID RESULTS OF YPD1/RESPONSE REGULATOR INTERACTIONS 50
FIGURE 4-2: YEAST TWO-HYBRID RESULTS OF YPD1/RESPONSE REGULATOR INTERACTIONS 52
FIGURE 4-3: SURFACE COMPARISON OF RESPONSE REGULATOR INTERACTIONS WITH YPD1 55
FIGURE 4-4: YEAST TWO-HYBRID RESULTS OF Q34 RANDOM MUTANTS 58
FIGURE 4-5: YEAST TWO-HYBRID RESULTS OF E58 RANDOM MUTANTS 61

CHAPTER 5 68

FIGURE 5-1: CO-CRYSTAL STRUCTURE OF THE YPD1/SLN1-R1 COMPLEX FROM S. CEREVISIAE 70
FIGURE 5-2: SURFACE MAP OF YPD1/SLN1-R1 INTERACTIONS 73
FIGURE 5-3: SURFACE MAP OF PROTEIN-PROTEIN INTERACTIONS 76
FIGURE 5-4: ACTIVE SITE ARRANGEMENT OF YPD1/SLN1-R1 IN TWO CRYSTAL FORMS 77

CHAPTER 6 83

FIGURE 6-1: THE SPO0F/SPO0B COMPLEX 88
FIGURE 6-2: STRUCTURAL ALIGNMENT OF YPD1 WITH HPT DOMAINS 91
FIGURE 6-3: NATIVE GEL SHIFT ASSAY 93
FIGURE 6-4: SURFACE COMPARISON OF HPT PROTEINS 99

List of Abbreviations

General Abbreviations

AD	Activation domain of GAL4
ATP	Adenosine triphosphate
CPRG	Chlorophenolred β-D-galactopyranoside
DBD	DNA binding domain of GAL4
DNA	Deoxyribonucleic acid
dNTP	Deoxyribonucleotide triphosphate
IPTG	Isopropyl-β-D-thiogalactoside
HPt	Histidine-containing phosphotransfer
LiAc	Lithium acetate
MAP	Mitogen activated protein
OD_x	Optical density at x nanometers
PCR	Polymerase chain reaction
PEG	Polyethylene glycol
rmsd	Root mean square deviation
SC	Synthetic complete (selection media for yeast)
YPAD	Yeast extract, peptone, adenine sulfate, dextrose (rich media for yeast)

Gene Designations

GPD1	glycerol-3-phosphate dehydrogenase 1

Protein Designations

ArcB	Anoxic redox control B; *E. coli*
CheY	Chemotaxis protein Y; *E. coli*
HOG1	High osmolarity glycerol response; *S. cerevisiae*
SKN7	
SLN1	Synthetic lethal of the N-end rule 1; *S. cerevisiae*
SSK1	Suppressor of the sensor kinase 1; *S. cerevisiae*
YPD1	Tyrosine (Y) phosphatase dependent 1; *S. cerevisiae*

Abstract

A histidine-containing phosphotransfer (HPt) protein, YPD1, plays a critical role in a multi-step phosphorelay signal transduction pathway in the yeast *Saccharomyces cerevisiae*. The SLN1-YPD1-SSK1 pathway controls activation of a downstream mitogen-activated protein (MAP) kinase in response to hyperosmotic stress. YPD1 is also involved in phosphoryl transfer in the SLN1-YPD1-SKN7 pathway involved in mediating cellular responses to cell wall damage and oxidative stress. It is known that YPD1 can interact with and transfer a phosphoryl group between the three response regulator domains (SLN1-R1, SSK1-R2 and SKN7-R3), however it is unknown how YPD1 distinguishes and interacts with the response regulators in order to elicit the correct response. Studies aimed at identifying a response regulator binding site as well as those aimed at addressing the question of specificity were initiated.

In order to identify a response regulator binding site on the surface of YPD1, studies were conducted that coupled alanine-scanning mutagenesis on the surface of YPD1 and a yeast two-hybrid screen with the response regulator domain of SSK1. Mapping the results of the yeast two-hybrid screen onto the surface of YPD1 revealed a response regulator binding site between the site of phosphorylation, H64, and the αA helix of YPD1. Furthermore, the surface of YPD1 used to bind the response regulator domain of SSK1 consists of a hydrophobic patch surrounded by polar and charged residues. Alignment of the sequence of YPD1 with other monomeric HPt proteins revealed conservation of the hydrophobic patch on the surface of other HPt proteins.

Similar assays were performed that screened YPD1 mutants created in the above assay for interactions with the remaining two response regulator domains in *S. cerevisiae*, SLN1-R1 and SKN7-R3. Results from the screens showed that YPD1 uses the same general surface to bind each response regulator. In addition, residues on the surface of YPD1 in the binding interface were identified that could be involved in the discrimination between the three response regulator domains. Two locations on the surface of YPD1 were randomly mutated to each of the twenty amino acids in order to identify trends between the type of residue at the binding interface and the strength of interaction between YPD1-response regulator complexes.

The results from the yeast two-hybrid screens were confirmed by the X-ray crystal structure of the SLN1-R1/YPD1 complex. This structure is the first to reveal protein-protein interactions between a monomeric HPt domain and a response regulator protein. Information gained in the study of response regulator interactions with YPD1 can be utilized to understand response regulator interactions with HPt proteins in other two-component pathways.

1. Introduction

1.1. Signal Transduction

In order to adapt to a constantly changing environment, organisms must continuously assess their surroundings. Prokaryotes exhibit a wide range of regulatory responses to adapt to environmental changes. External conditions such as osmolarity and nutrient availability are examples of the stimuli that organisms sense. In the chemotaxis response pathway of bacteria such as *Escherichia coli* and *Salmonella typhimurium*, swimming behavior is affected by the local concentration of nutrients and repellents in the medium (Blair, 1995; Falke *et al.*, 1997; Lukat & Stock, 1993; Stock & Mowbray, 1995). In the presence of chemoattractants cells exhibit smooth swimming behavior. However, when a low concentration of nutrients or higher levels of chemical repellents are detected at the cell surface it is observed that the smooth swimming behavior is replaced by random reorientation/tumbling until nutrients are detected again. The process of converting signals perceived at the cellular membrane into cellular responses is known as signal transduction.

Signal transduction processes or pathways utilize reversible protein phosphorylation as a common regulatory mechanism by which organisms interpret and

respond to certain environmental stimuli. The addition of a phosphoryl group has been demonstrated to affect kinetic and structural properties of proteins (Barford, 1991; Knowles, 1980; Westheimer, 1987; Witters, 1990). The eventual downstream effect of protein phosphorylation is a change in cellular processes or a change in protein expression patterns exhibited in the cell. In general the phosphorylation state of a sensory response protein is controlled by protein kinases and phosphatases. When appropriate stimuli are detected, protein kinases catalyze the phosphorylation of the sensory response protein using cytoplasmic ATP. The addition of the phosphoryl group can affect the kinetic properties of the protein and/or may affect the structure of the protein. The negatively charged phosphoryl group can cause a structural change in the protein by attracting positively changed residues or repelling negatively charged residues. The reorientation of residues near the site of phosphorylation can also be transmitted through the protein, altering the protein conformation in other locations. Changes in protein conformation can affect protein-protein interactions, substrate binding, ligand binding, and catalytic activity. The phosphorylation state of sensory response proteins may also be controlled by phosphatases which remove phosphoryl groups.

Numerous signal transduction pathways in eukaryotes employ protein phosphorylation as a means to amplify external signals through a mitogen-activated protein (MAP) kinase cascade (Cobb & Goldsmith, 1995; Crews & Erickson, 1993; Davis, 1993; Guan, 1994; Keyse, 2000; Nishida & Gotoh, 1993; Robinson & Cobb, 1997; Schaeffer & Weber, 1999; Seger & Krebs, 1995; West & Stock, 2001). MAP kinase cascades primarily regulate cellular differentiation and mitosis, but can control a variety of other responses in eukaryotic organisms (Fukuda *et al.*, 1997; Nishida &

Gotoh, 1993; Robinson & Cobb, 1997). In a MAP kinase cascade, the catalytic activity of three sequential kinases is affected by the phosphorylation of serine, threonine and tyrosine residues at the surface of the proteins. When the appropriate signal is detected the first protein, a MAP kinase kinase kinase (MAPKKK) is activated and serves to phosphorylate serine and threonine residues on a downstream MAP kinase kinase (MAPKK) protein. The MAPKK is activated by phosphorylation and serves to phosphorylate tyrosine and threonine residues on a MAP kinase protein. Phosphorylation of the MAP kinase acts as a molecular switch, turning on or off transcription of its target genes.

Prokaryotes also use reversible protein phosphorylation as a means for signal transduction. However, the mechanism employed to respond to external conditions is very different. In the so-called two-component signal transduction systems found in prokaryotes, phosphorylation occurs on histidine and aspartate residues located on a histidine kinase and a response regulator protein, respectively (Hoch, 2000; Parkinson & Kofoid, 1992; Stock & Mowbray, 1995; Stock *et al.*, 2000; Stock *et al.*, 1995; Swanson *et al.*, 1994; West & Stock, 2001).

1.2. Two-Component Signal Transduction

The most prevalent form of signal transduction in bacteria is the so-called two-component signal transduction pathway. This system employs protein phosphorylation as a mechanism to transmit signals and elicit the correct response (Figure 1-1).

A typical two-component system is composed of a histidine protein kinase, also referred to as a transmitter, and a response regulator protein, also referred to as a receiver

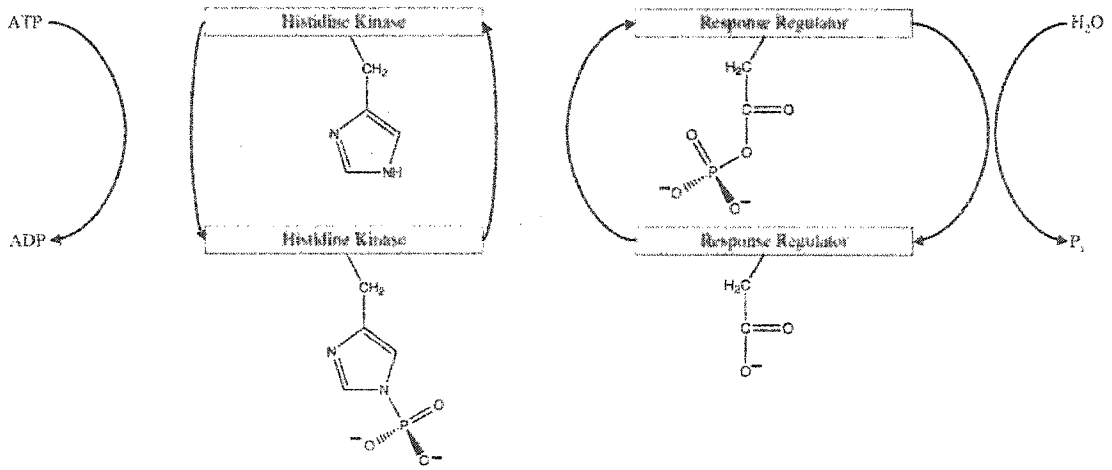

Figure 1-1
Flow of a Phosphoryl Group Through a Two-Component System. The γ-phosphoryl group of intracellular ATP is transferred to a conserved histidine on a histidine kinase protein. The phosphoryl group is subsequently shuttled to a conserved aspartate residue on a response regulator protein. The response regulator is returned to its inactive state by hydrolysis of the phosphoryl group.

(Figure 1-1) (Hoch, 2000; Hoch & Silhavy, 1995; Kofoid & Parkinson, 1988). The histidine protein kinase commonly functions as a transmembrane receptor that senses changes in external conditions. Upon ligand binding to the transmembrane portion of the protein a cytoplasmic histidine kinase domain autophosphorylates. The histidine kinase domain serves as a phospho-donor to the downstream response regulator protein. The response regulator is typically composed of an N-terminal regulatory domain and a C-terminal effector domain. The regulatory domain is phosphorylated on a conserved aspartate residue by the histidine kinase, which in turn alters the activity of the effector domain to modulate the response. In most cases, the effector domains have DNA binding or other regulatory functions that provide transcriptional control over gene targets.

It was originally thought that two-component systems were limited to prokaryotic organisms, but these pathways were later discovered in archaea (Lee & Stock, 1996; Rudolf *et al.*, 1995; Swanson *et al.*, 1996), plants (Chang *et al.*, 1993; Hua *et al.*, 1995; Imamura *et al.*, 1999; Kakimoto, 1996; Sakai *et al.*, 2001; Sakai *et al.*, 1998; Wilkinson

et al., 1995), fungi (Alex *et al.*, 1996; Brown *et al.*, 1994; Maeda *et al.*, 1994; Ota & Varshavsky, 1993; Shieh *et al.*, 1997), and protozoa (Chang *et al.*, 1998; Schuster *et al.*, 1996; Wang *et al.*, 1996; Zinda & Singleton, 1998). In all cases the modular design of the two-component paradigm is conserved.

1.3. Histidine Kinases

Histidine kinases are the initial phosphorylated protein in two-component signal transduction. Histidine kinases may be membrane bound (e.g. EnvZ) or soluble in the cytoplasm (e.g. CheA). Membrane bound histidine kinases typically contain two hydrophobic N-terminal membrane spanning sequences that traverse the inner membrane into the periplasmic space, and a cytoplasmic histidine kinase domain. The N-terminal extracellular region, also referred to as a sensory domain, is believed to be involved in environmental sensing. Soluble cytoplasmic histidine kinases, such as CheA, are typically bound to a membrane-bound chemoreceptor protein (MCP), but may also have additional sensory domains that are cytoplasmic. Structural and biochemical evidence shows that both membrane-bound and cytoplasmic histidine kinases form dimers *in vivo* (Jiang *et al.*, 2000; Qin *et al.*, 2003; Tomomori *et al.*, 1999; Yaku & Mizuno, 1997). When stimulated by appropriate environmental signals, the histidine kinase monomers trans-autophosphorylate a conserved histidine on the opposing monomer.

There is little sequence homology between the N-terminal sensory domains, which is expected due to the fact that these domains have evolved to sense a variety of different environmental stimuli. Compared to the sensory domains, however, the

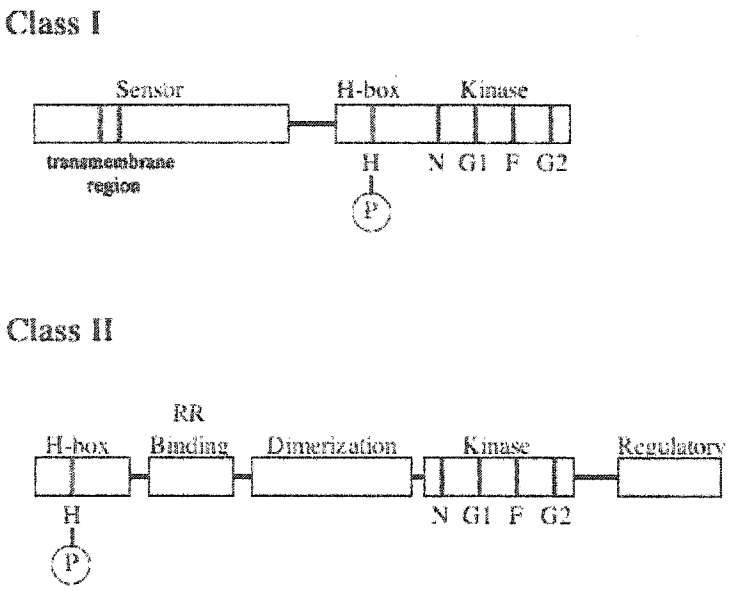

Figure 1-2
Class I versus Class II Histidine Kinases. Histidine kinases are divided into two classifications based on domain arrangement and sequence motifs. Figure adapted from (Bilwes *et al.*, 1999).

histidine kinase domains show a higher level of sequence conservation. The characteristic sequence motifs that comprise a histidine kinase domain have been termed the H (phosphorylatable histidine), N (asparagines), G1 (glycine rich), F (phenylalanine) and G2 (glycine rich 2) boxes. These sequence motifs are believed to be involved in important functions including ATP binding and enzymatic catalysis. Sequence homology analysis has been used to categorize more than 300 histidine kinases into two distinct classes based on domain architecture (Figure 1-2) (Dutta *et al.*, 1999; Grebe & Stock, 1999; Pirrung, 1999; Stock *et al.*, 2000). Class I histidine kinases typically consist of a sensory domain that monitors environmental conditions and a histidine kinase domain. The domain organization of a Class II histidine kinase (CheA) is much different than that of Class I histidine kinases. Class II histidine kinases contain five independent domains: The H-Box is a domain containing the four-helix bundle and the site of phosphorylation (P1), a response regulator binding domain (P2), a dimerization domain (P3), the catalytic

or kinase domain (P4), and a regulatory domain (P5).

Structural information is available for only two histidine kinases, the *E. coli* osmosensor EnvZ and the *E. coli* chemotaxis protein CheA. The solution structure of the homodimeric core domain class I histidine kinase EnvZ revealed the tertiary structure of its dimerization domain (Tomomori *et al.*, 1999). This N-terminal domain (amino acids 223-289) includes the site of phosphorylation (His243) and is arranged in a helix-turn-helix motif that dimerizes to form an up-down-up-down four-helix bundle (Figure 1-3A). The site of phosphorylation is located in the middle of the α1 helix on each monomer. The solution structure of the catalytic kinase domain of EnvZ has also been determined (Figure 1-3B) (Tanaka *et al.*, 1998). The structure revealed an α/β sandwich fold that contains a 5-stranded β-sheet surrounded on one face by three α-helices. The structure of the catalytic domain of EnvZ resembles the ATP binding domain of the bacterial class II histidine kinase CheA (Bilwes *et al.*, 2001). Both EnvZ and the P4 domain of CheA contain the sequence motifs that are believed to be involved in ATP binding, the G1, N and F boxes (Bilwes *et al.*, 2001; Tanaka *et al.*, 1998). In addition to the P4 domain of CheA, structural information exists for the P1 (Mourey *et al.*, 2001; Zhou *et al.*, 1995), P2 (Gouet *et al.*, 2001; McEvoy *et al.*, 1996) and P3-P4-P5 (Bilwes *et al.*, 1999) domains.

Though there has been a wealth of biochemical and some structural information about histidine kinases, very little is known about the actual mechanism of signal transduction across the membrane. Several theories have been postulated about the mechanism of how these signals are transmitted across the membrane, yet no consensus has been reached.

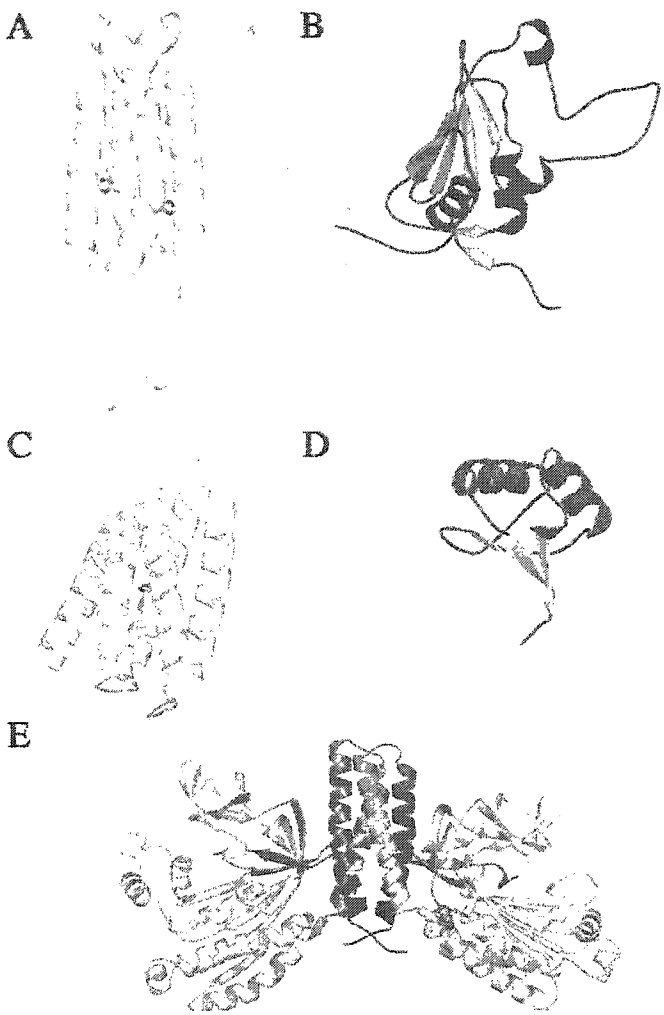

Figure 1-3

Structures of a Class I and Class II Histidine Kinase.

A. The structure of the homodimeric core domain of the class I *E. coli* histidine kinase EnvZ is shown. Two protein monomers dimerize to form a central four helix bundle. As a result two phosphorylation sites are present. (Tomomori *et al.*, 1999) (PDB code:1JOY)

B. NMR solution structure of the catalytic domain of the *E. coli* class I histidine kinase EnvZ is shown. The catalytic domain binds intracellular ATP and transfers the γ-phosphoryl group to the active site histidine. (Tanaka *et al.*, 1998)(PDB code: 1BXD)

C. Crystal structure of the P1 domain of the Class II histidine kinase CheA from *S. Typhimurium.* (Mourey *et al.*, 2001) (PDB code: 1I5N)

D. Crystal structure of the P2 response regulator binding domain of the Class II histidine kinase CheA from *E. coli.* (Welch *et al.*, 1998) (PDB code: 1A0O).

E. Crystal structure of the P3, P4 and P5 domains of the class II histidine kinase CheA from *Thermotoga maritima.* The dimerization domain (P3) is shown in dark blue. The catalytic domain (P4) is shown in green and light blue and the regulatory domain (P5) is shown in orange and yellow. (Bilwes *et al.*, 1999) (PDB code: 1B3Q)

1.4. Response Regulators

The second protein in a typical two-component signal transduction pathway is the response regulator protein. While the histidine kinase is usually involved in detecting changes in the extracellular environment, the response regulator typically modulates cellular responses to those environmental changes. A typical response regulator consists of two independently folded domains, a regulatory domain and an effector domain. The regulatory domain is usually located at the N-terminus of the protein and consists of approximately 125 amino acids. Although the sequence identity among various regulatory domains is relatively low (20-30% identity), the three-dimensional structures of these domains is well conserved (for review see (Stock & West, 2002; West & Stock, 2001)). NMR and X-ray structures of several regulatory domains show a nearly identical doubly-wound $(\beta\alpha)_5$ fold (Figure 1-4). The core of the protein is a 5-stranded central β-sheet sandwiched between α1 and α5 on one face and α2, α3, and α4 on the other. The protein is phosphorylated on a conserved aspartate residue located at the C-terminus of β3. The active site aspartate is surrounded by other conserved residues. Two aspartate residues located at the C-terminus of β1 are involved in binding a divalent magnesium. A conserved lysine residue located in the β5-α5 loop makes a salt-bridge to the active site aspartate residue in the unphosphorylated apo-state. Upon phosphorylation, a conserved hydroxyl-containing residue located at the C-terminus of β4 shifts along with an aromatic residue on β5 towards the active site (Pao *et al.*, 1994; Stock *et al.*, 2000; Stock & Da Re, 2000).

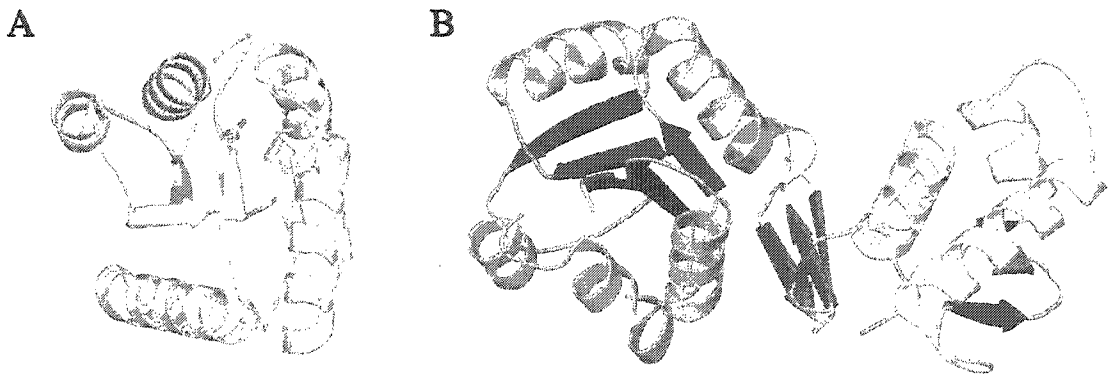

Figure 1-4
Structures of Response Regulator Proteins.
A. The prototypical response regulator CheY is shown. Every response regulator domain displays a doubly-wound $(\beta\alpha)_5$ fold. The core of the protein is a 5-stranded β-sheet surrounded by three α-helices on one face and two on the opposing face. The site of phosphorylation is located at the C-terminus of the third β-strand and is shielded from solvent by active site loops. (Bellsolell *et al.*, 1994) (PDB code: 1CHN)
B. The structure of the full-length response regulator DrrB. The regulatory domain (cyan and magenta) displays the classic fold typical of response regulator domains. The C-terminal effector domain (green and red) is linked to the regulatory domain through a small platform (red). (Robinson *et al.*, 2003)(PDB code: 1P2F)

The phosphorylation state of the regulatory domain modulates the activity of the attached or downstream effector domain. In most cases the response regulator under normal environmental conditions is in an unphosphorylated state. Under these conditions the position of the aromatic residue located on β5 is pointed away from the active site. However, once certain environmental conditions are met the response regulator is phosphorylated by the histidine kinase domain and the conserved aromatic residue shifts toward the active site. The attached effector domain is activated by conformational changes on β4-α4-β5 of the response regulator domain (West & Stock, 2001). Response regulators are capable of modulating responses to many different environmental stimuli. One reason for the wide range of adaptability is the variation that can occur in the effector domains. These domains commonly have DNA transcription activities, but have also been found to modulate protein-protein interactions and can have enzymatic activities.

1.5. Multi-step Phosphorelay Signal Transduction Systems

The traditional two-component system that has been described can be expanded into a multi-component phosphorelay system. In order to expand the traditional two-component system additional proteins must be involved, a histidine-containing phosphotransfer protein and a second (or more) response regulator domain. Phosphoryl groups are transferred through a series of four phosphotransfer reactions, ultimately to one or more response regulator proteins. In the first step, the γ-phosphoryl group of ATP is transferred to a histidine residue of the histidine kinase. The phosphoryl group is then transferred to a conserved aspartate residue on the first response regulator domain. Typically, in a multi-component phosphorelay system the first response regulator does not contain an attached effector domain. Instead the phosphoryl group is shuttled to a histidine-containing phosphotransfer (HPt) protein. HPt proteins are phosphorylated on a conserved histidine residue and then donate this phosphoryl group to a downstream response regulator. Phosphorylation of this response regulator protein, in turn, affects the activity of an attached effector domain.

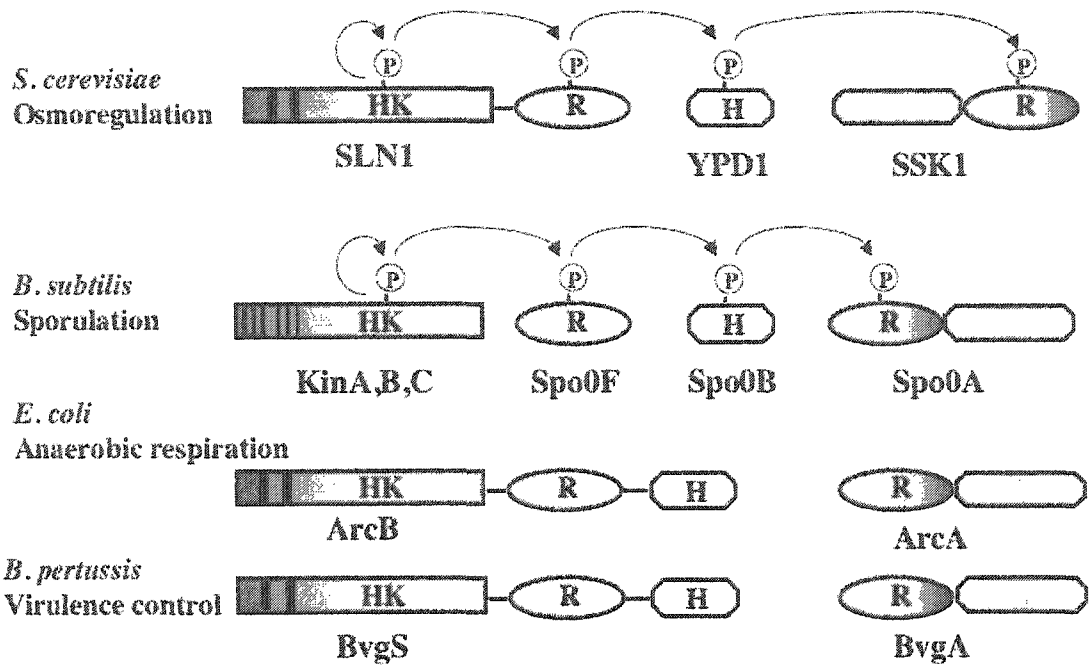

Figure 1-5
Examples of Multi-Step Phosphorelay Pathways. Although the basic histidine to aspartate phosphorelay is maintained, variations in the domain linkage exist in various phosphorelay systems. In all cases histidine kinases (HK) serve to phosphorylated a response regulator (RR). Histidine containing phosphotransfer proteins (H) act as an intermediate phosphotransfer step between two response regulators.

In multi-component systems the histidine-to-aspartate phosphotransfer reactions seen in the traditional two-component systems are conserved and the modular design of the system in conserved (Figure 1-5). Several systems, for example anaerobic respiration in *E. coli*, employ a hybrid histidine kinase that includes a histidine kinase domain, a response regulator domain and an HPt domain in a single polypeptide chain.

1.6. Osmoregulation in *Saccharomyces cerevisiae*

One of the best understood eukaryotic two-component systems is found in the yeast, *Saccharomyces cerevisiae*, and regulates cellular responses to changes in osmotic conditions (Albertyn *et al.*, 1994a; Blomberg & Adler, 1989; Brown *et al.*, 1994; Maeda *et al.*, 1994; Mager & Varela, 1993; Ota & Varshavsky, 1993; Posas *et al.*, 1996). When

S. cerevisiae is exposed to hyperosmotic conditions an adaptive response in the form of an increase in intracellular glycerol concentration, a compatible osmolyte, ensues. This response is initiated via the SLN1-YPD1-SSK1 phosphorelay pathway (Figure 1-6). The osmoregulation pathway in yeast utilizes two common mechanisms for signal transduction: the histidine to aspartate phosphorelay mechanism commonly observed in bacteria and the serine/threonine/tyrosine phosphorylated MAP kinase cascade typically found in eukaryotes.

The first protein in this pathway is the membrane-bound hybrid sensor kinase, SLN1 identified by Ota and Varshavsky (Ota & Varshavsky, 1992). At the N-terminus there are two predicted membrane spanning regions that surround an extracellular sensor domain. Following the second membrane spanning region is the histidine kinase (HK) domain. Located at the C-terminus of SLN1 is a response regulator domain, termed SLN1-R1. SLN1 is believed to exist as a dimer in the membrane and autophosphorylation occurs on a conserved histidine residue in the HK domain using cytosolic ATP as a phosphoryl donor (Posas *et al.*, 1996). SLN1-R1 catalyzes the transfer of the phosphoryl group from the HK domain to itself. Phosphoryl group transfer from SLN1 to SSK1, the downstream response regulator, occurs via the histidine-containing phosphotransfer protein YPD1 (Janiak-Spens *et al.*, 1999; Posas *et al.*, 1996).

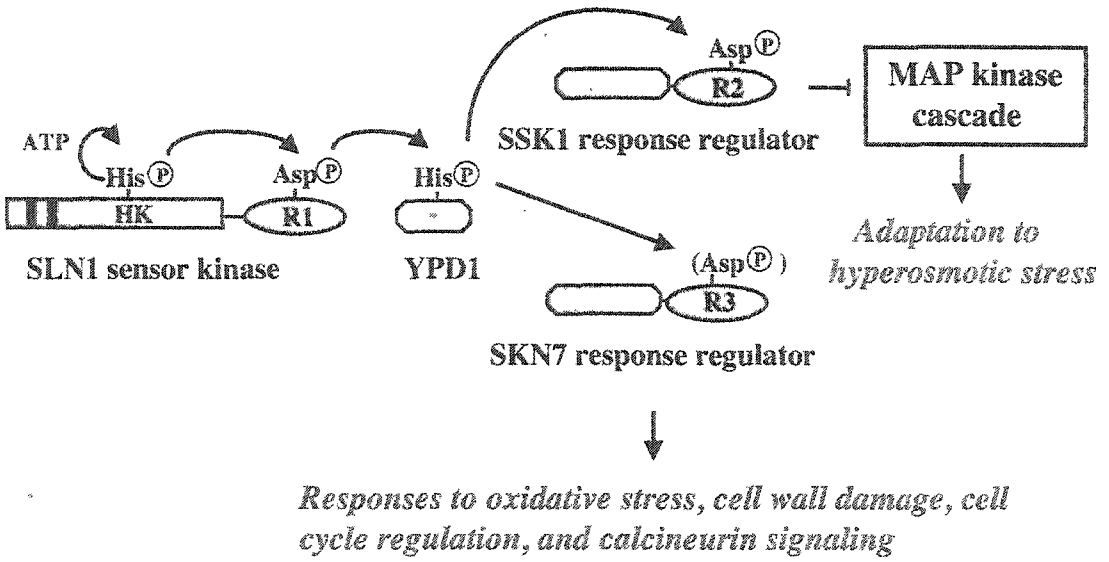

Figure 1-6

The Multi-Step Phosphorelay Signal Transduction System in *S. cerevisiae*. YPD1 interacts with and transfers a phosphoryl group between the regulatory domains SLN1-R1, SSK1-R2 and SKN7-R3. YPD1 also represents a bifurcation between pathways involved in different responses. Dephosphorylation of SSK1 results in activation of a downstream MAP kinase cascade resulting in adaptation to hyperosmotic stress. SKN7 has been implicated in a number of different cellular responses including oxidative stress and cell wall damage.

The domain organization of SSK1 is somewhat unorthodox when compared to bacterial response regulators. A traditional prokaryotic response regulator protein contains the response regulatory domain at the N-terminus and the DNA binding domain at the C-terminus. However, the response regulator domains of both SSK1 and SKN7 are located at the C-terminus and domains of unknown function are located at the N-terminus. Phosphorylation of SSK1 negatively regulates a downstream MAP kinase cascade (Posas *et al.*, 1996). Under normal osmotic conditions SLN1, YPD1, and SSK1 are maintained in a phosphorylated state. When *S. cerevisiae* is exposed to hyperosmotic conditions, however, SSK1 becomes dephosphorylated through an unknown mechanism and subsequently activates a downstream MAP kinase cascade, ultimately resulting in increased levels of intracellular glycerol.

SSK1 directly interacts with two redundant proteins in the downstream MAP kinase cascade. The MAP kinase kinase kinases SSK2 and SSK22 are activated in the presence of unphosphorylated SSK1 (Posas & Saito, 1998). These two kinases serve to activate the MAP kinase kinase PBS2 (Posas & Saito, 1997; Posas *et al.*, 1998), which in turn activates the MAP kinase in this pathway HOG1. Once phosphorylation of HOG1 occurs it regulates transcription of the gene target GPD1 (glycerol-3-phosphate dehydrogenase) through transcription factors (Brewster & Gustin, 1994; Posas & Saito, 1998) (Albertyn *et al.*, 1994b; Ferrigno *et al.*, 1998; Madhani & Fink, 1998; Schüller *et al.*, 1994; Wurgler-Murphy *et al.*, 1997). The resulting gene product, glycerol-3-phosphate dehydrogenase, catalyzes the reaction of dihydroxy-acetone phosphate into glycerol-3-phosphate, a precursor of glycerol.

It has also been shown that YPD1 can donate a phosphoryl group to another response regulator found in *S. cerevisiae*, SKN7 (Brown *et al.*, 1993; Morgan *et al.*, 1995). Like SSK1, the domain organization of SKN7 is not typical. Here, a domain showing homology to transcription factors is located at the N-terminus while the response regulator domain (SKN7-R3) is located at the C-terminus. SKN7 has been implicated in regulating responses to cell wall damage and oxidative stress (Alberts *et al.*, 1998; Brown *et al.*, 1994; Brown *et al.*, 1993; Ketela *et al.*, 1998; Li *et al.*, 1998; Morgan *et al.*, 1997). Cellular responses to cell wall damage occur in a SKN7 phosphorylation-dependent manner. Phosphorylation of SKN7 regulates transcription of the OCH1 gene encoding α-1,6 mannoyl transferase determined to be involved in repairing damage to the cell wall (Li *et al.*, 2002). SKN7 can also regulate gene transcription in a phosphorylation independent manner. Transcription of genes involved in cellular responses to oxidative

stress (TRX2, SSA1 and heat shock-like elements) are not dependent on the phosphorylation state of SKN7. It is believed that SKN7 undergoes an unknown modification or conformational change in response to oxidative stress.

1.7. Crystal structure of YPD1

The histidine-containing phosphotransfer protein YPD1 shuttles a phosphoryl group from the response regulator domain of SLN1 (SLN1-R1) to the response regulators domains of SSK1 and SKN7. Like other HPt domains, YPD1, does not possess enzymatic activity but instead appears to be a phosphorylated intermediate. The protein chain of YPD1 consists of 167 amino acids and has a calculated molecular weight of 19.2 kD.

YPD1 has been cloned into a bacterial expression vector, purified from *E. coli*, and crystallized by members of the laboratory. The crystal structure of YPD1 was determined to a resolution of 2.7Å using multiple isomorphous replacement and anomalous scattering methods (Xu *et al.*, 1999; Xu & West, 1999). YPD1 has an elongated shape with dimensions of 30x30x60 Å. It is an all-helical protein with six α-helices and one short 3_{10} helix (Figure 1-7). Two long helices, αB and αG, and two short helices, αC and αD, form an up-down-up-down four-helix bundle as the core of the protein. The phosphorylatable histidine residue (H64) is located in the middle of helix C and is completely exposed to the solvent. A higher resolution structure (1.8Å) of YPD1 was solved independently by another group (Song *et al.*, 1999).

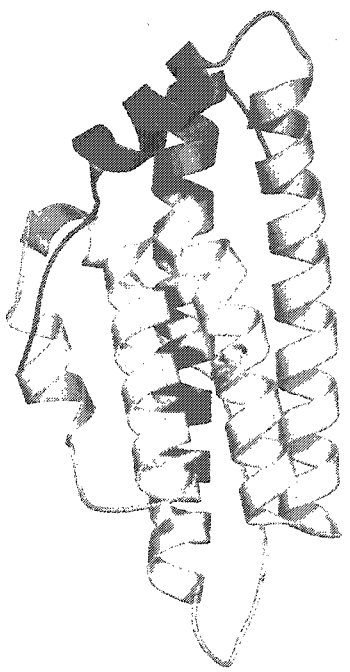

Figure 1-7
The Crystal Structure of the Yeast Histidine-Containing Phosphotransfer Protein YPD1. YPD1 is an all-helical protein, consisting of 6 α-helices and one 3_{10} helix (Xu & West, 1999) (PDB code 1QSP). The core of the protein is a four-helix bundle. The four-helix bundle core is elaborated upon by the addition of a helix at the N-terminus (blue) and a flexible linker connecting the D and the G helices. The site of phosphorylation, H64 (shown as stick model), is located in the middle of helix C and is exposed to solvent.

The structure of YPD1 is most similar to the C-terminal HPt domain of ArcB ($ArcB^c$) found in *E. coli* (Kato *et al.*, 1997). The resemblance suggests that both prokaryotes and eukaryotes use the same basic protein fold for phosphorelay signal transduction. Both HPt domains form a four-helix bundle as the core of the molecule. The similarity of the two proteins becomes more obvious when the two helices that surround the phosphorylatable histidine in each molecule are compared. A superimposition of the αC and αD helices from YPD1 and the corresponding helices in $ArcB^c$ give a root mean square deviation (rmsd) value of 0.36Å for backbone atoms and 0.30Å for Cα atoms. Although the two molecules share a common structural motif there are significant differences in the overall structure of the domains. In ArcB, the helices that correspond to the αB and αG helices in YPD1 are severely kinked giving the

molecule a kidney shape. The main difference in the two structures is a 45-residue insertion between the αD and αG helices in YPD1. This insertion partially covers the αG helix through hydrophobic interactions.

Knowledge of the molecular surface is critical to understanding how YPD1 recognizes differentiates the response regulator domains. In the view shown in Figure 1-7, the upper half of YPD1 is more hydrophobic than the lower half (Song *et al.*, 1999; Xu & West, 1999). The lower half of the molecule is characterized by the presence of several charged residues. A clustering of negatively charged residues also appears in the loop region connecting helices αA and αB. The location of these surface features around the histidine may be the key factors in the recognition and differentiation of the response regulators.

1.8. Significance of Studies Involving Two-Component Systems

Two-component signal transduction systems are relatively simple modular systems that can be modified to achieve several different responses. Unlike eukaryotic MAP kinase cascades, the two-component signal transduction systems in prokaryotes do not offer amplification of environmental signals beyond the original phosphorylation step. Since these systems regulate vital cellular responses to stimuli, regulation of the pathways is critical to maintaining homeostasis. The study of histidine kinases, response regulators, and histidine-containing phosphotransfer proteins has practical implications in developing new anti-microbial and, in the case of fungal organisms that employ two-component systems, anti-fungal treatments (Barrett *et al.*, 1998; Barrett & Hoch, 1998; Cardenas *et al.*, 1998; Fabret & Hoch, 1998; Hilliard *et al.*, 1999; Hlasta *et al.*, 1998;

Roychoudhury *et al.*, 1993). By taking advantage of the universal features of two-component systems or the specific interactions in a particular pathway, inhibitors could be designed for specific targets in a single organism or multiple targets in multiple organisms.

1.9. Research Focus

Two-component signal transduction systems are ubiquitous in bacteria and regulate a wide variety of cellular responses to environmental cues. These systems have also been discovered in single and multicellular lower eukaryotes, and in the plant *Arabidopsis thaliana* (Brandstatter & Kleber, 1998; Chang, 1996). Although the osmoregulation pathway in *S. cerevisiae* is the best characterized eukaryotic two-component system to date, there are still many questions that remain. (i) Which amino acids are crucial for YPD1/response regulator interactions? (ii) Does YPD1 bind response regulators through a common surface or do distinct binding sites exist for each of the response regulator domains on the surface of YPD1? (iii) How does YPD1 distinguish between each of the response regulators found in *S. cerevisiae* and shuttle a phosphoryl group to the appropriate response regulator?

Our laboratory is interested in defining the structural and biochemical basis for regulation of this pathway. Essentially, signal transduction is achieved through recognition, interaction, and phosphotransfer between components of the pathway. Therefore, the study of protein-protein interactions is the key to understanding regulation of the pathway. Since all chemical signals are shuttled through YPD1, studies investigating protein-protein interactions between YPD1 and each of the response

regulator domains found in *S. cerevisiae* were investigated in order to elucidate how YPD1 binds to and distinguishes between each of the three response regulator domains. Using alanine-scanning mutagenesis coupled with an *in vivo* yeast two-hybrid screen, my goals were to identify specific amino acid residues on the surface of YPD1 that are involved in interactions with each of the three response regulators. With the aim of identifying a response regulator binding site on the surface of YPD1, residues identified in the yeast-two hybrid screens will be mapped onto the surface of YPD1. Comparison of results from yeast two-hybrid screens with the three regulatory domains found in *S. cerevisiae* will provide insight into recognition and discrimination of YPD1 for the response regulator domains.

2. Materials and Methods

2.1. Materials

All chemicals used were of ultrapure grade. Oligonucleotide primers, *Sal I, Not I, Dpn I* restriction enzymes and T4 DNA ligase were obtained from Invitrogen. *Pfu*, *Pfu* Turbo, and *Pfx* DNA polymerases were purchased from Stratagene. Antibodies against SSK1-R2 and YPD1 were raised in rabbits by Cocalico Biologicals, Inc. Materials for the yeast two-hybrid analysis were obtained from Invitrogen. Chlorophenolred β-D-galactopyranoside (CPRG) was obtained from Roche. Culture media for bacterial and yeast growth were obtained from Difco. Low-melting agarose was purchased from Cambrex Bio Sciences. Plasmid DNA samples were submitted to Microgen (University of Oklahoma Health Sciences Center) to confirm point mutations on the surface of YPD1.

2.2. Construction of Vectors

For detection of protein-protein interactions between YPD1 and the response regulator domains of SLN1, SSK1, and SKN7 plasmids were constructed for use in the ProQuest yeast two-hybrid system (Gibco BRL) (Figure 2-1). Two synthetic oligonucleotides were used in the amplification of the YPD1 gene fragment, a 5' primer

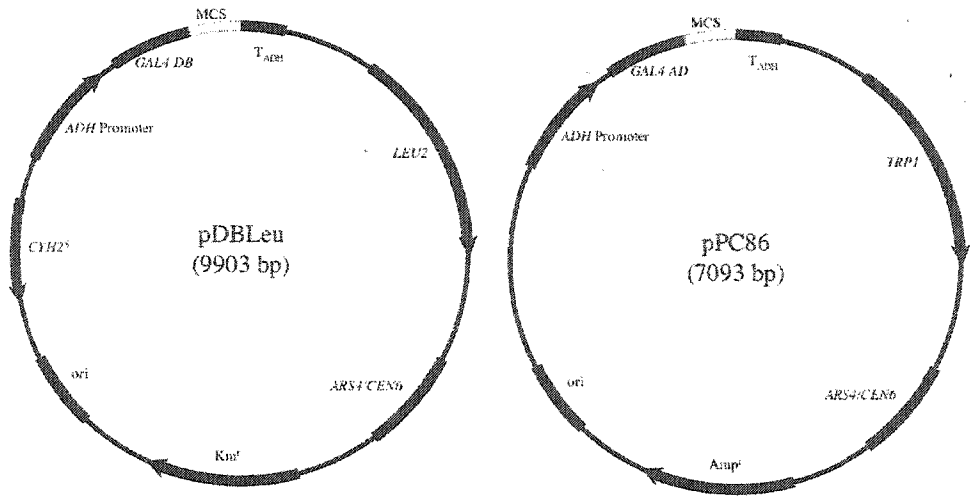

Figure 2-1

Yeast Two-Hybrid Vectors. Vectors utilized in the yeast two-hybrid system are shown. pDBLeu (left) contains the DNA binding domain of *GAL4* from yeast. An *E. coli* replication of origin (ori) is included as well as a kanamycin resistance gene for cloning. A replication of origin for yeast (*ARS/CEN6*) is present as well as a gene for selection in yeast (*LEU2*). Similar features are present in pPC86 with the exception the activation domain of *GAL4* (*GAL4 AD*), and selection markers for *E.coli* (Amp^r) and yeast (*TRP1*).

in which a *Sal* I restriction site was added and a 3' primer in which a *Not* I restriction site was added. The PCR reaction (100µl) contained both primers (AHW 158 and AHW 159, 50 µM each), plasmid DNA template (100 ng), dNTP's (200 µM), and *Pfu* DNA polymerase (2.5 units). The gene fragment for full-length YPD1 was amplified by PCR, digested with *Sal* I and *Not* I restriction enzymes, and cloned into the pDBLeu vector. The resulting vector, pDBLeu-YPD1, expresses a GAL4 DNA binding domain-YPD1 (DBD-YPD1) fusion protein in yeast. The response regulator domain of SLN1 (amino acids 1084-1220), SSK1 (amino acids 495-712) and SKN7 (amino acids 361-622) were prepared similarly as the YPD1 fusion gene, but were cloned into pPC86. These vectors (OU61 for SSSK1-R2, OU150 for SLN1-R1 and OU151 for SKN7-R3) express a GAL4-activator domain-response regulator domain fusion protein in yeast.



Figure 2-2

Selection of Surface Residues for Mutation. YPD1 surface residues in the vicinity of H64 (green) were selected for alanine scanning mutagenesis and are colored yellow. Alanine and glycine surface residues in this location were not mutated.

2.3. QuikChange Mutagenesis

Using the structure of YPD1, surface-exposed residues in the vicinity of H64 were selected for alanine-scanning mutagenesis. With the aid of a molecular surface representation of YPD1 (Figure 2-2), all non-alanine and non-glycine residues on the same face as H64 were selected for mutagenesis. A total of 37 selected amino acid residues were mutated individually using the QuikChange of mutagenesis (Papworth *et al.*, 1996). The QuikChange site-directed mutagenesis method (Stratagene) is based on whole plasmid PCR. The template for the PCR is any double-stranded plasmid that contains the gene insert of interest and must be purified from a host that is capable of methylating DNA (Figure 2-3). Two complementary oligonucleotide primers containing

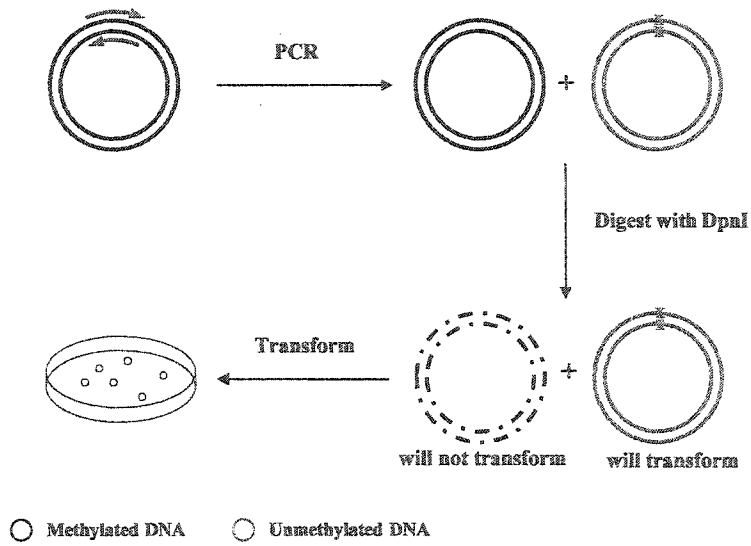

Figure 2-3
Overview of the QuikChange Mutagenesis System. Whole plasmid amplification utilizing mutant primers yields an unmethylated plasmid containing the desired mutation. Digestion with *DpnI* destroys the template leaving only newly synthesized plasmid (red) for vector transformation.

the desired mutation (Table 2-1, 50μM each) were included with the template DNA (OU64, pDBLeu-YPD1, 100ng) in the PCR reaction. The oligonucleotide primers were extended during the thermocycling by *Pfu* Turbo DNA polymerase (2.5 units, Stratagene) in a reaction buffer (10 mM KCl, 10 mM ammonium sulfate, 20 mM Tris-HCl pH 8.8, 2 mM MgSO4, 0.1% Triton X-100, 0.1mg/ml bovine serum albumin) supplied by Stratagene. A total of sixteen rounds of denaturation (94°C, 1 min.), annealing (40-55°C, 1 min.) and extension (68°C, 20 min.) were performed. Upon completion of the polymerase chain reaction two populations of plasmids remain in the reaction mix, the methylated parental template and the unmethylated nicked plasmid that contains the desired mutation. Newly synthesized plasmid DNA was selectively retained by adding *Dpn I* (10 units) to the product of the polymerase chain reaction and incubating at 37°C for 2 hours. Additionally, *Dpn I* will only digest its recognition sequence (GATC) when the adenosine in this sequence is methylated. The parental plasmid DNA (OU64,

Table 2-1

Oligonucleotide Primers Used for Site-Directed Mutagenesis of YPD1

Oligo	Description	Sequence
AHW 156	SSK1-R2 Y2H 5′ primer	ACGTCGACCACCACAAGTGAAAAAGTTTTCCCC
AHW 157	SSK1-R2 Y2H 3′ primer	ATGCGGCCGCTCACAATTCTATTTGAGTGGGCGAGAG
AHW 158	YPD1 Y2H 5′ primer	ACGTCGACCTCTACTATTCCGTCAGAAATC
AHW 159	YPD1 Y2H 3′ primer	ATGCGGCCGCTTATAGGTTTGTGTTGTATATTTAG
AHW 169	YPD1 T57A 3′ primer	GATTGTCTAATTCGG**C**AAGATTTTTTTAAAATG
AHW 170	YPD1 E58A 3′ primer	CCCAGATTGTCTAAT**G**CGGTAAGATTTTTTTAAAATG
AHW 171	YPD1 D60A 3′ primer	GGCCCAGATTG**G**CTAATTCGGTAAG
AHW 172	YPD1 N61A 3′ primer	ATGGCCCAGA**GC**GTCTAATTCGGTAAG
AHW 173	YPD1 H64A 3′ primer	CCCTTTAAAAAA**GC**GCCCAGATTGTCTAATTCGG
AHW 174	YPD1 F65A 3′ primer	GAACCCTTTAAA**GC**ATGGCCAAGATTGTC
AHW 175	YPD1 S69A 3′ primer	GCCTAATGCAGCAG**C**AGAACCCTTTAAAAAATG
AHW 176	YPD1 L73A 3′ primer	GGCAATTCTTTGTAAGCCT**GC**TGCAGCAGAAGAACC
AHW 178	YPD1 F27A 3′ primer	GAATAATTAGACCTTTAGAA**GC**ATCGGAATCATCG
AHW 179	YPD1 L31A 3′ primer	CGATAAATTGAATAATT**GC**ACCTTTAGAAAAATCGG
AHW 180	YPD1 Q34A 3′ primer	GCCTGGTCGATAAAT**GC**AATAATTAGACC
AHW 181	YPD1 Q38A 3′ primer	GCAAAAGTTGTTTGTGCC**GC**GTCGATAAATTG
AHW 182	YPD1 T42A 3′ primer	GAGCAAAAG**C**TGTTTGTGCTTGGTCG
AHW 183	YPD1 E83A 3′ primer	CCCAAGTTTTGAATTCTT**G**CACAAACCCAGGC
AHW 184	YPD1 N87A 3′ primer	CCATTTTTCTTCCCAAG**GC**TTGAATTCTTTCAC
AHW 188	YPD1 Q45A 3′ primer	GTCGTTGCATT**GC**AGCAAAAGTTGTTTG
AHW 189	YPD1 W80A 3′ primer	GAATTCTTTCACAAACC**GC**GGCAATTCTTTG
AHW 191	YPD1 I13A 3′ primer	GATATAATTTCATTTAAG**GC**GGTCCAATTG
AHW 192	YPD1 E16A 3′ primer	CCATAGATATAATT**G**CATTTAAGATG
AHW 193	YPD1 I17A 3′ primer	CATCCATAGATATA**GC**TTCATTTAAG
AHW 194	YPD1 S19A 3′ primer	GTCATCCATAG**C**TATAATTTCATTTAAG
AHW 195	YPD1 M20A 3′ primer	CATCGTCATCC**GC**AGATATAATTTC
AHW 196	YPD1 D21A 3′ primer	CGGAATCATCGTCAT**G**CATAGATATAATTTC
AHW 197	YPD1 T41A 3′ primer	GAGCAAAAGTTG**C**TTGTGCCTGGTCG
AHW 198	YPD1 R48A 3′ primer	CACCGTCCAGCTGT**GC**TTGCATTTGAGC
AHW 199	YPD1 E53A 3′ primer	CGGTAAGATTTTTT**G**CACCGTCCAGC
AHW 200	YPD1 N55A 3′ primer	CTAATTCGGTAAGA**GC**TTTTTCACCG
AHW 201	YPD1 Q76A 3′ primer	CCCAGGCAATTCTT**GC**TAAGCCTAATGC
AHW 213	YPD1 L31A 5′ primer	CCGATTTTTCTAAAGGT**GC**AATTATTCAATTTATCG
AHW 214	YPD1 Q34A 5′ primer	GGTCTAATTATT**GC**ATTTATCGACCAGGC
AHW 215	YPD1 T41A 5′ primer	CGACCAGGCACAA**G**CAACTTTTGCTC
AHW 216	YPD1 Q45A 5′ primer	CAAACAACTTTTGCT**GC**AATGCAACGAC
AHW 217	YPD1 F65A 5′ primer	GACAATCTGGGCCAT**GC**TTTAAAGGGTTC
AHW 218	YPD1 Q76A 5′ primer	GCATTAGGCTTA**GC**AAGAATTGCCTGGG
AHW 219	YPD1 W80A 5′ primer	CAAAGAATTGCC**GC**GGTTTGTGAAAGAATTC
AHW 220	YPD1 N87A 5′ primer	GTGAAAGAATTCAA**GC**CTTGGGAAGAAAAATGG
AHW 223	YPD1 T12A 5′ primer	GAAATCATCAATTGG**G**CCATCTTAAATG
AHW 224	YPD1 T12A 3′ primer	CATTTAAGATGG**C**CCAATTGATGATTTC
AHW 225	YPD1 D23A 5′ primer	CTATGGATGAC**GC**TGATTCCGATTTTTC
AHW 226	YPD1 D23A 3′ primer	GAAAAATCGGAATCA**GC**GTCATCCATAG
AHW 227	YPD1 D24A 5′ primer	CTATGGATGACGAT**GC**TTCCGATTTTTC
AHW 228	YPD1 D24A 3′ primer	GAAAAATCGGAA**GC**ATCGTCATCCATAG
AHW 229	YPD1 S69A 5′ primer	CCATTTTTTAAAGGGT**G**CTTCTGCTGC
AHW 230	YPD1 S69A 3′ primer	GCAGC**A**GAAG**C**ACCCTTTAAAAAATGG
AHW 240	SLN1-R1 Y2H 5′ primer	GAGGTCGACTAATGAAACAAGTGTC
AHW 241	SLN1-R1 Y2H 3′ primer	GGAGGCGGCCGCTCATTTGTTATTTTTCTTTCCC
AHW 242	SKN7-R3 Y2H 5′ primer	GAGGTCGACTAGCCTAACACCAAATGCTCAAAATAAC
AHW 243	SKN7-R3 Y2H 3′ primer	GGAGGCGGCCGCTTATGATAGCTGGTTTTCTTGAAGTGTAG

pDBLeuYPD1) was originally purified from an *E. coli* host, DH5α, which is capable of methylating its DNA. Thus, the template DNA will be digested by *Dpn I* leaving the newly synthesized mutated vector intact and linear DNA fragments from the parental DNA. A small aliquot (10 µl of 50 µl total volume) of the digestion was used for a vector transformation into the *E. coli* host. The transformation mixture was applied to LB-agar plates containing kanamycin (25 µg/ml) and grown overnight at 37°C. Individual colonies appearing on the transformation plate were selected and grown in LB-kanamycin at 37°C overnight for DNA isolation. Isolated vector DNA was sent for sequencing (Microgen, University of Oklahoma Health Sciences Center) to confirm the YPD1 mutation and catalogued (Table 2-2).

2.4. Megaprimer Mutagenesis

Mutants created for the site-directed random mutagenesis (Chapter 4) could not be created using the QuikChange method of site-directed mutagenesis. Another method, megaprimer mutagenesis, was used to create these mutants (Colosimo *et al.*, 1999; Ekici *et al.*, 1997). In this method three oligonucleotides were used in two subsequent polymerase chain reactions. In the first PCR, one oligonucleotide flanked the gene of interest. A second oligonucleutide contained the mutation somewhere inside the gene. The product from the reaction was a gene fragment that contained the mutation of interest. The gene fragment was purified and utilized as a primer in the second polymerase chain reaction. Another oligonuclotide flanking the opposite end of the gene was included in the second PCR and the resulting product was a gene expressing the mutant of interest.

Table 2-2
Plasmids Used in the YPD1-Reponse Regulator Yeast Two-Hybrid Screen

Plasmid	Parent Vector	Insert	Protein Expressed
OU 61	pPC86	SSK1-R2	Gal4 AD-SSK1-R2
OU 64	pDBLeu	YPD1	Gal4 DBD-YPD1
OU 65	pDBLeu	YPD1 K67A	Gal4 DBD-YPD1 K67A
OU 66	pDBLeu	YPD1 Q86L	Gal4 DBD-YPD1 Q86L
OU 67	pDBLeu	YPD1 G68Q	Gal4 DBD-YPD1 G68Q
OU 69	pDBLeu	YPD1 R90A	Gal4 DBD-YPD1 R90A
OU 79	pDBLeu	YPD1 E58A	Gal4 DBD-YPD1 E58A
OU 80	pDBLeu	YPD1 D60A	Gal4 DBD-YPD1 D60A
OU 81	pDBLeu	YPD1 N61A	Gal4 DBD-YPD1 N61A
OU 82	pDBLeu	YPD1 H64A	Gal4 DBD-YPD1 H64A
OU 84	pDBLeu	YPD1 I17A	Gal4 DBD-YPD1 I17A
OU 85	pDBLeu	YPD1 S19A	Gal4 DBD-YPD1 S19A
OU 86	pDBLeu	YPD1 T42A	Gal4 DBD-YPD1 T42A
OU 87	pDBLeu	YPD1 R48A	Gal4 DBD-YPD1 R48A
OU 88	pDBLeu	YPD1 E53A	Gal4 DBD-YPD1 E53A
OU 89	pDBLeu	YPD1 N55A	Gal4 DBD-YPD1 N55A
OU 90	pDBLeu	YPD1 T57A	Gal4 DBD-YPD1 T57A
OU 91	pDBLeu	YPD1 L73A	Gal4 DBD-YPD1 L73A
OU 93	pDBLeu	YPD1 Q86A	Gal4 DBD-YPD1 Q86A
OU 97	pDBLeu	YPD1 S70A	Gal4 DBD-YPD1 S70A
OU 97	pDBLeu	YPD1 I13A	Gal4 DBD-YPD1 I13A
OU 98	pDBLeu	YPD1 E16A	Gal4 DBD-YPD1 E16A
OU 99	pDBLeu	YPD1 M20A	Gal4 DBD-YPD1 M20A
OU100	pDBLeu	YPD1 D21A	Gal4 DBD-YPD1 D21A
OU101	pDBLeu	YPD1 F27A	Gal4 DBD-YPD1 F27A
OU102	pDBLeu	YPD1 Q38A	Gal4 DBD-YPD1 Q38A
OU103	pDBLeu	YPD1 E83A	Gal4 DBD-YPD1 E83A
OU120	pDBLeu	YPD1 T12A	Gal4 DBD-YPD1 T12A
OU121	pDBLeu	YPD1 D23A	Gal4 DBD-YPD1 D23A
OU122	pDBLeu	YPD1 D24A	Gal4 DBD-YPD1 D24A
OU123	pDBLeu	YPD1 L31A	Gal4 DBD-YPD1 L31A
OU124	pDBLeu	YPD1 T41A	Gal4 DBD-YPD1 T41A
OU125	pDBLeu	YPD1 Q45A	Gal4 DBD-YPD1 Q45A
OU126	pDBLeu	YPD1 S69A	Gal4 DBD-YPD1 S69A
OU127	pDBLeu	YPD1 Q76A	Gal4 DBD-YPD1 Q76A
OU128	pDBLeu	YPD1 W80A	Gal4 DBD-YPD1 W80A
OU129	pDBLeu	YPD1 N87A	Gal4 DBD-YPD1 N87A
OU155	pDBLeu	YPD1 Q34A	Gal4 DBD-YPD1 Q34A
OU224	pDBLeu	YPD1 F65A	Gal4 DBD-YPD1 F65A

Table 2-3
Oligonucleotide Primers Used for Random and Site-Directed Mutagenesis of YPD1 Q34 and E58 mutants

Oligo	Description	Sequence
AHW 158	YPD1 Y2H 5′ primer	ACGTCGACCTCTACTATTCCGTCAGAAATC
AHW 159	YPD1 Y2H 3′ primer	ATGCGGCCGCTTATAGGTTTGTGTTGTATATTTAG
AHW 252	YPD1 Q34X 3′ primer	GCCTGGTCGATAAA**ANN**AATAATTAGACC
AHW 256	YPD1 Q34K 3′ primer	GCCTGGTCGATAAA**TTT**AATAATTAGACC
AHW 262	YPD1 Q34W 3′ primer	GCCTGGTCGATAAA**CCA**AATAATTAGACC
AHW 287	YPD1 E58X 3′ primer	CCCAGATTGTCTAA**TNN**GGTAAGATTTTTTTCACCG
AHW 351	YPD1 Q34M 3′ primer	GTGCCTGGTCGATAAA**CAT**AATAATTAGACCT
AHW 360	YPD1 Q34E 3′ primer	GTGCCTGGTCGATAAA**TTC**AATAATTAGACCT
AHW 379	YPD1 E58F 3′ primer	CCCAGATTGTCTAA**AAA**GGTAAGATTTTTTTC
AHW 382	YPD1 E58M 3′ primer	CCCAGATTGTCTAA**CAT**GGTAAGATTTTTTTC
AHW 387	YPD1 E58Y 3′ primer	CCCAGATTGTCTAA**ATA**GGTAAGATTTTTTTC
AHW 388	YPD1 E58H 3′ primer	CCCAGATTGTCTAA**ATG**GGTAAGATTTTTTTC
AHW 390	YPD1 E58N 3′ primer	CCCAGATTGTCTAA**ATT**GGTAAGATTTTTTTC
AHW 392	YPD1 E58C 3′ primer	CCCAGATTGTCTAA**ACA**GGTAAGATTTTTTTC
AHW 393	YPD1 E58W 3′ primer	CCCAGATTGTCTAA**CCA**GGTAAGATTTTTTTC
AHW 400	YPD1 E58D 3′ primer	CCCAGATTGTCTAA**ATC**GGTAAGATTTTTTTC

Two sites on the surface of YPD1 (Q34 and E58) were chosen for site-directed random mutagenesis (Chapter 4). Oligonucleotides containing random bases at the first two positions of the Q34 and E58 codons were obtained from Invitrogen. Additional primers for specific mutations at each locus were kindly donated by Dr. Bruce Roe (University of Oklahoma) (Table 2-3). The first round of PCR included 1μM each primer (random, AHW252 and AHW 287; 3', AHW159), 1X *Pfx* reaction buffer (Invitrogen), 1 mM $MgSO_4$, 5 μl Invitrogen enhancer buffer, 0.1 μg template (OU64), and 3.2 mM each dNTP in a final volume of 100 μl. The reaction tube was subjected to 30 rounds of thermocycling (94°C for 30 seconds, 40-50°C for 30 seconds, and 68°C for 2 minutes). Newly synthesized megaprimer was separated from reaction components by electrophoresis in a 1% low-melt agarose gel. The megaprimer DNA fragment was cut from the gel, heated to 67°C to melt the agarose, and purified by phenol:chloroform extraction. The megaprimer was then used as a primer in the second round of PCR. Components of the second round of PCR were the same as the first round with the

exception of the primers (5' AHW158). The product from the second round of PCR was purified as before, and cloned into pDBLeu as previously described (Table 2-4).

2.5. Yeast Two-Hybrid Assay

Plasmids containing the AD-response regulator and DBD-YPD1 fusion proteins were co-transformed into the host strain, MaV203, using the PEG-LiAc method (Burke *et al.*, 2000). Transformation mixtures were plated onto synthetic complete (SC) –leu –trp agar media and grown at 30°C for 48 hours. Three isolated colonies of each mutation were selected and assayed three times (for a total of at least nine datapoints for each mutant) for β-galactosidase activity. Each colony was incubated in 2.5 ml SC –leu –trp at 30°C overnight and 1 ml of the culture was used to inoculate 5 ml of YPAD media (1% yeast extract, 2% peptone, 0.01% adenine sulfate, 2% dextrose, pH 6.0). Inoculants were incubated at 30°C until an optical density at 600 nm (OD_{600}) of 1.0 was reached. Cells were harvested from 1.5 ml aliquots and washed twice with 1.0 ml assay buffer (100 mM HEPES, 150 mM NaCl, 5 mM L-aspartate, 1% BSA , 0.05% Tween 20, pH 7.3). Cell pellets were resuspended in 100 µl assay buffer and lysed by repeated rounds of immersion in liquid nitrogen and incubation in a 37°C waterbath. Assay buffer (900 µl) containing 2 mM CPRG was added to the cell lysate. The reaction mixture was incubated at room temperature overnight. The reaction was then quenched by addition of 250 µl 6 mM $ZnCl_2$ and the time was recorded. Cellular debris was removed by centrifugation. The OD_{574} of the supernatant was recorded. β-galactosidase units were calculated using the equation, β-gal units = 1000 x OD_{574}/ (t x V x OD_{600}), where t is the

Table 2-4
Plasmids Used in the YPD1 Q34 and E58 Random Mutant Yeast Two-Hybrid Assay

Plasmid	Parent Vector	Insert	Protein Expressed
OU 61	pPC86	SSK1-R2	Gal4 AD-SSK1-R2
OU 64	pDBLeu	YPD1	Gal4 DBD-YPD1
OU150	pPC86	SLN1-R1	Gal4 AD-SLN1-R1
OU151	pPC86	SKN7-R3	Gal4 AD-SKN7-R3
OU152	pDBLeu	YPD1 Q34K	Gal4 DBD-YPD1 Q34K
OU154	pDBLeu	YPD1 Q34W	Gal4 DBD-YPD1 Q34W
OU203	pDBLeu	YPD1 Q34G	Gal4 DBD-YPD1 Q34G
OU204	pDBLeu	YPD1 E58G	Gal4 DBD-YPD1 E58G
OU205	pDBLeu	YPD1 E58D	Gal4 DBD-YPD1 E58D
OU208	pDBLeu	YPD1 E58T	Gal4 DBD-YPD1 E58T
OU209	pDBLeu	YPD1 E58S	Gal4 DBD-YPD1 E58S
OU211	pDBLeu	YPD1 E58R	Gal4 DBD-YPD1 E58R
OU212	pDBLeu	YPD1 E58P	Gal4 DBD-YPD1 E58P
OU213	pDBLeu	YPD1 E58L	Gal4 DBD-YPD1 E53L
OU214	pDBLeu	YPD1 E58Q	Gal4 DBD-YPD1 E58Q
OU215	pDBLeu	YPD1 E58K	Gal4 DBD-YPD1 E58K
OU216	pDBLeu	YPD1 E58I	Gal4 DBD-YPD1 E58I
OU217	pDBLeu	YPD1 E58T	Gal4 DBD-YPD1 E58T
OU218	pDBLeu	YPD1 Q34C	Gal4 DBD-YPD1 Q34C
OU219	pDBLeu	YPD1 Q34Y	Gal4 DBD-YPD1 Q34Y
OU220	pDBLeu	YPD1 Q34R	Gal4 DBD-YPD1 Q34R
OU221	pDBLeu	YPD1 E58Y	Gal4 DBD-YPD1 E58Y
OU222	pDBLeu	YPD1 Q34P	Gal4 DBD-YPD1 Q34P
OU223	pDBLeu	YPD1 Q34D	Gal4 DBD-YPD1 Q34D
OU227	pDBLeu	YPD1 E58V	Gal4 DBD-YPD1 E58V
OU228	pDBLeu	YPD1 Q34F	Gal4 DBD-YPD1 Q34F
OU229	pDBLeu	YPD1 Q34S	Gal4 DBD-YPD1 Q34S
OU230	pDBLeu	YPD1 Q34N	Gal4 DBD-YPD1 Q34N
OU231	pDBLeu	YPD1 Q34H	Gal4 DBD-YPD1 Q34H
OU233	pDBLeu	YPD1 Q34L	Gal4 DBD-YPD1 Q34L

time in minutes and V is the volume of the initial aliquot. β-galactosidase activity for each of the mutants was compared to that of wild-type YPD1.

2.6. Western Blots

Protein expression levels of the two-hybrid fusion proteins were determined by Western blotting (Towbin *et al.*, 1979). Cell concentrations were normalized to the optical density at 600 nm of the culture. Aliquots were taken and cells were pelleted by centrifugation at 8000 x g for 1 minute. Cell pellets were washed in buffer (100 mM HEPES, 150 mM NaCl, 5 mM L-aspartate, 1% bovine serum albumin, 0.05% Tween 20, pH 7.3). Cells were resuspended in 100 µl of the same buffer and then lysed by repeated rounds of immersion in liquid nitrogen, followed by incubation at 37°C in a water bath for 2 minutes. Sample loading buffer (4X: 250 mM Tris (pH 6.8), 40% glycerol, 8% SDS) was added to each tube and the samples were loaded onto a 10%-SDS-polyacrylamide gel and electrophoresed at 200 V for 30 minutes. Samples were electroblotted onto polyvinylidene difluoride (PVDF) membranes in transfer buffer (25 mM Tris (pH 8.3), 192 mM glycine, 20% methanol, 0.1% SDS). Membranes were probed with a YPD1-specific antibody (1:10000 dilution) followed by an alkaline phosphatase-conjugated goat anti-rabbit secondary antibody. The blots were analyzed using the enhanced chemifluorescense detection system from Amersham Biosciences.

2.7. Pull down assay

An *in vitro* pull down assay was performed between SSK1-R2 and YPD1 or YPD1-G68Q. In this assay, SSK1-R2 was fused to an intein affinity tag (CYB-R2),

purified and bound to chitin beads according to published procedures (Janiak-Spens & West, 2000).

Bead-bound GST-HK (21 μM, 25 μl) was aliquoted into two tubes. Each tube was washed three times with 100 μl of buffer A (50 mM Tris-pH 8.0, 100mM KCl, 10 mM $MgCl_2$, and 20% glycerol). The beads were resuspended in 50 μl buffer A. Reduced glutathione (5 μl of 10X stock) was added to the resuspended beads. Radiolabeled [γ-^{32}P] ATP (333 μM, 1.5 μl) was added to phosphorylate HK and incubated at room temperature for 30 minutes. The reaction was separated into supernatant and pellet by centrifugation (300g for 2 minutes) and the supernatant removed to a new tube.

CYB-R2 (2x75 μl of 5 μM) was washed as stated before. The pellet was resuspended in 75 μl of buffer A and 50 μl of HK was added to each tube. The mixture was incubated for 1.5 hours while being mixed every 15 minutes. Mixtures were again separated into supernate and pellet. The pellet (CYB-R2) was resuspended in 75 μl buffer A.

YPD1 (2 μl of 43μM stock) was added to one reaction tube and incubated for 10 minutes. YPD1-G68Q (3 μl of 27.2 μM stock) was added to the other reaction tube and incubated for 10 minutes. The mixtures were separated into supernatant and pellet as previously stated and removed to separate tubes. The pellet was washed with an additional 100 μl of buffer A. The volume of both supernatant and pellet were resuspended 100 μl Laemmli buffer. Samples were loaded onto a 15% SDS polyacrylamide gel and electrophoresed until the bromphenolblue band ran off the gel. The gel was exposed to a phosphorimaging plate overnight and developed using a phosphorimager (Molecular Dynamics).

2.8. Native Gel-Shift Assay

Phosphorylation of the response regulator domain of SSK1 was achieved by incubating bead-bound GST-HK with ATP according to published procedures (Janiak-Spens *et al.*, 2000). The phosphorylated and unphosphorylated SSK1-R2 (16 μM) was added to parallel reactions containing YPD1 (1.6 μM) and YPD1 mutants (1.6 μM) in reaction buffer (50 mM Tris-HCl (pH 8.0), 100mM KCl, 10mM $MgCl_2$, 2mM DTT, 20% glycerol) for 5 minutes at room temperature. Protein samples were loaded onto a native 15% polyacrylamide gel and electrophoresed at 250 V for 40 minutes. Proteins were electroblotted onto polyvinylidene difluoride (PVDF) membranes in transfer buffer (25 mM Tris (pH 8.3), 192 mM glycine, 20% methanol). Duplicate membranes were probed with anti-SSK1-R2 or anti-YPD1 antisera and developed using the Immun-Star chemiluminescence kit (BioRad).

3. Identification of the SSK1-R2 Response Regulator Binding Site on YPD1

3.1.Introduction

The histidine-containing phosphotransfer protein, YPD1, plays a central part in responses to hyperosmotic and other environmental stress responses in *Saccharomyces cerevisiae*. YPD1 is required for phosphoryl transfer between an upstream response regulator domain, SLN1-R1, and two downstream response regulator domains, SSK1-R2 and SKN7-R3. The interaction between YPD1 and SSK1-R2 appears to be quite different than the one between YPD1 and the other two response regulator domains, SLN1-R1 and SKN7-R3. A detectable complex between YPD1 and SSK1-R2 has been observed by yeast two-hybrid analysis *in vivo* (Posas *et al.*, 1996) and in a native gel shift assay *in vitro* (Janiak-Spens *et al.*, 2000). The presence of YPD1 has also been shown to affect the stability of phospho-SSK1-R2 in *in vitro* experiments by preventing hydrolysis of the phosphoryl group. The phosphorylated half-life of the response regulator in the absence and presence of YPD1 is 14 minutes and 42 hours, respectively (Janiak-Spens *et al.*, 2000). This stabilizing effect of YPD1 was not observed with either SLN1-R1 or SKN7-R3. Furthermore, in the presence of equimolar concentrations of the two

downstream response regulator domains, SSK1-R2 and SKN7-R3, YPD1 preferentially donates a phosphoryl group to SSK1-R2 (Fabiola Janiak-Spens, unpublished observations). Thus YPD1 clearly interacts differently with the three response regulator domains in *S. cerevisiae.*

In order to address the question of specificity of interaction between YPD1 and the response regulator domains, studies were performed utilizing alanine-scanning mutagenesis coupled with a yeast two-hybrid screen to identify critical residues on the surface of YPD1 that mediate protein-protein interactions with SSK1-R2.

3.2. Results

The crystal structure of YPD1 was solved by Qingping Xu previously in our laboratory (Xu & West, 1999) and independently by another group (Song *et al.*, 1999). Using the structure of YPD1 as a guide, several site-specific mutations were engineered on the surface of the molecule near His64, the site of phosphorylation. All non-alanine and non-glycine surface residues in this area were selected for alanine-scanning mutagenesis. Each mutant was then screened for loss of interaction with the response regulator domain of SSK1 (SSK1-R2) using the well-established yeast two-hybrid system (Chien *et al.*, 1991; Fields & Song, 1989; Fields & Sternglanz, 1994).

The yeast two-hybrid system has become a valuable technique in the identification of protein-protein interactions (Bartel & Fields, 1997; Chien *et al.*, 1991; Maher, 2002; Robinson & Brasch, 1998; Serebriiskii *et al.*, 2001; White, 1996). The system was originally devised to identify proteins that interact *in vivo* with a particular protein of interest. However, over time many variations of the system have been developed, including the yeast one-hybrid, three-hybrid, and reverse two-hybrid systems

(Vidal *et al.*, 1996a; Vidal *et al.*, 1996b). The yeast two-hybrid system utilizes a transcription factor found in yeast that possesses unique qualities.

The GAL4 transcription factor contains two independently functioning domains: a DNA-binding domain (DBD) at the N-terminus and an activation domain at the C-terminus (AD). The DNA-binding domain of GAL4 recognizes and binds to promoter regions in the galactose operon. The activation domain interacts with RNA polymerase and initiates transcription of genes in the galactose operon. For gene transcription to occur the two GAL4 domains must be physically linked. If the two domains are co-expressed and not physically linked transcription of the galactose genes does not occur. The yeast two-hybrid system takes advantage of this phenomenon by creating two hybrid proteins. The first hybrid protein is a protein of interest fused to the DNA-binding domain of GAL4. Another fusion protein is created between a protein believed to interact with the protein of interest fused to the activation domain of GAL4. In the yeast two-hybrid system, if the two proteins of interest interact, the GAL4 transcription factor is reconstituted, and transcription occurs (Figure 3-1). Proteins that do not interact, however, will not reconstitute the GAL4 transcription factor and RNA polymerase will not transcribe the reporter gene. The two possibilities presented above represent the extreme cases possible in the yeast two-hybrid system. The benefit of the yeast two-hybrid system is protein-protein interactions can be detected between weakly interacting protein pairs as well as strongly interacting protein pairs yielding a graded response that can be quantified.

In this assay proteins that interact strongly will have a higher level of expression of the reporter gene than protein pairs that interact weakly. In the ProQuest yeast two-

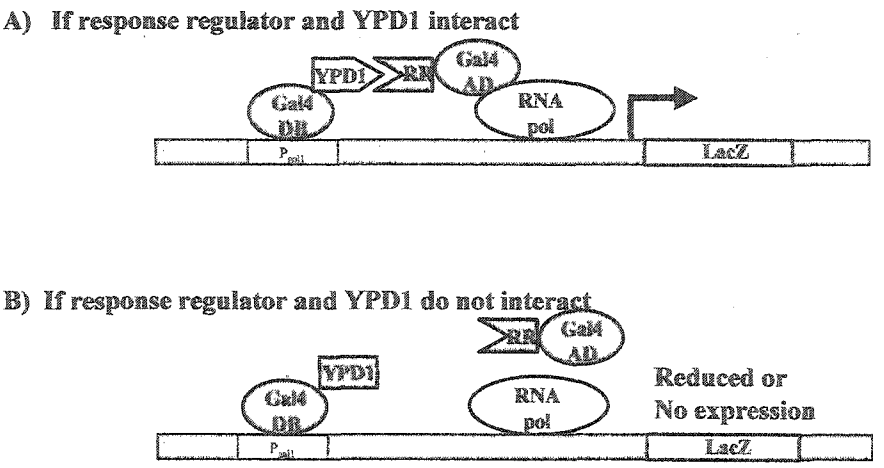

Figure 3-1
Overview of the Yeast Two-Hybrid System. Reconstitution of the *GAL4* transcription factor occurs upon interaction between the two fusion proteins resulting in expression of the *lacZ* reporter gene. Fusion proteins that do not interact or interact poorly will display a reduced expression of β-galactosidase.

hybrid system three reporter genes (*HIS3*, *URA3* and *lacZ*) are integrated into the host genome. The reporter genes are located downstream of the GAL_1 upstream activation sequence (UAS) and allow users of the system three independent methods of determining protein-protein interactions *in vivo*. The *E. coli lacZ* gene encoding β-galactosidase can be used in a liquid assay to determine the relative strength of interaction between protein pairs (Serebriiskii & Golemis, 2000).

Experiments aimed at comparing *in vitro* affinities for protein with yeast two-hybrid data proved successful (Estojak *et al.*, 1995). The results from the assay indicated that the strength of interaction predicted in the yeast two-hybrid system correlated well with data obtained *in vitro* and there was a direct correlation between the strength of interaction observed in the screen and the level of reporter gene expression. Thus, yeast two-hybrid data obtained in the screen of wild-type YPD1 and YPD1 mutants with yeast response regulator domains will provide useful information in identifying surface

residues from YPD1 that are involved in interactions with the response regulator domains.

Residues selected were mutated to alanine for several reasons. First, it was reasoned based on the structure of YPD1 that mutation of these selected surface residues would have a minimal effect on the overall structure of the molecule, thus, the folding of the protein would be preserved. YPD1 is an all-helical protein, and alanine has a propensity for forming α–helices. Second, in studies where there is no known protein structure available, alanine-scanning mutagenesis has proven to be a valuable tool in identifying possible protein docking sites (Wells, 1991). Finally, mutation of a residue to a lower volume side chain would reduce the possibility of receiving a false positive resulting from steric hindrance, which could force the two molecules apart.

Each of the YPD1 alanine mutants was screened for loss of interaction with SSK1-R2 using the yeast two-hybrid assay. In addition to the mutants created specifically for this project, several other previously engineered mutants that displayed weakened *in vitro* phosphotransfer activity, were included in the screen (Janiak-Spens & West, 2000).

Before screening the YPD1 mutants the feasibility of the assay was tested with the wild-type proteins. The ProQuest two-hybrid system from BRL/Invitrogen included several controls of various interaction strengths for determination of the relative strength of interaction between the proteins of interest. Results from the assay revealed that YPD1 and SSK1-R2 interact relatively weakly with one another. The level of interaction was roughly twice that of the weakest control pair provided, the human E2F1 and retinoblastoma (Rb) proteins (Vidal *et al.*, 1996a) (Figure 3-2). Each of the YPD1

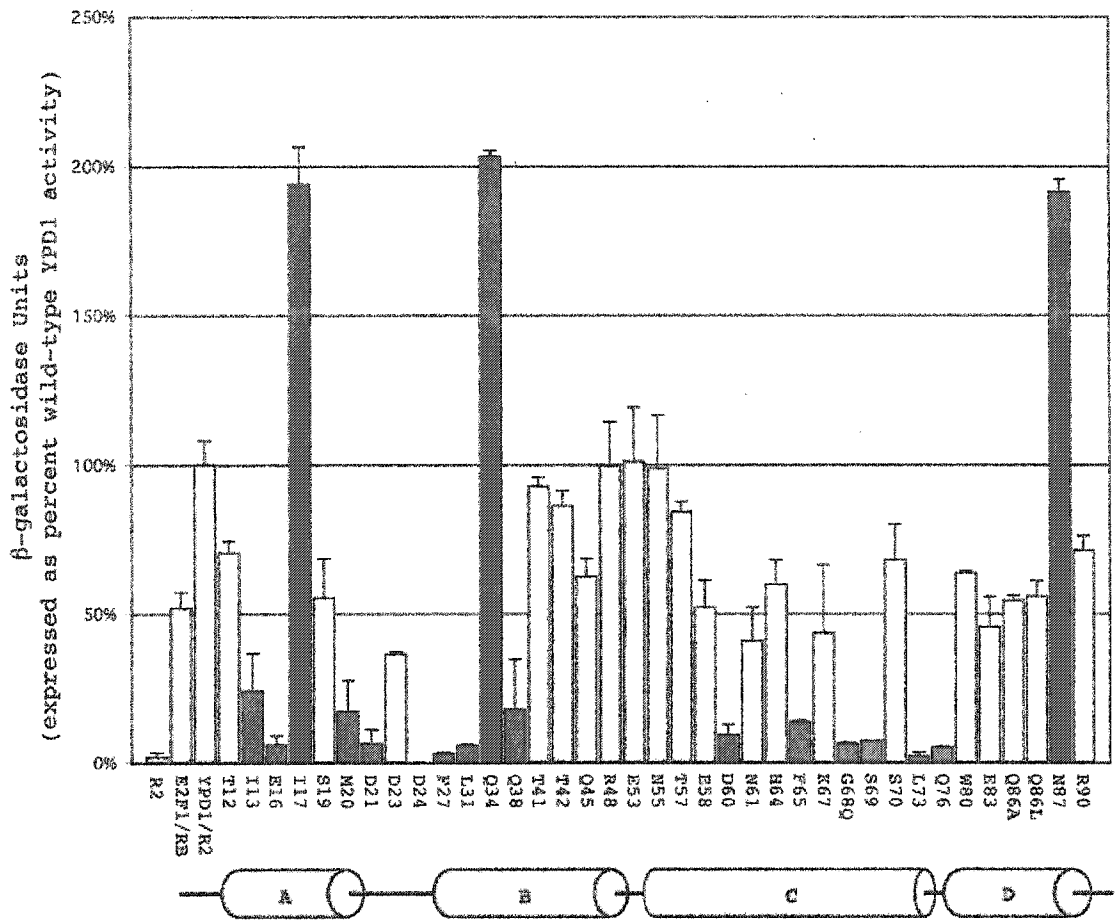

Figure 3-2

***In vivo* Protein-Protein Interaction Screen Between YPD1 and SSK1-R2.** YPD1 mutants were screened for loss of interaction with the response regulator domain of SSK1 using a yeast two-hybrid assay. Results from a liquid β-galactosidase assay were reported as units of activity and compared to that of the wild-type YPD1 interaction. Each data point represents three independent colonies assayed in triplicate and the standard deviation from the mean is shown. Mutants in green displayed a near wild-type interaction while residues in yellow and red displayed a moderate and severe disruption of interaction with SSK1-R2, respectively. The three mutants displaying an enhanced interaction phenotype are shown in blue. The secondary structure assignment for each residue is located below the graph. Unless otherwise noted all residues were mutated to alanine. Figure taken from (Porter *et al.*, 2003).

mutants was then screened using CPRG as a substrate for loss of interaction with SSK1-R2 and the results compared to that of the wild-type interaction (Table 3-1) (Eustice *et al.*, 1991). To ensure that the results obtained were an accurate representation of the strength of the protein-protein interaction being measured and not due to differences in protein expression a Western blot analysis was performed using α-YPD1 antibodies (Figure 3-3). Results show that all YPD1 mutants were expressed at the same level.

Table 3-1
YPD1/SSK1-R2
Yeast Two-Hybrid Interactions

YPD1 Mutant	SSK1-R2	Location
wild-type	100 ± 4	N/A
T12A	70 ± 4	A Helix
I13A	24 ± 13	A Helix
E16A	6 ± 3	A Helix
I17A	194 ± 12	A Helix
S19A	55 ± 13	A Helix
M20A	17 ± 10	A Helix
D21A	6 ± 5	A-B loop
D23A	36 ± 1	A-B loop
D24A	0 ± 0	A-B loop
F27A	3 ± 0	B Helix
L31A	6 ± 0	B Helix
Q34A	203 ± 2	B Helix
Q38A	18 ± 17	B Helix
T41A	93 ± 3	B Helix
T42A	86 ± 5	B Helix
Q45A	62 ± 6	B Helix
R48A	99 ± 15	B Helix
E53A	101 ± 18	B-C loop
N55A	99 ± 18	C Helix
T57A	84 ± 3	C Helix
E58A	52 ± 9	C Helix
D60A	9 ± 4	C Helix
N61A	41 ± 11	C Helix
H64A	60 ± 8	C Helix
F65A	14 ± 1	C Helix
K67A	43 ± 23	C Helix
G68Q	6 ± 0	C Helix
S69A	7 ± 0	C Helix
S70A	68 ± 12	C Helix
L73A	2 ± 1	C Helix
Q76A	5 ± 0	D Helix
W80A	64 ± 0	D Helix
E83A	45 ± 10	D Helix
Q86A	54 ± 2	D Helix
Q86L	56 ± 5	D Helix
N87A	191 ± 4	D Helix
R90A	71 ± 5	D Helix

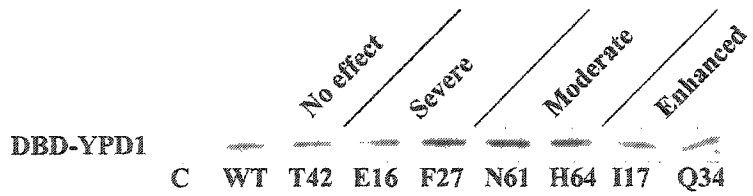

Figure 3-3
Protein Expression Profile of DBD-YPD1 Fusion Proteins in Yeast Strain MaV203.
Proteins from equivalent whole cell lysates of yeast colonies expressing the DNA binding domain-YPD1 mutant fusion protein were separated on an SDS-PAGE gel followed by transfer to a PVDF membrane and probed with an anti-YPD1 antibody. A negative control was included (C) that lacked a DBD-YPD1 expression plasmid. Representatives from each of the four classifications were included, near wild-type (T42), severe (E16 and F27), moderate (N61 and H64), and enhanced (I17 and Q34). Figure taken from (Porter *et al.*, 2003).

The YPD1 mutants screened showed a level of interaction ranging from no interaction to a two-fold enhancement of the interaction with SSK1-R2 as compared to wild-type. The mutants were divided into four categories: no effect, moderately disrupting, severely disrupting, and enhanced interaction. Only 6 of the 39 residues screened (T41, T42, R48, E53, N55, and T57) were observed to have no appreciable effect (76-100% wild-type interaction) with respect to interaction with SSK1-R2. These residues seem to cluster around the C-terminus of αB and the N-terminus of αC. A large number of mutants (T12, S19, D23, Q45, E58, N61, H64, K67, S70, W80, E83, Q86A, Q86L, and R90) displayed a moderate disruption (25-75% wild-type interaction) of the interaction with SSK1-R2. These 14 residues are clustered along the αA, αC and αD helices. Mutation of another 14 residues (I13, E16, M20, D21, D24, F27, L31, Q38, D60, F65, G68Q, S69, L73, and Q76) had a significant disruptive effect (< 25% wild-type interaction) on protein-protein interactions. These residues seem to be essential for proper interaction between YPD1 and SSK1-R2. They are located throughout the A helix, at the N-terminus of αB and the C-terminus of αC. Unexpectedly, three YPD1 mutants displayed an enhanced interaction with SSK1-R2. These mutants (I17A, Q34A

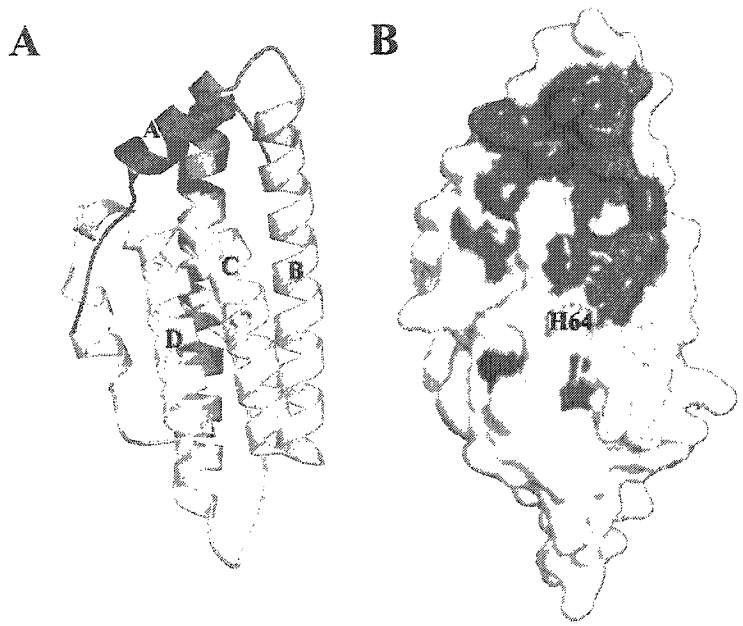

Figure 3-4

A. Ribbon Diagram of YPD1. YPD1 is an all-helical protein with a four-helix bundle core. The site of phosphorylation, H64, is located in the middle of helix C shown in stick model.

B. Molecular Surface Representation of YPD1. The molecular surface of YPD1 was generated using the program PYMOL (DeLano, 2002). Mutations that resulted in a moderate and severe disruption of interactions with SSK1-R2 are colored yellow and red, respectively. Those that displayed no significant change in strength of interaction are shaded green and mutants that resulted in an enhanced interaction phenotype are shaded blue. The mutated residues that resulted in a severe disruption with SSK1-R2 are located between H64 and the αA helix. One residue (D60) falls just outside this area and is located one turn below H64. Figure taken from (Porter *et al.*, 2003).

and N87A) displayed a two-fold increase in interaction strength compared to that of wild-type YPD1 interaction.

The goal of this project was to identify the response regulator binding site on the surface of YPD1. This was accomplished for the SSK1-R2 domain by mapping the results from the yeast two-hybrid assay onto the molecular surface of YPD1 generated in the molecular graphics program PYMOL (Figure 3-4). From this representation it is immediately apparent that mutations that severely disrupted interaction with SSK1-R2 cluster on the surface of YPD1. The binding site is located mainly between the site of

phosphorylation (H64) and the αA helix and encompasses approximately 750Å^2 as estimated by the molecular graphic program GRASP (Nicholls *et al.*, 1991). Thirteen of the fourteen severely disrupting mutations reside in this area. Only one mutation (D60) is located outside of this area, one turn below the site of phosphorylation and could easily be within the buried surface of a YPD1-response regulator complex.

Mutants that displayed a moderate disruption of interaction of the protein pair were located around the patch of severely disrupting mutations. In every case the location of a moderately disrupting mutation was located adjacent to a severely disrupting mutation. The mutations that had no significant effect are shown in green and are primarily located in one area on the surface of YPD1 away from the site of phosphorylation. The three mutations that resulted in an enhanced interaction were found near the periphery of the proposed binding site and surrounded the phosphorylation site.

3.3. Discussion

3.3.1 SSK1-R2 Binding Site on YPD1

Upon further examination of the surface of YPD1, it was apparent that a large hydrophobic patch is located between the phosphorylation site, H64, and the αA helix. This is the same area that was identified as the SSK1-R2 response regulator binding surface. The hydrophobic patch is surrounded by polar and charged residues. The surface area of the hydrophobic patch was calculated using the molecular graphics program GRASP (Nicholls *et al.*, 1991) and was found to be approximately 690Å^2 (Figure 3-5A). This is slightly smaller than the calculated surface area of the binding site that is occupied

by severely disrupting residues. The presence of the hydrophobic patch is interesting because it could represent a general binding surface for other response regulator domains.

To determine if the hydrophobic domain on the surface of YPD1 is a general characteristic of HPt domains, a sequence alignment was performed (Figure 3-5B). Alignment of YPD1 with five other HPt domains (*Schizosaccharomyces pombe* MPR1, *Candida albicans* YPD1, *Arabidopsis thaliana* AHP2, *Dictyostelium discoideum* RdeA, and *Escherichia coli* ArcB) revealed eight residues found in the hydrophobic patch of YPD1 are conserved in each of the other HPt domains as well. These residues are located on αA (I13, I17 and M20), the N-terminus of αB (F27 and L31), and the C-terminus of αC (G68, L73 and G74). It is also interesting to note that the residues from the other HPt domains, corresponding to A71 and A72 in YPD1, are mainly hydrophobic and presumably are located in the same area of the molecule. These two positions were not tested in the yeast two-hybrid assay, but could contribute to the binding interface as indicated by analysis of the sequence alignment.

Thus, the hydrophobic patch on the surface of YPD1 that serves as a response regulator binding site is likely to be a general feature found in other HPt domains. Further evidence for this binding site comes from the two-component system in *Escherichia coli* involved in anaerobic respiration. Analysis of the HPt domain of the anaerobic hybrid sensor ArcB also revealed a hydrophobic patch located in a similar position on the surface. Mutation of the residues within this area exhibited decreased phosphotransfer activity, which the authors attributed to a loss of interaction with its cognate response regulator ArcA (Kato *et al.*, 1999; Matsushika & Mizuno, 1998a).

A



B

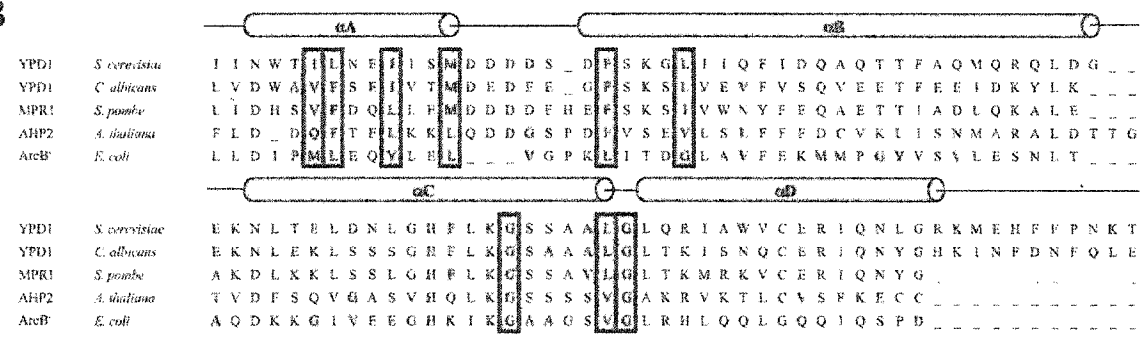

Figure 3-5

A. Hydrophobic Surface Map of YPD1. The molecular surface of YPD1 is colored according to its chemical properties. Residues that are polar or charged are shaded yellow, while hydrophobic residues are shaded grey. A cluster of hydrophobic residues is located on the surface in the same region as the patch of severely disrupting mutations.

B. HPt Sequence Alignment. The sequence of YPD1 was aligned with HPt domains from other organisms *Schizosaccharomyces pombe* MPR1, *Candida albicans* YPD1, *Arabidopsis thaliana* AHP2, and *Escherichia coli* ArcB. * Shaded residues (grey for hydrophobic, yellow for polar) are surface exposed residues in YPD1 and corresponding residues on other HPt domains. Boxed residues are those that were determined to be in the hydrophobic patch of YPD1 and are conserved among the aligned HPt domains.

The results from the yeast two-hybrid assay also underscore the importance of this hydrophobic patch. From the eight conserved residues identified in the sequence alignment, mutation of six (I13, M20, F27, L31, G68, and L73) resulted in a severe loss of interaction with SSK1-R2 and one residue (I17) was found to enhance the interaction with SSK1-R2. The remaining residue, G74, was not tested in the two-hybrid system due

to the fact that it is located in a β-hairpin turn between helix C and D. It has been noted that expression of this mutant did not yield any soluble protein (Janiak-Spens & West, 2000). It was speculated that mutation of this residue to alanine alters the structure of the molecule such that, at least when expressed in *Escherichia coli*, the protein was misfolded. Therefore is may also give an unreliable result in the *in vivo* yeast two-hybrid system.

It is possible that residues that make up the hydrophobic patch represent a general binding surface for all response regulators and that the remaining polar residues that display a severely disrupting phenotype outside this area are responsible for determining the specificity for individual response regulators. This will have to be determined by a comparative study whereby several response regulators will be screened against the same HPt domain, for example YPD1 screened against SLN1-R1, SSK1-R2 and SKN7-R3 (Chapter 4). We may then be able to determine which residues are needed for general recognition of response regulators and which are specific for a particular response regulator.

There are several explanations for the three mutations that resulted in an enhanced interaction with SSK1-R2. First, mutation of the polar residues to an alanine residue could extend the hydrophobic patch, increasing the "general" recognition site for the response regulator. Second, the mutation to alanine decreased the side chain volume of each of the residues. This might reduce steric hindrance at the interface of the complex allowing the two molecules to come closer in a complex. Finally, the corresponding residues on the surface of SSK1-R2 may have chemical properties that are more suited to the chemical properties of the alanine in these positions on YPD1. These possibilities

were further investigated by randomly mutating amino acid residues in the positions that displayed enhanced interactions and assaying those mutants in the yeast two-hybrid system (Chapter 4). Furthermore, a detailed discussion of all YPD1/response regulator interactions in context with other HPt/response regulator as well as their implications to the broader topic of two-component signal transduction will follow in Chapter 6.

4. YPD1-Response Regulator Domain Interactions: A Comparative Study

4.1. Introduction

In the previous chapter protein-protein interactions between YPD1 and the regulatory domain of SSK1 were investigated by alanine-scanning mutagenesis coupled to a yeast two-hybrid screen. Studies were first performed on YPD1 and SSK1-R2 because of the previously observed higher affinity of YPD1 for SSK1-R2 than for SLN1-R1 or SKN7-R3 (F. Janiak-Spens, unpublished observations). Results from the yeast-two hybrid screen revealed that the SSK1-R2 response regulator binding site on the surface of YPD1 is located between the αA helix of YPD1 and the site of phosphorylation, H64. Moreover, a large hydrophobic patch is located in the center of the SSK1-R2 binding site. A sequence alignment between YPD1 and other monomeric HPt domains from bacteria, fungi, and plants revealed that residues that make up the hydrophobic patch on the surface of YPD1 is a conserved feature of HPt domains. Based on these observations it was theorized that the hydrophobic patch on the surface of YPD1 represents a common response regulator binding site. A ring of polar and charged residues surrounds the hydrophobic patch on the surface of YPD1. It was further speculated that these polar and charged amino acid residues are involved in determination of response regulator

specificity, although further studies screening YPD1 with other response regulators are needed to support this hypothesis.

Results from the yeast two-hybrid assay between YPD1 and SSK1-R2 also revealed an interesting observation. Three YPD1 alanine mutants displayed a two-fold enhanced interaction phenotype when screened for interactions with SSK1-R2. The three mutations were located near the periphery of the hydrophobic patch on the surface of YPD1. It was hypothesized that these observations could result from (i) increasing the surface area of the hydrophobic patch, (ii) reducing steric hindrance at the protein-protein interface, or (iii) residues on the surface of the response regulator domain of SSK1 may have chemical properties that are more suited to the mutation on the surface of YPD1.

In this chapter the question of HPt/response regulator specificity will be addressed. The YPD1 alanine mutants were screened for loss of interaction with the remaining two response regulator domains in *S. cerevisiae*, SLN1-R1 and SKN7-R3 using the yeast two-hybrid screen. Through this comparative study we hoped to identify residues on the surface of YPD1 that contribute to specific interactions with each of the response regulator domains. Furthermore, a study coupling site-directed random mutagenesis with the yeast two-hybrid screen aimed at examining the enhanced interaction mutants will be presented.

4.2. Results

4.2.1 SLN1-R1 and SKN7-R3 Interaction Screen with YPD1

While a complex could be observed *in vitro* between YPD1 and phosphorylated SSK1-R2 using a native gel-shift assay, no complex was observed between YPD1 and

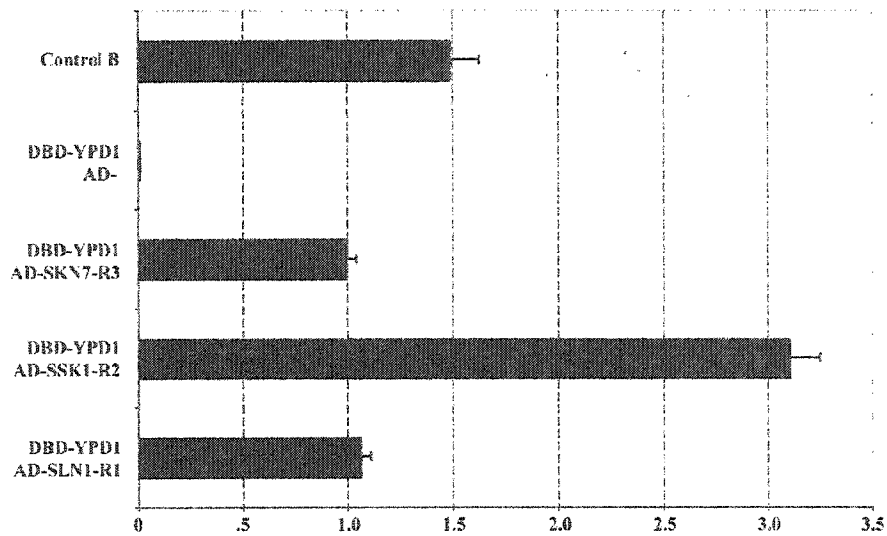

Figure 4-1.
Yeast Two-Hybrid Results of YPD1/Response Regulator Interactions. YPD1 was screened for strength of interaction with each of the three response regulator domains found in *S. cerevisiae*. A positive control (control B) was included in the screen and includes two weakly interacting proteins, E2F1/Retinoblastoma. A negative control was also included lacking a response regulator domain.

SLN1-R1 or SKN7-R3 (F. Janiak-Spens, unpublished observations). To determine if interactions could be detected *in vivo* between YPD1 and SLN1-R1 or SKN7-R3, a yeast two-hybrid assay was performed. Results demonstrated that the complexes could be detected and show that a YPD1/SLN1-R1 complex and a YPD1/SKN7-R3 complex have approximately the same strength of interaction (Figure 4-1). The strength of interaction for the two complexes was about one third as strong as that determined for the YPD1/SSK1-R2 complex.

YPD1 alanine mutants created to identify the SSK1-R2 binding site, as described in the previous chapter, were screened for loss of interaction with the upstream response regulator, SLN1-R1, and the downstream response regulator involved in oxidative stress responses and cell wall synthesis, SKN7-R3. Mutants were categorized into one of four

groups according to their relative strength of interaction with each of the response regulator domains. Mutants displaying a near wild-type (75-100%) interaction with the response regulators have little effect on the interaction of the two proteins. Mutants that disrupted the interaction between the two proteins were classified as moderately disrupting (25-74% wild-type interaction) and severely disrupting (<25% wild-type interaction). Several mutants displayed an enhanced interaction (>150% wild-type interaction) with the response regulators. The graph comparing the interaction profile of the response regulators with the YPD1 mutants clearly identifies severely disrupting mutants located on αA (E16A, M20A, D21A), the N-terminus of αB (F27A, L31A) and the C-terminus of αC (D60A, F65A, G68Q, S69A, L73A) which showed similar interaction patterns when tested against all response regulators (Figure 4-2 and Table 4-1). Mutants that have no significant effect on the interaction of the response regulators with YPD1 appear to cluster near the C-terminus of αB and the N-terminus of αC. These residues are located away from the proposed response regulator-binding surface on YPD1 as discussed in the previous chapter.

While many of the severely disrupting mutants showed the same behavior in all three interaction screens, several YPD1 mutants were categorized as severely disrupting with one response regulator and fell into another interaction category with the other response regulators. Results show that there is one mutant (S19A) that displays a severely disrupting phenotype when assayed with SLN1-R1, but displays a moderate disruption phenotype with SSK1-R2 and a wild-type phenotype with SKN7-R3. This residue appears to be involved in specific interactions with SLN1-R1 (Table 4-2). There were no YPD1 surface residues that seem to be specific for interactions with SSK1-R2,

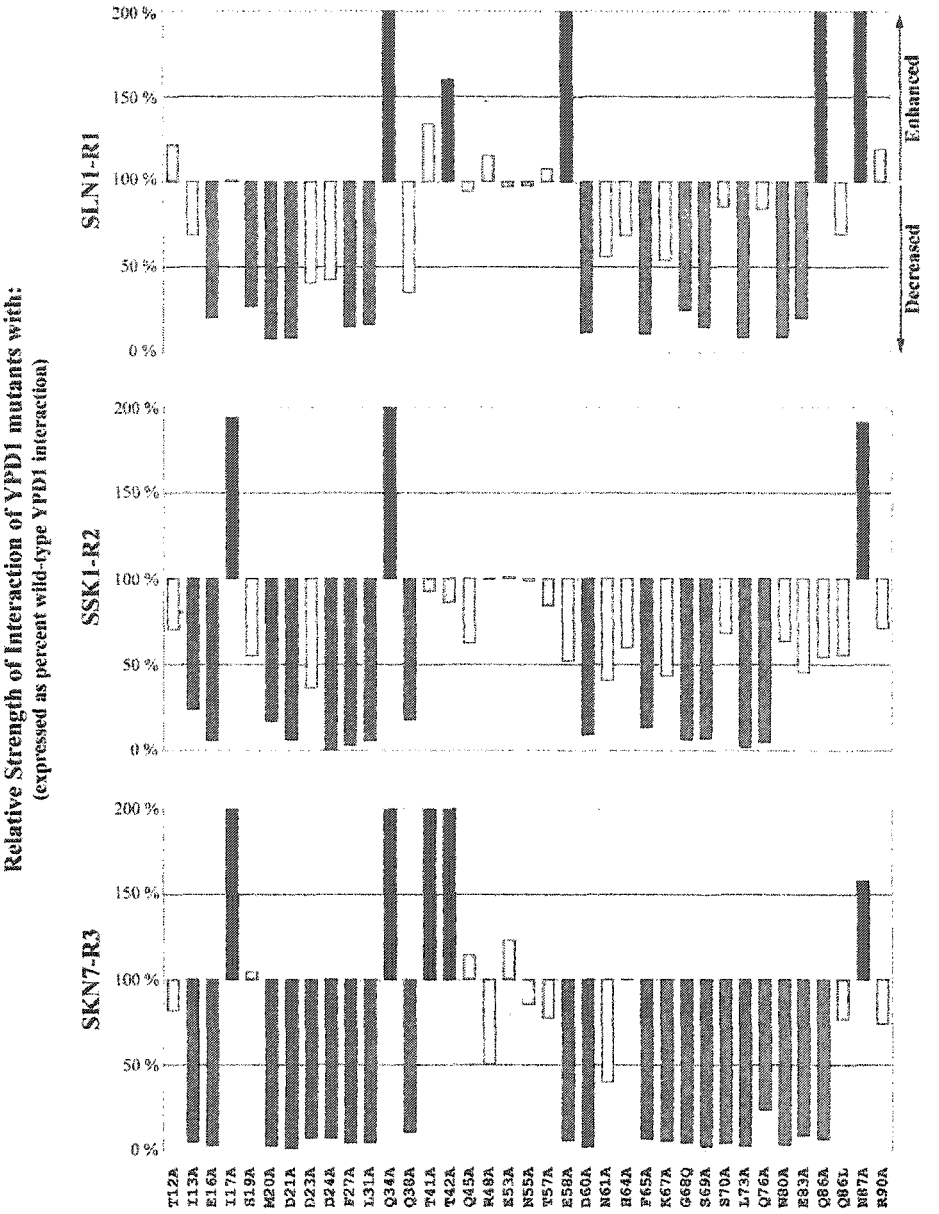

Figure 4-2

Yeast Two-Hybrid Results of YPD1-Response Regulator Interactions. A graph of the results from the yeast two-hybrid screens of YPD1 with all three yeast response regulator domains was constructed. Note the absolute values of enhanced interactions above 200% (blue) are not shown in this scale (results in Table 4-1). Mutants resulting in a moderate or severe disruption between YPD1 and the response regulators are shown in yellow and red, respectively. Mutants displaying no significant deviation from wild-type interactions are shown in green. Bars below the 100% indicate disruption of YPD1-response regulator interactions, while bars above the line indicate enhanced interactions.

Table 4-1
YPD1-Response Regulator
Yeast Two-Hybrid Interactions

YPD1 Mutant	Percent Interaction with: SLN1-R1	SSK1-R2	SKN7-R3	Location
wild-type	100 ± 8	100 ± 4	100 ± 4	N/A
T12A	122 ± 17	70 ± 4	82 ± 4	A Helix
I13A	69 ± 6	24 ± 13	5 ± 1	A Helix
E16A	20 ± 3	6 ± 3	3 ± 1	A Helix
I17A	101 ± 7	194 ± 12	1007 ± 96	A Helix
S19A	27 ± 7	55 ± 13	104 ± 9	A Helix
M20A	8 ± 1	17 ± 10	3 ± 1	A Helix
D21A	8 ± 2	6 ± 5	1 ± 0	A-B loop
D23A	41 ± 4	36 ± 1	8 ± 2	A-B loop
D24A	42 ± 5	0 ± 0	7 ± 0	A-B loop
F27A	15 ± 1	3 ± 0	4 ± 1	B Helix
L31A	16 ± 1	6 ± 0	5 ± 1	B Helix
Q34A	272 ± 18	203 ± 2	470 ± 70	B Helix
Q38A	35 ± 6	18 ± 17	11 ± 1	B Helix
T41A	134 ± 23	93 ± 3	239 ± 14	B Helix
T42A	160 ± 15	86 ± 5	244 ± 35	B Helix
Q45A	94 ± 16	62 ± 6	114 ± 17	B Helix
R48A	115 ± 3	99 ± 15	50 ± 9	B Helix
E53A	97 ± 8	101 ± 18	123 ± 10	B-C loop
N55A	97 ± 3	99 ± 18	85 ± 8	C Helix
T57A	108 ± 19	84 ± 3	78 ± 15	C Helix
E58A	671 ± 24	52 ± 9	6 ± 0	C Helix
D60A	12 ± 2	9 ± 4	2 ± 0	C Helix
N61A	56 ± 19	41 ± 11	40 ± 2	C Helix
H64A	68 ± 7	60 ± 8	100 ± 5	C Helix
F65A	11 ± 1	14 ± 1	7 ± 1	C Helix
K67A	54 ± 7	43 ± 23	6 ± 1	C Helix
G68Q	25 ± 2	6 ± 0	5 ± 4	C Helix
S69A	15 ± 4	7 ± 0	2 ± 1	C Helix
S70A	85 ± 18	68 ± 12	4 ± 1	C Helix
L73A	9 ± 3	2 ± 1	3 ± 2	C Helix
Q76A	84 ± 11	5 ± 0	24 ± 2	D Helix
W80A	9 ± 1	64 ± 0	3 ± 0	D Helix
E83A	20 ± 2	45 ± 10	9 ± 2	D Helix
Q86A	656 ± 55	54 ± 2	7 ± 1	D Helix
Q86L	69 ± 5	56 ± 5	77 ± 2	D Helix
N87A	213 ± 27	191 ± 4	158 ± 2	D Helix
R90A	119 ± 7	71 ± 5	74 ± 5	D Helix

Table 4-2
YPD1 Surface Residues Involved in Specific Interactions with:

SLN1-R1	S19
SSK1-R2	None
SKN7-R3	D23, E58, K67, S70 and Q86
SLN1-R1 and SKN7-R3	W80 and E83
SSK1-R2 and SKN7-R3	I13, D24, Q38, Q76

but five residues (D23, E58, K67, S70, and Q86) appear to be specific for interactions with SKN7-R3. There were also residues that displayed a severely disrupting phenotype with only two out of the three response regulators. Two YPD1 residues (W80 and E83) appear to be involved in response regulator binding to SLN1-R1 and SKN7-R3, while four residues (I13, D24, Q38, and Q76) appear to be involved in interactions with SSK1-R2 and SKN7-R3. Mutants displaying severely disrupting phenotype in the yeast two-hybrid assay were mapped onto the surface of YPD1 as described in chapter 3 (Figure 4-3A). The interaction map of SLN1-R1 with YPD1 shows the fewest number of surface residues (13 of 37) that comprise the binding interface with a surface area of 662 $Å^2$. The interaction map of SSK1-R2 was comprised of 14 residues, resulting in a surface area of 763 $Å^2$. The interaction between SKN7-R3 and YPD1 involved the greatest number of residues (21 of 37) as revealed by the two-hybrid screen. The surface area of the residues that when mutated disrupted the interaction between SKN7-R3 and YPD1 was 1031$Å^2$. This result is surprising when one considers that the interaction between wild-type YPD1 and SSK1-R2 was three-fold tighter than the interaction between wild-type YPD1 and SKN7-R3. A composite map of the three response regulator maps was constructed (Figure 4-3C) to visualize the common surface used to bind each response regulator (red) and to identify regions of response regulator specificity around the common interface

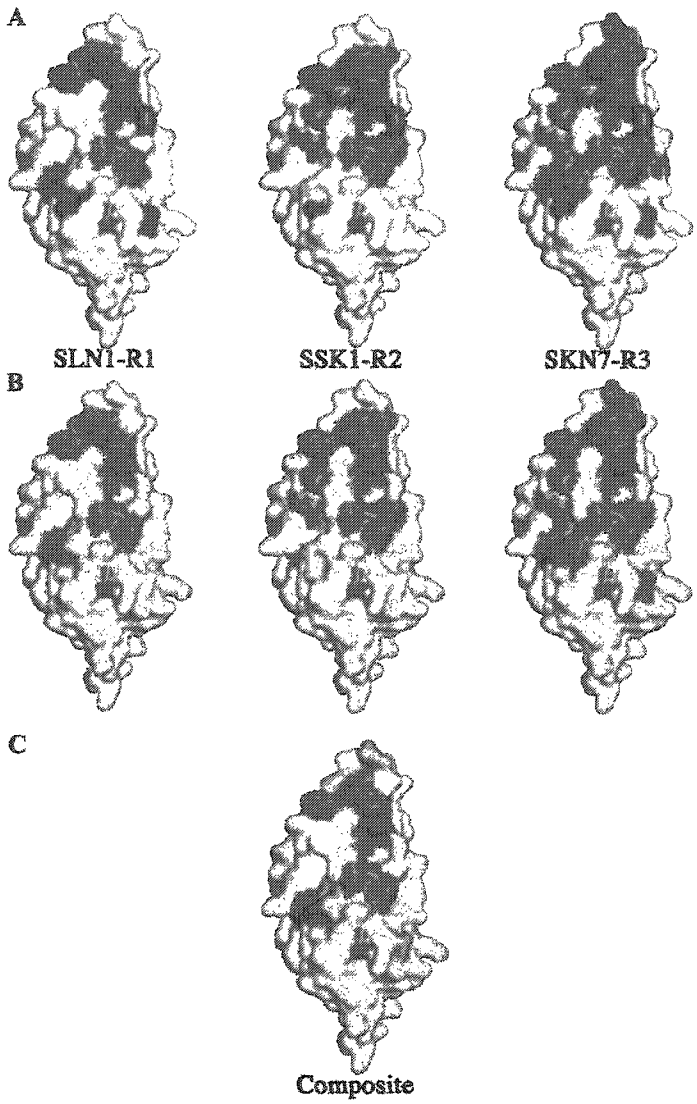

Figure 4-3

Surface Comparison of Response Regulator Interactions with YPD1.

A. Results from the yeast two-hybrid screens were mapped onto the surface of YPD1 using the same coloring scheme as previously described (red, severely disrupting; yellow, moderately disrupting, green, wild-type interactions; blue, enhanced interactions).

B. Mutants resulting in a severe disruption of interaction are shown in red. The patch of red represents the proposed response regulator binding site on the surface of YPD1 for each response regulator.

C. Residues on the surface of YPD1 resulting in a severe disruption of interaction with any of the response regulators were colored according to protein-protein interactions with the response regulators. Residues in red were involved in interactions with all three response regulator domains. Those in orange and blue are specific for SLN1-R1 and SKN7-R3 respectively. Residues in cyan were involved in interactions with both SSK1-R2 and SKN7-R3 while those in magenta were involved in interactions with SLN1-R1 and SKN7-R3.

(orange, SLN1-R1; blue, SKN7-R3; magenta, SLN1-R1 and SKN7-R3; cyan, SSK1-R2 and SKN7-R3). The common surface area of YPD1 that is used to bind each response regulator is located between H64 and αA. The residues in this area are mostly hydrophobic in nature, consisting of six hydrophobic residues (M20, F27, L31, F65, G68, and L73) flanked by four polar or charged residues (E16, D21, D60, and S69). Areas of specific response regulator interaction are located on either side of the stripe of general interactions.

As reported in Chapter 3 there were three YPD1 surface mutations (I17A, Q34A and N87A) that resulted in an enhanced interaction of YPD1 with SSK1-R2. Results from the yeast two-hybrid screen with SLN1-R1 and SKN7-R3 identified five mutants with similar enhanced interactions in each of the screens. Mutations resulting in enhanced interaction with SLN1-R1 were Q34A, T42A, E58A, Q86A and N87A, while those with SKN7-R3 were I17A, Q34A, T41A, T42A, and N87A. Two mutants (Q34A and N87A) displayed the enhanced phenotype in all three screens. Interestingly, one YPD1 mutant (E58A) displayed an enhanced, moderately disrupting and a severely disrupting phenotype with SLN1-R1, SSK1-R2 and SKN7-R3, respectively.

4.2.2 Analysis of YPD1 Q34 Mutants

To further investigate the enhanced interaction phenotypes two residues, Q34 and E58, were selected for random mutagenesis. It was hypothesized that mutants displaying an enhanced interaction did so due to the increased hydrophobicity of the alanine mutation. Since the Q34A mutation resulted in an enhanced interaction with each of the three response regulators, this position was randomly mutated to each of the remaining eighteen amino acid residues and assayed in the yeast two-hybrid system to reveal any

Table 4-3
YPD1 Q34X-Response Regulator
Yeast Two-Hybrid Interactions

YPD1 Mutant	Fold Interaction with: SLN1-R1	SSK1-R2	SKN7-R3
wild-type	1.00 ± 0.03	1.00 ± 0.04	1.00 ± 0.09
Q34A	2.72 ± 0.18	2.03 ± 0.02	4.7 ± 0.69
Q34C	60.07 ± 4.39	23.94 ± 0.93	60.8 ± 3.32
Q34D	0.13 ± 0.01	0.3 ± 0.04	0.14 ± 0.04
Q34E	0.15 ± 0.01	0.38 ± 0.06	0.08 ± 0.01
Q34F	62.72 ± 1.60	461.15 ± 34.45	46.64 ± 4.17
Q34G	0.24 ± 0.02	0.41 ± 0.15	0.24 ± 0.02
Q34H	0.24 ± 0.06	0.42 ± 0.04	0.21 ± 0.03
Q34I	217.59 ± 16.26	132.91 ± 11.94	242.27 ± 6.41
Q34K	0.08 ± 0.02	6.43 ± 0.11	0.07 ± 0.01
Q34L	90.96 ± 9.53	45.09 ± 2.39	93.5 ± 5.19
Q34M	47.24 ± 6.30	26.39 ± 2.67	58.36 ± 1.46
Q34N	0.15 ± 0.06	0.36 ± 0.06	0.11 ± 0.03
Q34P	0.07 ± 0.01	0.07 ± 0.01	0.07 ± 0.01
Q34R	0.07 ± 0.01	0.3 ± 0.11	0.08 ± 0.02
Q34S	1.73 ± 0.09	0.99 ± 0.16	1.00 ± 0.03
Q34T	9.49 ± 0.63	4.65 ± 0.39	17.92 ± 0.76
Q34V	656.29 ± 41.21	565.91 ± 89.03	1034.64 ± 24.27
Q34W	108.76 ± 25.32	5.64 ± 0.27	10.96 ± 0.65
Q34Y	96.21 ± 11.07	9.19 ± 1.17	24.16 ± 0.92

patterns in changes of strength of interaction (Figure 4-4 and Table 4-3). A similar interaction profile is observed with each of the three response regulators. The following pattern is evident when looking at the graph. Mutation of residue 34 on YPD1 from glutamine to a hydrophobic residue dramatically enhances (up to 1000-fold) the interaction of YPD1 with each of the three response regulator domains, while mutation to a polar or charged residue disrupts the interaction. The mutation resulting in the highest level of enhanced interaction was Q34V. This mutant displayed a 656-, 566- and 1035-fold enhancement in interaction with SLN1-R1, SSK1-R2 and SKN7-R3, respectively (Table 4-3). Trends from this interaction assay seem to follow the hydrophobicity scale determined by Kyte and Doolittle (Kyte & Doolittle, 1982). In this scale of hydrophobicity, amino acid residues are ranked according to physiochemical properties.

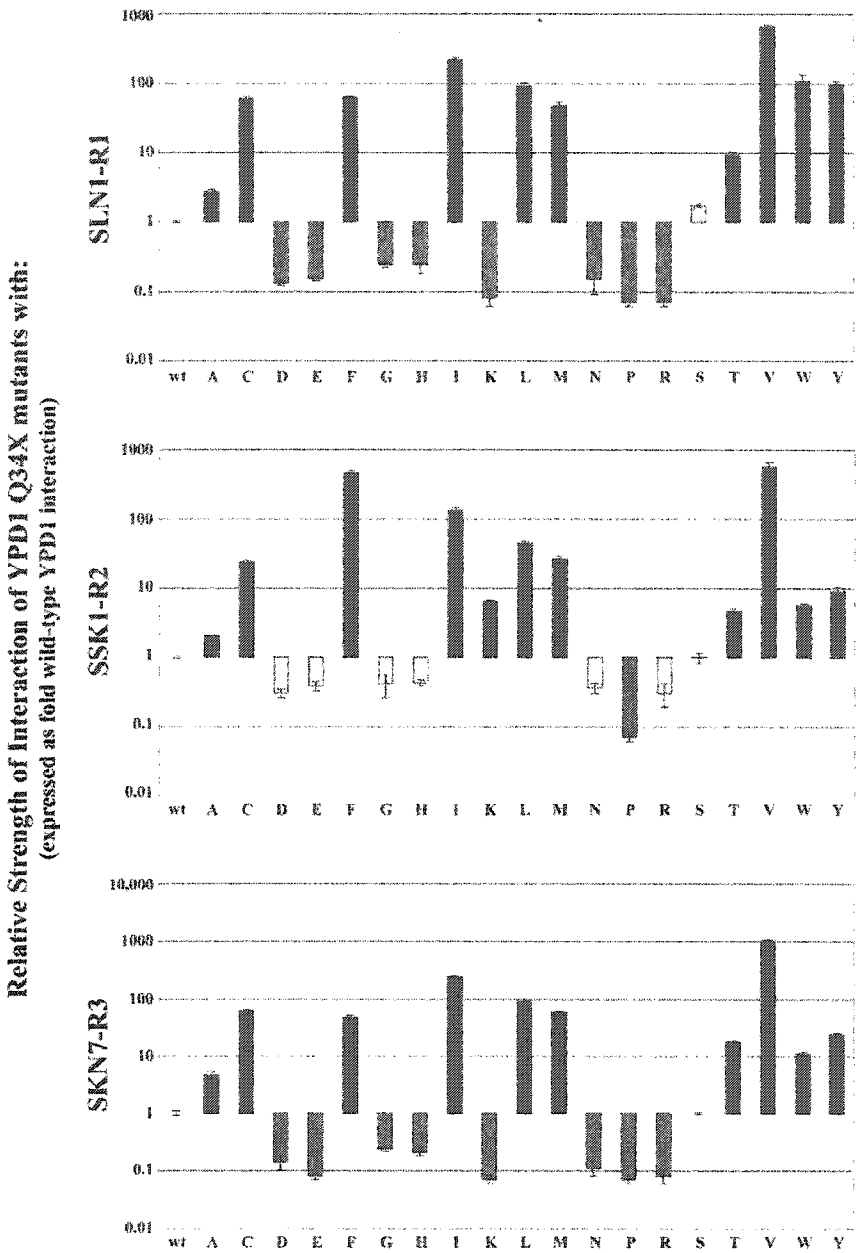

Figure 4-4

Yeast Two-Hybrid Results of Q34 Random Mutants. A graph of the yeast two-hybrid screens between YPD1 Q34 mutants and each response regulator domain was constructed. Mutants severely disrupting or moderately disrupting the interaction with the response regulator are colored red and yellow respectively. Mutants resulting in an enhanced interaction with the response regulator are colored blue. Note the Y-axis shows strength of interaction in log scale. Bars above the line marked 1 indicate an enhanced interaction between the protein pair and those below indicate a disrupted interaction of the protein-pair.

According to the scale isoleucine, valine and leucine have the highest level of hydrophobicity. Coincidentally, mutation of Q34 to any of these three amino acids results in the greatest enhanced interaction in the yeast two-hybrid screens with each response regulator. Amino acids classified as moderately hydrophobic (phenylalanine, cystine, methionine, and alanine) also display an enhanced interaction, although the extent of enhancement is not as great as that observed with the isoleucine, valine and leucine mutants. Amino acids that are charged or polar appear to disrupt the interaction of YPD1 with the response regulators. Kyte and Doolittle list seven amino acids (histidine, asparagine, glutamine, aspartate, glutamate, lysine, and arginine) that fall into this classification. With the obvious exception of glutamine, all mutations of Q34 to these amino acids resulted in disruption of the interaction of YPD1 with the response regulator. Agreement between the yeast two-hybrid results and the Kyte and Doolittle hydrophobicity scale tends to break down for residues that are slightly hydrophobic/hydrophilic (glycine, threonine, serine, tryptophan, tyrosine, and proline). However, a pattern was observed between the results from the yeast two-hybrid assay and the side chain volume of these residues. Q34 mutants that have a small side chain volume, glycine and proline, disrupted the interaction of YPD1 with the response regulators. Conversely, residues with a large side chain volume (threonine, tryptophan, and tyrosine) resulted in an enhanced interaction with the response regulators. The mutation of Q34 to serine displayed a near wild-type interaction with YPD1 in the yeast two-hybrid screens. Coincidentally, the side chain volume of serine is between the other groups of residues described. It appears that both hydrophobicity and side chain volume at this position on the surface of YPD1 affect binding to response regulators.

4.2.3 Analysis of YPD1 E58 Mutants

Since E58A resulted in a different phenotype in each of the response regulator interaction screens, it was thought that this residue may contribute to specificity for response regulators. This position was randomly mutated to further investigate the effect of residue type on the interaction of YPD1 with the response regulators. Overall, results from the interaction screen of E58 mutants were not as dramatic as those observed in the Q34 interaction screen (Figure 4-5, Table 4-4). The greatest level of enhancement any of the screens was 6.7-fold higher than the wild-type interaction.

The interaction screen between the YPD1 E58 mutants and SLN1-R1 reveals only one mutation (E58A) that resulted in an enhanced phenotype (Figure 4-5, Table 4-4). Several mutants resulted in a severely disrupting phenotype (E58F, E58G, E58H, E58K, E58P, E58R, E58S, and E58T), while four each were classified as moderately disrupting (E58M, E58N, E58V, and E58Y) or near wild-type (E58D, E58I, E58L, and E58W). Based on the polarity and size effect observed in the Q34 mutant, it was speculated that the mutation of E58 to aspartate, a slightly smaller, negatively charged residue, would maintain the same level of interaction with the response regulator. This was confirmed with the results of the yeast two-hybrid screen. However, further analysis of the results revealed no other pattern between chemical properties or volume of the amino acid residue and strength of interaction in the yeast two-hybrid assay.

One enhanced interaction (E58Y) was observed between the YPD1 E58 mutants and SSK1-R2. Only four mutants (E58H, E58P, E58R, and E58S) resulted in a severe disruption of interaction with SSK1-R2. There were five mutants that displayed a moderately disrupting phenotype (E58A, E58F, E58G, E58K, and E58T) and six that

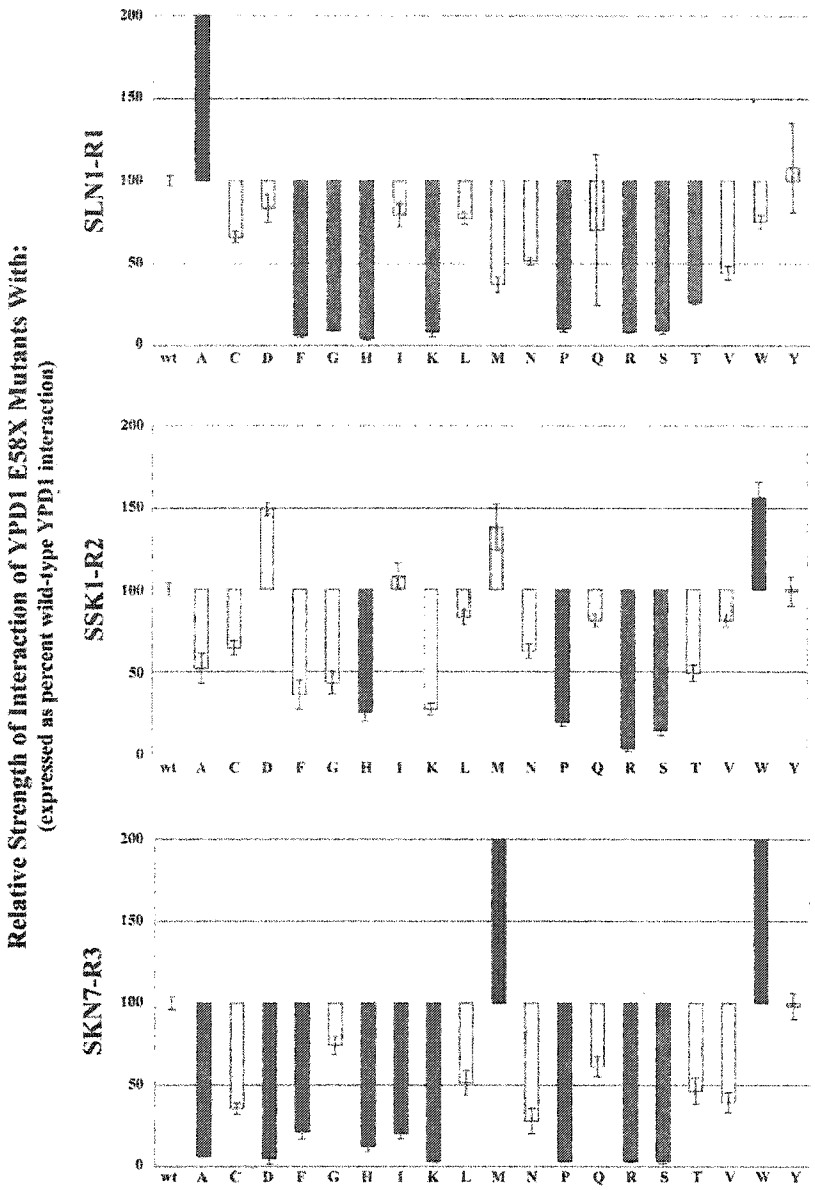

Figure 4-5

Yeast Two-Hybrid Results of E58 Random Mutants. A graph of the yeast two-hybrid screens between YPD1 Q34 mutants and each response regulator domain was constructed. Mutants severely disrupting or moderately disrupting the interaction with the response regulator are colored red and yellow respectively. Mutants resulting in an enhanced and near wild-type interaction with the response regulator are colored blue and green, respectively. Bars above the line marked 100% indicate an enhanced interaction between the protein pair and those below indicate a disrupted interaction of the protein pair.

Table 4-4
YPD1 E58X-Response Regulator
Yeast Two-Hybrid Interactions

	Percent Interaction with:		
Ypd1 Mutant	SLN1-R1	SSK1-R2	SKN7-R3
wild-type	100 ± 3	100 ± 4	100 ± 4
E58A	671 ± 24	52 ± 9	6 ± 0
E58C	66 ± 4	64 ± 4	35 ± 3
E58D	83 ± 8	149 ± 4	5 ± 4
E58F	6 ± 1	36 ± 9	21 ± 4
E58G	9 ± 1	43 ± 7	74 ± 6
E58H	4 ± 1	25 ± 6	12 ± 3
E58I	79 ± 7	108 ± 8	20 ± 3
E58K	8 ± 3	27 ± 4	3 ± 1
E58L	77 ± 3	83 ± 4	51 ± 8
E58M	37 ± 5	138 ± 14	220 ± 16
E58N	51 ± 2	62 ± 5	28 ± 8
E58P	10 ± 2	19 ± 3	3 ± 0
E58Q	70 ± 45	81 ± 4	61 ± 6
E58R	8 ± 1	3 ± 2	3 ± 0
E58S	9 ± 2	14 ± 3	3 ± 1
E58T	26 ± 1	49 ± 5	46 ± 8
E58V	44 ± 4	81 ± 4	39 ± 6
E58W	75 ± 4	156 ± 10	215 ± 19
E58Y	108 ± 27	99 ± 9	98 ± 8

displayed a wild-type phenotype (E58D, E58I, E58L, E58M, E58V, and E58W). In this interaction screen it appears that mutation of E58 to a polar or positively charged residue disrupts the interaction with SSK1-R2. The only exceptions to this observation are E58D and E58Y. While it was expected that mutation of E58 to aspartate would have a similar interaction as the wild-type interaction, it was unexpected that mutation to tyrosine would have an enhanced effect. Tyrosine is an aromatic amino acid with a large side-chain volume and a terminal hydroxyl group. The oxygen of the hydroxyl group may mimic the interaction of glutamate with the corresponding amino acid on the response regulator.

The interaction profile between the YPD1 E58 mutants and SKN7-R3 is very different than that observed with the other two response regulators. In this interaction screen that were two mutants (E58M and E58Y) that showed an enhanced interaction

phenotype, five (E58G, E58L, E58Q, E58T, and E58V) with a moderately disrupting phenotype, nine (E58A, E58D, E58F, E58H, E58I, E58K, E58P, E58R, and E58S) with a severely disrupting phenotype. Only one mutant (E58W) displayed a near wild-type phenotype. Thus, in this interaction screen nearly all mutations resulted in a loss of interaction with SKN7-R3. The two residues that displayed an enhanced interaction phenotype have neutral charges and bulky side chains that contain atoms with lone pairs of electrons near the end of the side chain. No other pattern in the data was observed.

4.3. Discussion

4.3.1 Comparison of Wild-Type YPD1/Response Regulator Interactions

I have examined the relative strength of interaction between YPD1 and each of the three *S. cerevisiae* response regulator domains using the yeast two-hybrid system. The results showed that YPD1 had the greatest level of interaction with the regulatory domain of SSK1. This interaction was about three-fold stronger than the interaction observed between YPD1 and the other two response regulator domains, SLN1-R1 and SKN7-R3. This is consistent with previously reported data that showed preferential phosphotransfer between YPD1 and SSK1-R2 (F. Janiak-Spens, unpublished observations) as well as a detectable complex in native gel shift assay only with the YPD1/SSK1-R2 complex in *in vitro* assays (Janiak-Spens *et al.*, 2000). While a YPD1/SLN1-R1 and a YPD1/SKN7-R3 complex could not be detected in native gel shift assays, they were detected using the yeast two-hybrid system. One reason for this observation here could be the sensitivity level of the two assays. The strength of protein-

protein interactions in the yeast two-hybrid assay is measured through transcription of a reporter gene, *lacZ*. The level of *lacZ* expression was determined using a liquid β-galactosidase assay that permits detection of low levels of β-galactosidase *in vivo*. The yeast two-hybrid system is also capable of detecting transient interactions between proteins. Proteins need only to associate briefly for transcription of the *lacZ* gene to occur. Native gel shift assays, however, require the interaction of the proteins in a complex to be stable throughout the electrophoresis time period. Weakly interacting proteins and/or proteins that only associate transiently, as apparently YPD1 and SLN1-R1 or SKN7-R3 do, would not be expected to be detectable.

4.3.2 Comparison of YPD1/Response Regulator Binding Interfaces

YPD1 alanine mutants created for the yeast two-hybrid screen with SSK1-R2 were also screened for loss of interaction with SLN1-R1 and SKN7-R3 respectively. Results from the screens revealed that YPD1 uses the same overall surface to bind all three response regulators. This surface on YPD1, located between H64 and the αA helix, was also found to contain a hydrophobic patch at its center. Furthermore, it was previously speculated that residues at the periphery of the hydrophobic patch contribute to specificity for the binding of a particular response regulator.

Comparison of the results of the two-hybrid screens reveals ten residues (E16, M20, D21, F27, L31, D60, F65, G68, S69, and L73) on the surface of YPD1 that are implicated in binding all three response regulator domains. These residues are located in a stripe along the surface of YPD1 and are located on the αA, αB and αC helices. Of the ten residues that comprise the core binding site six are hydrophobic and four are polar.

Comparison of these results to the theoretical model of a complex between YPD1 and the bacterial response regulator CheY proposed by Qingping Xu (Porter *et al.*, 2003), indicates that the majority of interactions of these core response regulator binding residues are to the α1 helix of CheY. The remaining interactions are observed in contacts to the β5-α5 and the β3-α3 loops of CheY.

Several other residues were observed to be involved in interactions with one or two response regulator domains. These residues were found to contribute to the specificity of interaction with the response regulator domains. These residues are located on either side of the stripe of core response regulator binding residues. Mapping of the location of these residues on the surface of YPD1 to the previously mentioned YPD1/CheY theoretical complex shows that these residues make contact to active site loops on the surface of the response regulator. When compared to other response regulator sequences, these loops (β1-α1, β3-α3 and β4-α4) are more variable in sequence composition and thus are probably responsible for making specific interactions with YPD1.

4.3.3 Site-Specific Enhanced Interaction Mutants.

Mutation of several residues resulted in an enhanced interaction phenotype. This may due to either a reduction in steric hindrence by the mutant residue or an expansion of the hydrophobic patch on the surface of YPD1. To test this theory site-specific random mutagenesis was performed at two locations on the surface of YPD1. The first site, Q34, was selected because it was found to have an enhanced interaction phenotype in the two-hybrid screen with all three response regulators, SLN1-R1, SSK1-R2 and SKN7-R3. The

other site on the surface of YPD1, E58, displayed three different interactions with the three response regulator domains in the yeast two-hybrid screens.

Results from the screen of the Q34 mutants showed that mutation of this residue to a more hydrophobic residue increased the strength of interaction between YPD1 and all response regulators. Q34 is located at the periphery of the hydrophobic patch on the surface of YPD1 on the B helix. Substitution at this location to a hydrophobic residue will extend the hydrophobic patch on YPD1, thereby increasing the surface area available for general interaction with the response regulators.

Side chain volume also plays an important role in determining the of strength of interaction between the two proteins. YPD1 Q34 mutants that have approximately the same hydrophobicity displayed stronger interactions with the response regulators when the side chain volume of the mutants was larger. This observation suggests that while hydrophobicity is the determining factor of strength of interaction with response regulators at this location, residues with larger side chain volume can also serve to extend the hydrophobic surface at this location.

While hydrophobicity and side chain volume can explain the trend in protein-protein interactions between the response regulators and YPD1 Q34 mutants, no such trend was observed with the library of YPD1 E58 mutants. It is important to note that E58 is not located near the hydrophobic patch on the surface of YPD1. However, data from the E58 random mutant screens could be used in *in vivo* assays to investigate the effects of altering the flow of phosphate in the two-component system.

4.3.4 Summary

Through alanine-scanning mutagenesis coupled to a yeast-two hybrid analysis, the response regulator binding site has been located on the surface of YPD1. Comparisons of data obtained from interaction screens between YPD1 and each of the three response regulator domains in *S. cerevisiae* revealed that, in general, the same surface on YPD1 is used for all three response regulators. Ten residues on the surface of YPD1 were identified as being involved in mediating contacts to all three response regulators and thus make up the core response regulator binding surface. Residues located on either side of the core residues are involved in making contacts to specific response regulators. We speculate these residues contribute to the specificity of the protein-protein interactions. Comparison of the results of the yeast two-hybrid screens with the YPD1/CheY theoretical complex shows that the core residues make contact to residues from the α1 helix of CheY. In contrast, residues contributing to specific interactions with a response regulator mainly make contact to the flexible active site loops near the site of phosphorylation.

5. Structural Analysis of the YPD1/SLN1-R1 Complex

5.1. Introduction

Two complementary approaches were used to investigate the interaction between YPD1 and the response regulator domains in *S. cerevisiae*. Previous chapters have focused on yeast two-hybrid analysis of wild-type and mutant YPD1 with each of the response regulator domains. It was found that the response regulator binding site on the surface of YPD1 between the site of phosphorylation, H64, and the αA helix (Porter *et al.*, 2003). This binding surface is composed of a large hydrophobic patch surrounded by polar and charged residues at the periphery. Each of the three response regulators in *S. cerevisiae* used this surface, to varying degrees, for interactions with YPD1 (Chapter 4). Residues within the hydrophobic patch are highly conserved in other HPt domains from other organisms (Porter *et al.*, 2003).

Concurrent to the yeast two-hybrid assays, work aimed at co-crystallization of YPD1 with any one of the response regulator domains was being attempted by members of our laboratory. Attempts to co-crystallize the SLN1-R1 domain with YPD1 were successful (Chooback & West, 2003). Thus, information regarding specific protein-protein contacts could now be obtained at an atomic level. While the structure of YPD1 was previously known, no direct structural information about any of the response

regulator domains involved in osmoregulation in *S. cerevisiae* was known. However, based on sequence and functional homology it is speculated that the structure of the yeast response regulator domains would be similar to CheY.

In this chapter, I will provide a detailed analysis of the SLN1-R1/YPD1 co-crystal structure. This structure allowed us not only to visualize the SLN1-R1 response regulator domain but also to carry out a detailed analysis of the protein-protein interface between YPD1 and SLN1-R1. Additionally, due to the high structural homology observed in HPt proteins and response regulator domains, we demonstrated that this complex can serve as a model for interactions between other HPt-response regulator complexes.

5.2. Results

5.2.1 Structure of the Complex

Co-crystallization of the YPD1/SLN1-R1 complex yielded crystals in two different space groups under similar crystallization conditions (Chooback & West, 2003). The previously solved YPD1 structure (Xu & West, 1999) was used as a search model and the structure of the complex was determined by molecular replacement (Carter & Sweet, 1997). The $P2_12_12_1$ crystal form contained only one complex in the asymmetric unit, while the $P3_2$ crystal form contained six complexes in the asymmetric unit. The structures of each crystal form were solved and refined to a resolution of 2.3 Å and 2.1 Å for the models obtained in the $P2_12_12_1$ and $P3_2$ space groups, respectively (Figure 5-1) (Xu *et al.*, 2003).

No significant differences were observed between the structures of the individual proteins in either crystal form. Moreover, the structure of YPD1 in each complex

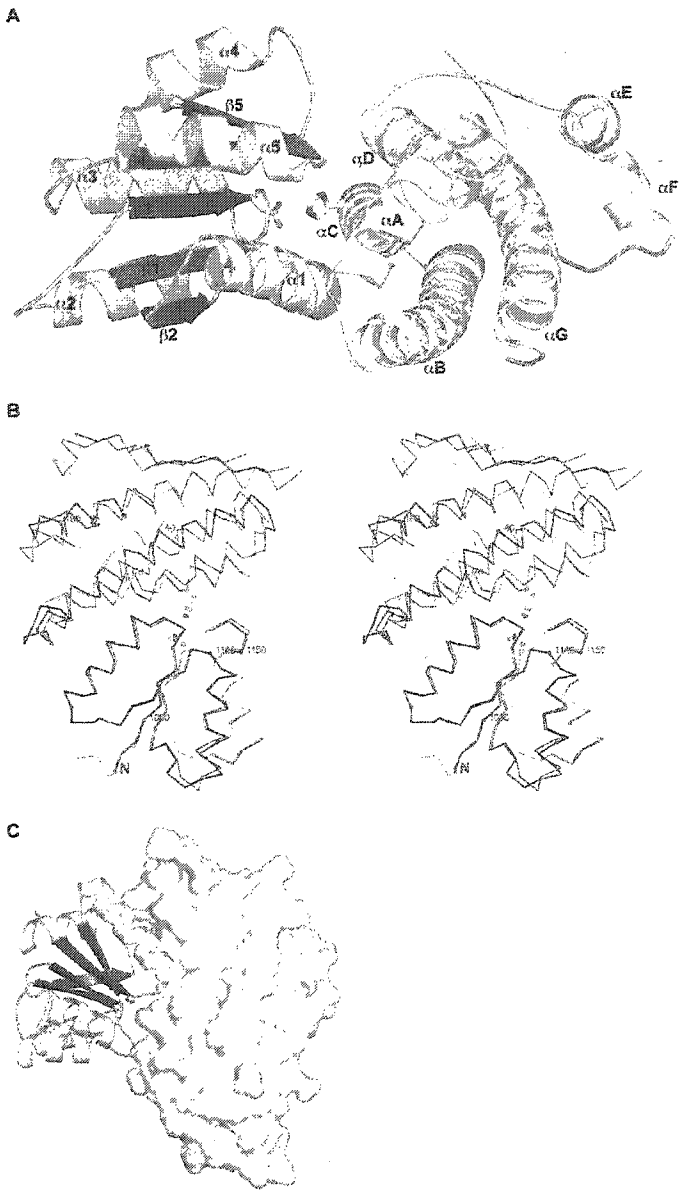

Figure 5-1. Co-Crystal Structure of the YPD1/SLN1-R1 Complex from *S. cerevisiae*.

A. Ribbon diagram of the complex. The fold of the SLN1-R1 domain is similar to all other known response regulator structures. A central five-stranded β-sheet (magenta) comprises the core of the protein. The structure of the HPt protein YPD1 is shown in yellow. The two phosphorylatable active site residues, D1144 of SLN1-R1 and H64 of YPD1, are displayed in stick model.

B. Backbone overlay of the complex in the two crystal forms. A stereoview of the structural alignment of the two crystal forms reveals a displacement of YPD1 relative to SLN1-R1 from the $P2_12_12_1$ (blue) to the $P3_2$ (red) crystal form.

C. Surface complementarity of the complex. A 90° rotation of the complex from the view shown in (B) displays the molecular surface of YPD1 and a ribbon representation of the SLN1-R1 domain, which highlights the surface complementarity of the complex. Figure taken from (Xu *et al.*, 2003).

displays no significant difference from the previously determined structure of YPD1 (r.m.s. deviation of 1.12 Å and 0.56 Å for the $P2_12_12_1$ and $P3_2$ complex, respectively).

The regulatory domain of the SLN1 hybrid sensor kinase consists of 136 residues (residues 1084-1220) and is located at the C-terminus of the molecule. The structure of the SLN1-R1 domain as solved in the co-crystal structure displays the same overall tertiary fold $(\beta\alpha)_5$ as all other response regulators solved to date (Robinson *et al.*, 2000; Stock *et al.*, 2000; West & Stock, 2001). The core of the protein is a five-stranded parallel β-sheet surrounded by five α-helices. Two α-helices are located on one face of the β-sheet while three α-helices are located on the opposing face. The site of phosphorylation, D1144, is situated at the C-terminus of β3 and is shielded from solvent by loops connecting the C-terminus of the β-strands to the α-helices.

Structural alignment of SLN1-R1 with the prototypical response regulator CheY from *E. coli* revealed an r.m.s. deviation of only 1.27 Å for 117 aligned Cα atoms (Volz & Matsumura, 1991). The major distinction between the two structures is the length of the α5 helix, which is five residues shorter in the SLN1-R1 structure. Residues located at the C-terminus of the SLN1-R1 domain (1211-1220) form an extended loop displaying no secondary structure. Backbone conformations of the central β-sheet and loops in and around the active site are highly conserved, while greater sequence and structural variability exists for the loops on the side of the molecule opposite from the active site. These loops connect the C-terminus of the α-helices to the β-strands and are located away from the protein-protein interface. Three loops that comprise the active site (β1-α1, β2-α2 and β3-α3) exhibit greater structural conservation (i.e. lower r.m.s.d.) than other loops in the same area (β4-α4, β5-α5).

Though the regulatory domain of SLN1-R1 is the first fungal response regulator structure solved, its tertiary structure is similar to that of bacterial response regulator domains and the response regulator ETR1 from the plant *Arabadopsis thaliana* (Baikalov *et al.*, 1996; Birck *et al.*, 1999; Djordjevic *et al.*, 1998; Djordjevic & Stock, 1998; Madhusudan *et al.*, 1996; Stock *et al.*, 1993; Volkman *et al.*, 1995). This suggests that structure and function of response regulator domains is evolutionary conserved across species (bacteria, fungi and plants).

The relative positioning of YPD1 to SLN1-R1 is such that the central β-sheet of SLN1-R1 is nearly perpendicular to the four-helix bundle of YPD1. The active site of SLN1-R1 containing the phosphorylatable aspartate (D1144) and the β-α loops are located in close proximity to H64 of YPD1 in both crystal forms. Superimposition of the structures in the two crystal forms reveals a displacement of SLN1-R1 relative to YPD1 (Figure 5-1 (B)). SLN1-R1 appears to have rotated approximately 10° around the α1 helix. As a result differences exist in the binding interface between the two crystal forms.

5.2.2 Analysis of the Protein-Protein Interface

As previously mentioned, there are slight but significant differences in the positioning of SLN1-R1 relative to YPD1 in the two different crystal forms. The SLN1-R1 domain appears to have rotated approximately 10° around the α1 helix from one crystal form to another. As a result, the binding interface in the $P2_12_12_1$ crystal form contains nearly 300 $Å^2$ more surface area than the interface in the $P3_2$ crystal form (Figure 5-2). Although there are fewer residues at the protein-protein interface in the $P3_2$ crystal form, the ratio of polar to non-polar residues at the interface remains constant

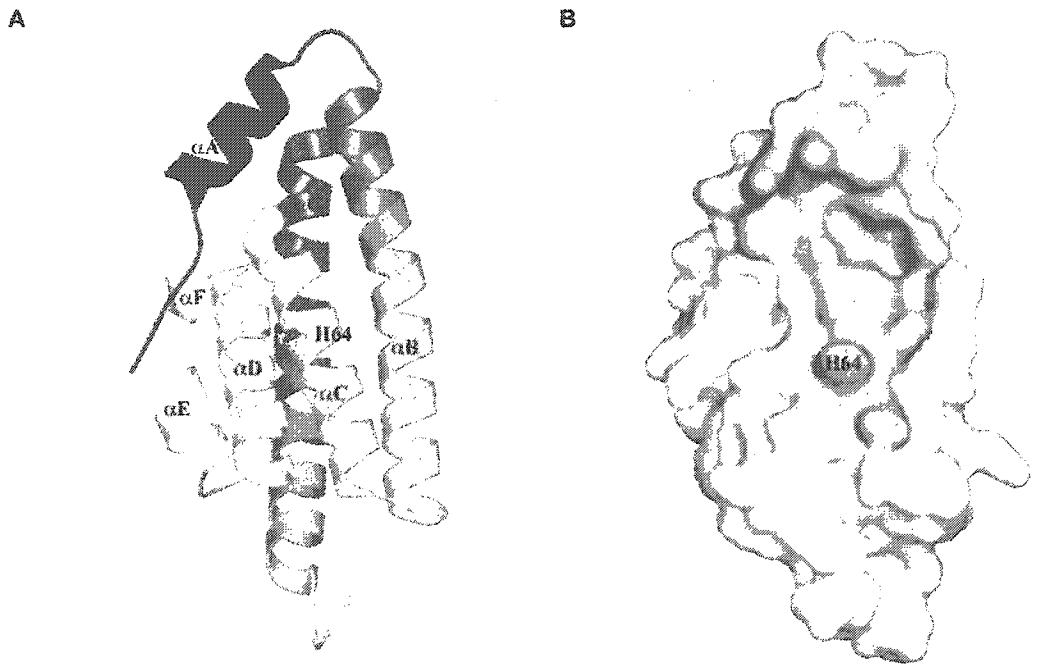

Figure 5-2. Surface Map of YPD1/SLN1-R1 Interactions in the $P2_12_12_1$ and $P3_2$ Crystal Forms.

A. A ribbon representation is shown in the same orientation as the surface view shown in (B). The site of phosphorylation, H64, is shown in stick model.

B. Surface view of YPD1 highlighting protein-protein interactions with the SLN1-R1 domain. The common surface used to bind SLN1-R1 in each crystal form is colored blue. Interactions specific to the $P2_12_12_1$ (yellow) or the $P3_2$ (green) crystal form are also colored. Figure taken from (Xu *et al.*, 2003).

(Table 5-1). Both complexes have protein-protein interfaces that are about 65% non-polar.

The binding interface of the $P2_12_12_1$ complex includes a buried patch of hydrophobic residues flanked on two sides by hydrophilic interactions. A small portion of the total surface area of YPD1 (11.5%) is buried in this complex representing 953 $Å^2$ of the YPD1 surface area. Consistent with the results from the yeast two-hybrid system, residues from the αA, the N-terminus of αB, the C-terminus of αC and the αD helix of YPD1 comprise the binding interface with SLN1-R1 (Table 5-1). As expected, several surface-exposed residues on αA (I13, E16, I17, and M20) make contact with the SLN1-

Table 5-1
YPD1/SLN1-R1 Intermolecular Contacts

A. *$P2_12_12_1$ complex*

YPD1 residue	Location	SLN1-R1 residue(s)	Location
*Hydrophobic interactions**			
Ile13	αA	Pro1196	β5-α5 loop
Ile17	αA	Val1102	α1
Met20	αA	Arg1105, Met1106, Leu1109	α1
Phe27	αB	Arg1105	α1
Leu31	αB	Val1102	α1
Ser69	αC	Val1098	α1
Ala71	αC	Pro1196	β5-α5 loop
Ala72	αC	Pro1196, Val1102	β5-α5 loop, α1
Glu83	αD	Phe1175	β4-α4 loop
Hydrogen-bond interactions†			
Glu16 Oε1	αA	Arg1199 N	α5
Met20 O	αA	Arg1105 Nη2	α1
Gln34 Nε2	αB	Glu1101 Oε2	α1
Gln34 Oε1	αB	His1097 Nδ1	α1
Gln38 Nε2	αB	Asn1096 Oδ1	β1-α1 loop
Gln38 Oε1	αB	Asn1096 Nδ2	β1-α1 loop
Asp60 Oδ1	αC	Gln1146 Nε2	β3-α3 loop
His64 Nε2	αC	Asp1095 Oδ2	β1-α1 loop
Phe65 O	αC	Asn1096 Nδ2	β1-α1 loop
Gly68 O	αC	Asn1099 Nδ2	α1
Gln86 Oε1	αD	Gln1146 Nε2	β3-α3 loop
Arg90 Nη2	αD	Gln1146 Oε1	β3-α3 loop

B. *$P3_2$ complex*

*Hydrophobic interactions**			
Ile13	αA	Pro1196	β5-α5 loop
Ile17	αA	Val1102	α1
Met20	αA	Arg1105, Met1106, Leu1109, Arg1199	α1, α5
Phe27	αB	Arg1105	α1
Leu31	αB	Glu1101, Val1102	α1
Gln34	αB	Val1098	α1
Ser69	αC	Val1098	α1
Hydrogen-bond interactions†			
Glu16 Oε1	αA	Arg1199 N	α5
Ser19 Oγ	αA	Arg1199 Nη2	α5
Met20 O	αA	Arg1105 Nη1, Arg1105 Nε	α1
Gln38 Nε2	αB	Asn1096 Oδ1	β1-α1 loop
Gln38 Oε1	αB	Asn1096 Nδ2	β1-α1 loop
His64 Nε2	αC	Asp1095 Oδ2	β1-α1 loop
Phe65 O	αC	Asn1096 Nδ2	β1-α1 loop
Gly68 O	αC	Asn1099 Nδ2	α1

*identified using the programs LigPlot (Wallace et al., 1995), SURFNET (Laskowski, 1991), and by visual inspection.

†identified using the HBPLUS algorithm as implemented in LigPlot (Wallace et al., 1995) with donor-acceptance cutoff distance of Š 3.2 Å.

Figure taken from (Xu, Porter et al. In Press).

R1 domain. A hydrogen bond exists between E16 of YPD1 and R1199 of SLN1-R1, while the remainder of the interactions between the αA helix of YPD1 and SLN1-R1 are hydrophobic in nature. The αB helix of YPD1 is also involved in making significant contacts with SLN1-R1 though these are mostly polar in nature. Two residues (F27 and L31) of αB make hydrophobic contacts to the response regulator while a total of four hydrogen bonds are observed between Q34 and Q38 to the response regulator. There are also a total of four hydrogen bonds observed between four residues of αC (D60, H64, F65, and G68) to SLN1-R1 along with three residues (S69, A71 and A72) displaying hydrophobic interactions. Interactions were also observed between residues of αD (E83, N86, and R90) and SLN1-R1. Each of the four helices of YPD1 involved in making contact with the SLN1-R1 domain contribute a significant portion of the surface at the protein-protein interface.

As expected a large part of the binding interface of the SLN1-R1 domain is composed of residues located in the β-α loops near the active site of the response regulator. Four loops (β1-α1, β3-α3, β4-α4 and β5-α5) were observed in making contact to YPD1. The remaining active site loop, β2-α2, is located at the edge of the interface, but makes no contacts to YPD1. The α1 helix of SLN1-R1 also makes contact to YPD1 and is positioned such that residues on the surface make contact to the hydrophobic patch on the surface of YPD1. Similar to the hydrophobic patch on the surface of YPD1 representing the core binding interface for the response regulator, the surface of the α1 helix of the SLN1-R1 domain represents the core binding interface for YPD1. This point is illustrated in Figure 5-3 where the binding interface of each protein

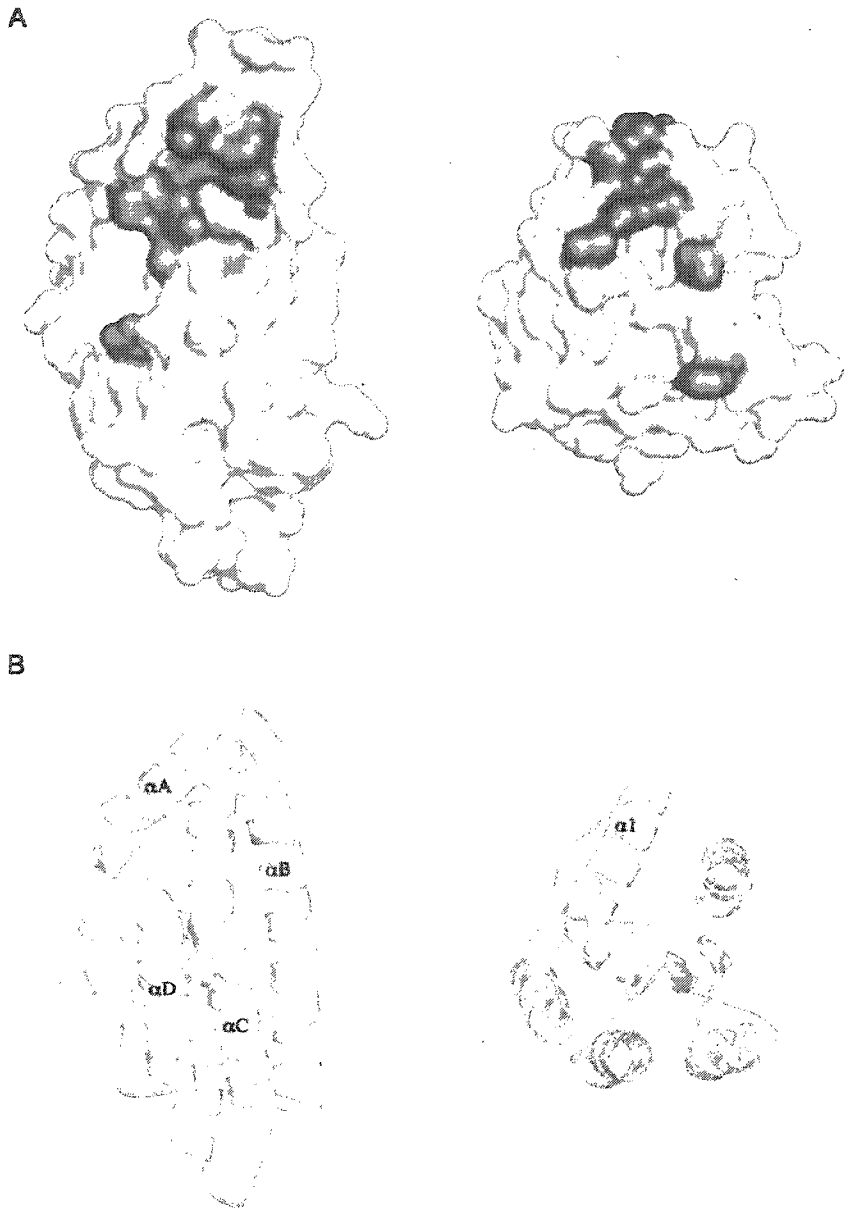

Figure 5-3. Surface Map of Protein-Protein Interactions Colored According to Chemical Properties.

A. The two molecules in the $P2_12_12_1$ crystal form were rotated 90° in opposite directions to show the buried surface of the complex. YPD1 is shown on the left while SLN1-R1 is showed on the right. The binding surfaces are colored according to their chemical properties. Surfaces displayed in grey represent hydrophobic interactions while surfaces colored green represent polar interactions.

B. The same view as in panel A is shown but the surface of the molecules is made transparent allowing the underlying secondary structure elements to be visualized. Active site residues are again shown in stick model. Figure taken from (Xu *et al.*, 2003).

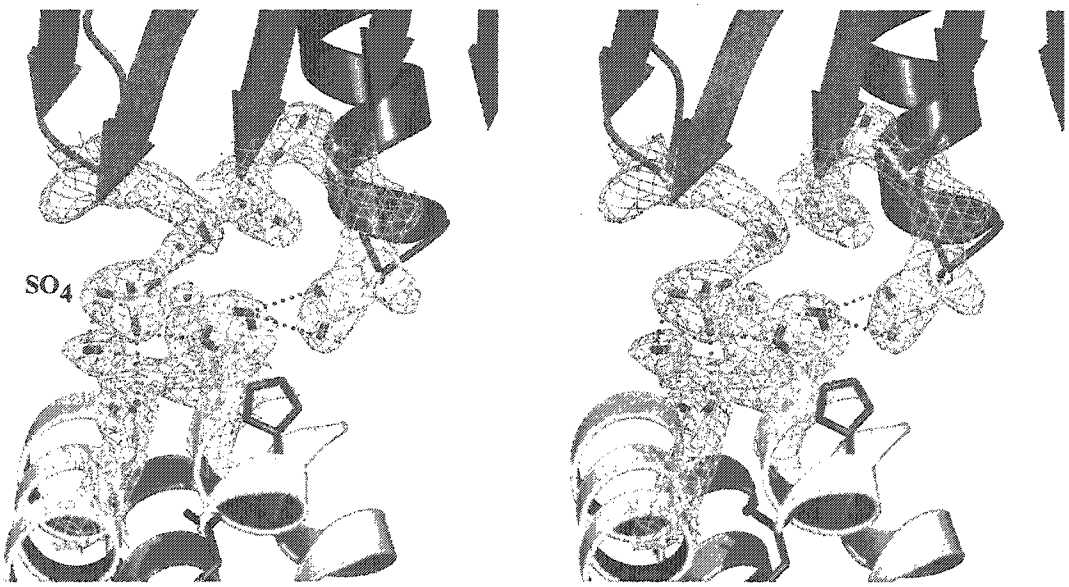

Figure 5-4. Active Site Arrangement of YPD1 and SLN1-R1 in Two Crystal Forms. An electron density map of the active site of the YPD1/SLN1-R1 complex in the $P2_12_12_1$ crystal from is displayed in stereoview. A structural alignment of the SLN1-R1 domain was performed and the structure of the $P3_2$ crystal form was overlaid onto the $P2_12_12_1$ crystal form. Helices C and D from YPD1 are shown for both the $P2_12_12_1$ crystal form (green) and the $P3_2$ crystal form (grey). The displacement of the C and D helices in the $P3_2$ crystal form highlights the conformational differences between the active sites in the two crystal forms. Figure taken from (Xu *et al.*, 2003).

in the complex is colored according to the type of interaction (hydrophobic or hydrophilic) and displayed over the secondary structure of the corresponding protein.

Slight but significant differences at the protein-protein interface are observed between the $P2_12_12_1$ and the $P3_2$ crystal forms. Due to the rotation around α1 of SLN1-R1, contacts observed between the β4-α4 loop of SLN1-R1 and αD of YPD1 in the $P2_12_12_1$ crystal form are not present in the $P3_2$ crystal form (Figure 5-2). As a result, the buried surface area is substantially reduced (from 953 $Å^2$ to 678 $Å^2$) in the $P3_2$ complex. In both complexes hydrophobic contacts between the hydrophobic patch on the surface of YPD1 and α1 of SLN1-R1 are preserved.

Another important distinction between the $P2_12_12_1$ and the $P3_2$ crystal forms is the distance of the site of phosphorylation, H64, in YPD1 to the active site of SLN1-R1.

H64 of YPD1 is closer and in a much better alignment with D1144 of SLN1-R1 for phosphoryl transfer in the $P2_12_12_1$ crystal form compared to the $P3_2$ crystal form (Figure 5-4). In the $P2_12_12_1$ complex, the Nε2 atom of H64 is 3.9 Å away from Oδ2 atom of D1144. However, in the $P3_2$ complex these atoms have moved 1.9 Å away from one another. The relative movement of the active sites away from each other in the $P3_2$ crystal form exposes the two active sites to solvent.

Further analysis of the protein-protein interface in each crystal form reveals a high degree of surface complementarity. A low gap index (discussed further in Chapter 6) of 2.26 and 2.53 was calculated for the co-crystal structures in the $P2_12_12_1$ and the $P3_2$ crystal forms respectively (Laskowski, 1995). The high degree of surface complementarity between the two proteins is an interesting feature of the complex due to the relatively low ratio (11.5 %) of buried surface area to total surface area of the complex. The low ratio of buried surface area to total surface area of the complex is consistent with complexes that are transient in nature (Nooren & Thornton, 2003).

5.3. Discussion

5.3.1 Comparison of the YPD1/SLN1-R1 Co-Crystal Structure to Yeast Two-Hybrid Results

The response regulator binding interface of YPD1 as revealed in the X-ray crystal structure correlates very well with the yeast two-hybrid data obtained between YPD1 and SLN1-R1 (Chapter 4). With each method, the response regulator binding site was identified as the surface area between H64 and the αA helix of YPD1. Residues from

YPD1 involved in response regulator binding that were identified in each study are located on αA (E16, S19 and M20), αB (F27, L31, and Q34), αC (D60, F65, G68, and S69), and αD (E83). A small number of residues on the surface of YPD1 were observed in interactions with SLN1-R1 in the co-crystal structure that were not classified as severely disrupting in the yeast two-hybrid screen. Two residues I13 and I17 make hydrophobic interactions with the response regulator and displayed moderate and wild-type interactions in the two-hybrid analysis. It is interesting to note that both of these residues are located on the edge of the protein-protein interface and were identified as being involved in interactions with SSK1-R2 and SKN7-R3. Another residue, R90, was observed to make hydrogen bond interactions in the $P2_12_12_1$ crystal form but was not identified in the two-hybrid assay. This residue is also located at the edge of the protein-protein interface and is only involved in interactions in one crystal form. Two other residues, A71 and A72, were not tested in the yeast two-hybrid system due to the fact that only non-alanine and glycine residues were selected for mutation. It was speculated by sequence alignment that these residues were involved in hydrophobic interactions in the core of the protein-protein interface. The involvement of the two residues in protein-protein interactions was confirmed by the X-ray structure of the YPD1/SLN1-R1 complex in the $P2_12_12_1$ crystal form. Finally, Q38 was observed to make a hydrogen bond to the SLN1-R1 domain in the crystal structure. Yeast two-hybrid data showed a moderate disruption (35% wild-type) of interaction with SLN1-R1 for the Q38A YPD1 mutant. This is near the cutoff (25% wild-type interactions) for mutations classified as severely disrupting.

There were also three residues on the surface of YPD1 that were identified by the yeast two-hybrid system as being involved in interactions with SLN1-R1 that were not observed in the co-crystal complex. Those residues (D21, L73 and W80) are located just outside the interaction surface but adjacent to a residue that is involved in response regulator interaction. Two possibilities exist for this result. First, mutation of these residues to a smaller alanine residue could allow greater side chain movement in adjacent surface residues. Second, two crystal forms have been observed with the YPD1/SLN1-R1 complex. This may suggest that there are multiple modes of binding between YPD1 and SLN1-R1. There could be an additional binding mode where SLN1-R1 is shifted in such a way that these residues become part of the protein-protein interface.

5.3.2 Specificity Determinants of Protein-Protein Interactions.

In Chapter 4, residues on the surface of YPD1 involved in interactions with one or more of the response regulators were put into one of two classifications, (i) those which were observed in making contacts with each of the three response regulators (core response regulator binding residues), (ii) and those which were observed in interactions with one, or a combination of two response regulators (specific response regulator binding residues). A total of 10 residues made up the core response regulator binding surface as identified by the yeast two-hybrid studies. Six residues are hydrophobic in nature (M20, F27, L31, F65, G68 and L73) and are flanked by four polar residues (E16, D21, D60 and S69). Eight of the ten core response regulator binding residues were observed in making contacts to the SLN1-R1 domain in the X-ray structure. Two residues, D21 and L73, were not observed in the crystal structure. The cutoff for hydrophobic interactions in the programs LigPlot and SURFNET is 4.0 Å (Wallace *et al.*,

1995). The distance between L73 of YPD1 and V1098 of SLN1-R1 is very near the cutoff values for hydrophobic interactions for these programs. It is possible that the result from the two-hybrid assay is valid and L73 represents a true interaction between YPD1 and SLN1-R1. Two residues that were speculated to be involved in YPD1-response regulator interactions by sequence alignment (A71 and A72) are also involved in making hydrophobic contacts. The two residues are located in the center of the hydrophobic surface and also should be classified as core response regulator binding residues.

Yeast two-hybrid analysis identified three residues on the surface of YPD1 (S19, W80 and E83) other than the core response regulator binding residues that are involved in interactions with SLN1-R1. These residues were determined to be involved in determining specificity for one response regulator over another. Yeast two-hybrid assays showed only one residue (S19) specific for interactions with SLN1-R1, while two residues (W80 and E83) were observed to be involved in interactions with SLN1-R1 and SKN7-R3. The YPD1 surface residue specific for SLN1-R1, S19, is involved in making a hydrogen bond to the Nη2 atom of R1199 on SLN1-R1 in the $P3_2$ complex. While no interaction was observed between W80 and SLN1-R1 in either crystal form, a hydrophobic contact was observed between E83 and F1175 of SLN1-R1.

5.3.3 Summary

The results from the yeast two-hybrid assays reported in the previous chapters are consistent with the co-crystal structures of the YPD1/SLN1-R1 complex. However, it appears that the results of the yeast two-hybrid system represent an average of the possible binding modes between YPD1 and the response regulators since some of the

mutants displaying a severely disrupting phenotype were only verified by interactions in one of the two crystal forms. For example, S19A was found to severely disrupt the interaction between YPD1 and SLN1-R1 in the yeast two-hybrid assay but contacts are only observed between S19 of YPD1 and SLN1-R1 in the $P3_2$ crystal form of the complex. Furthermore, the only discrepancy between the yeast two-hybrid results and the co-crystal structures is the classification of a few residues on the surface of YPD1 located near the edge of the binding interface with SLN1-R1. Again these differences could occur through several different scenarios. First, the original cut-off for the classification in the yeast two-hybrid system was set arbitrarily. Disruption of interactions fell into two categories, moderately disrupting at 26-75% of wild-type interactions and severely disrupting at below 25% of wild-type interactions. In order to resolve some of the discrepancies between the two-hybrid system and the solved structures of the complex, the cut-off value of severely disrupting mutants should be raised from 25% to around 35% of the wild-type interaction. Second, the fact that two crystal forms were observed under similar crystallization conditions suggests that there are multiple binding modes between YPD1 and SLN1-R1. It is possible that another binding mode exists that accounts for the remaining residues identified in the two-hybrid system that were not observed in the co-crystal structures. Finally, it is also possible that mutation of the residues affected the orientation of adjacent residues and this combined rearrangement resulted in a loss of interaction between the two proteins. However, information about the location of the response regulator binding site is still obtained in these cases.

6. Discussion of Protein-Protein Interactions

6.1. Introduction

Organisms must detect and respond to a wide variety of environmental cues. Two-component signal transduction systems have evolved as a means to convert signals at the cellular membrane into meaningful responses that allow the organism to adapt and survive. The modular design of these systems could allow for new signaling modules to divergently evolve through gene duplication. Bacteria, such as *E. coli* and *B. subtilis* possess 30-40 pairs of two-component systems each involved in regulating unique responses to stimuli (Mizuno, 1997). Given the abundance of two-component signaling systems in a particular organism, and the modular design of the two-component system, the question arises as to how each system can identify components found in a specific response pathway and interact with only proteins in that pathway? In essence, how is cross-talk avoided between distinct two-component systems?

The key to understanding the fidelity of two-component systems is studying the protein-proteins interactions involved in the phosphoryl transfer from one protein to another. Some systems have evolved to include additional modules thus forming a multi-step His-Asp phosphorelay. The protein-protein interactions that occur in two-component and the simplest multi-step phosphorelay systems involving a histidine

kinase, response regulator, and a HPt protein all involve interaction of a response regulator with a four-helix bundle from either the histidine kinase or the HP domain. The co-crystal structures of SLN1-R1/YPD1 (Xu *et al.*, 2003) and Spo0F/Spo0B (Zapf *et al.*, 2000) provide two similar but distinctive models of HPt protein interaction with their cognate response regulators. Further details about these interactions were elucidated through a study comparing the surface and the residues YPD1 uses to bind each of the three response regulator domains found in *S. cerevisiae* (Porter *et al.*, 2003). Given that two-component proteins of similar function (e.g. histidine kinases, response regulators or HPt proteins) have similar three-dimensional structures, information gained from the study of protein-protein interactions in the osmoregulatory signal transduction pathway of *S. cerevisiae* could be applied to two-component systems in other organisms. Furthermore, knowledge of the protein-protein interfaces in two-component systems could be utilized to develop inhibitors designed to disrupt these interactions. In this chapter I will discuss the principles of HPt protein-response regulator interactions using YPD1 as a model HPt protein.

6.2. Discussion

6.2.1 Survey of Protein-Protein Interfaces

Proteins can associate with one another through both covalent and non-covalent interactions (Jones & Thornton, 1996; Ofran & Rost, 2003). Covalent interactions can occur through linkage of sulfhydryl groups on the surface of the protein monomer subunits. The di-sulfide bond is a common mechanism for oligomerization. For proteins that must associate and dissociate rapidly, non-covalent interactions are the primary

means of interaction (Ho *et al.*, 2002; Pawson & Nash, 2000). Non-covalent dimerization of proteins also occurs through amino acid side chains located on the surface of a protein monomer, but these interactions only include hydrophilic and hydrophobic interactions.

Through studies involving insulin, trypsin and hemoglobin two basic tenets of protein-protein interactions were defined (Chothia & Janin, 1975). Stability of the protein-protein association is directly related to the hydrophobicity of the interface, and protein association is selectively determined by shape complementarity at the interface. The "classic" protein-protein interaction is defined as an interface dominated by a hydrophobic core with polar and charged residues forming a ring along the periphery of this core (Larsen *et al.*, 1998). It is believed that the initial or nonspecific interaction occurs through the association of the hydrophobic surfaces while orientation of the two proteins occurs through hydrogen bonding and salt-bridges located on the edge of the hydrophobic patch.

A visual survey of 136 dimeric proteins in the Protein Data Bank (PDB) revealed that only one-third of the protein complexes adhered to the "classic" definition of protein-protein interactions (Larsen *et al.*, 1998). Great diversity exists among the remaining two-thirds of the protein complexes. Several interfaces have small patches of hydrophobic character with hydrogen bonds and water distributed throughout the interface. Thus, no hydrophobic core was formed that excluded water from the interface. Other protein complexes were interwoven and had convoluted interfaces. It is thought that these protein chains associate while folding to form a stable dimer. The study revealed that the "classic" protein-protein interface represents only a minority of the interacting proteins (Larsen *et al.*, 1998).

As discussed in Chapter 3, the surface of YPD1 contains a large cluster of hydrophobic residues between His64 and the αA helix. The cluster of hydrophobic residues is surrounded by polar and charged residues at the periphery. Yeast two-hybrid screen results from the interaction between YPD1 and the response regulator domains of SLN1, SSK1 and SKN7 revealed that the hydrophobic patch on the surface of YPD1 is intimately involved in response regulator binding. The co-crystal structure of the YPD1/SLN1-R1 complex allowed, for the first time, to visualize the interaction of a monomeric HPt protein with its cognate response regulator. The protein-protein interface of the complex revealed that the interaction between YPD1 and SLN1-R1 adheres to the definition of a "classic" protein-protein interaction.

The size of the protein-protein interface is typically reported as the change in accessible surface area (ΔASA). In most cases the greater the ΔASA, the stronger the interaction between the two monomers. The ΔASA varies widely for homodimers and has an average value of 1685 $Å^2$ (Jones & Thornton, 1996). Heterodimers, as expected, on average have a smaller protein-protein interface (ΔASA of 1101 $Å^2$) (Jones & Thornton, 1996). This lower value can be explained by the more transient nature of the proteins that form heterodimers (Nooren & Thornton, 2003). For example, in signal transduction the rapid association and dissociation of two-component proteins is essential for a quick response to a potentially harmful change in environmental conditions. The change in ASA for the YPD1/SLN1-R1 complex is 953 $Å^2$, which is slightly lower than the average value reported for heterodimers. This suggests that the association of YPD1 with SLN1-R1 is relatively weak and is transient in nature. The lower value for ΔASA is not surprising given that upon phosphorylation YPD1 must dissociate from SLN1-R1 and

interact with and transfer a phosphoryl group to either SSK1 or SKN7 in order to elicit a timely response to changes in external conditions.

Surface complementarity also plays an important role in determining protein-protein interactions. One measure of surface complementarity is the gap volume defined by Laskowski (Laskowski, 1995; Laskowski *et al.*, 1993). The gap volume index is reported as the volume between the molecules (gap volume) divided by the accessible surface area at the protein interface. Protein complexes with a high level of complementarity at the interaction interface have a low gap volume index. Using the protein-protein interaction server (http://www.biochem.ucl.ac.uk/bsm/PP/server/) and the program SURFNET (Laskowski, 1995) a gap volume index of 2.26 was calculated for the YPD1/SLN1-R1 complex. This value is more similar to the average value reported for homodimers (2.20) than that of heterodimers (2.48) (Jones *et al.*, 2000; Jones & Thornton, 1996). While the interaction between YPD1 and SLN1-R1 is relatively weak when compared to the average ΔASA of heterodimers, the surface complementarity between the proteins is high. This is likely due to the fact that HPt proteins have evolved not only to rapidly transmit a signal from one response regulator to another, but have also evolved to distinguish between response regulators in a particular response pathway.

6.2.2 Comparison to the Spo0B/Spo0F Complex.

The co-crystal structure of the Spo0B/Spo0F complex from *Bacillus subtillus* was the first to illuminate interactions between an HPt protein and a response regulator (Figure 6-1A) (Zapf *et al.*, 2000). The structure of the HPt protein Spo0B reveals that it consists of two domains, an α-helical domain located at the N-terminus and a α/β domain

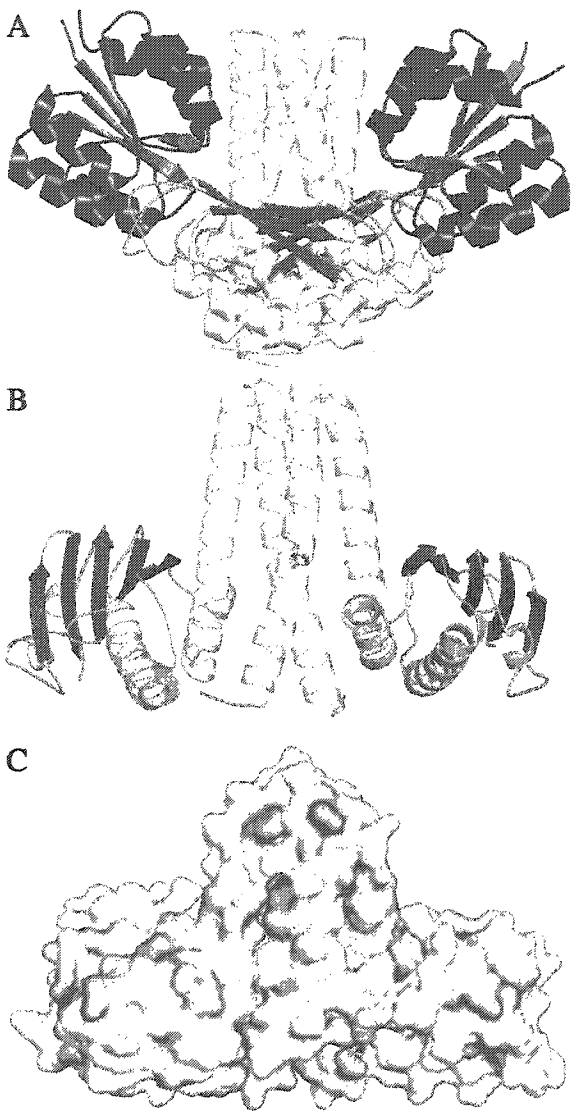

Figure 6-1

A. Spo0B/Spo0F Complex. The structure of the *B. subtilis* Spo0B/Spo0F complex is shown in ribbon representation. The response regulator Spo0F is shows in red and blue while the HPt Spo0B is shown in yellow magenta and cyan.

B. Spo0B Dimer. Spo0B forms a stable dimer. The four-helix bundle (yellow) contains the sites of phosphorylation (H30) and is flanked by an α/β domain at the C-terminus (magenta and cyan).

C. Surface Map of Spo0B. The surface of Spo0B was colored according to its chemical properties. Polar and changed residues are colored yellow, while hydrophobic residues are colored grey.

located at the C-terminus (Figure 6-1B). The helical domain at the N-terminus contains two α-helices with a hairpin turn. The C-terminal domain contains a 5-stranded β-sheet and three α-helices. The helices are located on one face of the β-sheet leaving the other face of the β-sheet exposed to solvent. The site of phosphorylation, H30, is located in the middle of α1 and, like that of YPD1, is completely exposed to solvent. To date, all known HPt proteins contain a four-helix bundle core with the site of phosphorylation in the middle of a helix. In Spo0B, the four-helix bundle is formed by dimerization of two Spo0B monomers. As a result of this dimerization, Spo0B has two phosphorylatable histidines and two flanking α/β domains. The structure of the response regulator, Spo0F, is similar to those of the other response regulator domains solved to date.

Spo0F is bound to Spo0B through a hydrophobic patch (approximately 1200 $Å^2$) found on the surface of the four-helix bundle of Spo0B (Figure 6-1C). The hydrophobic patch is located in the equivalent position to that of the patch on the surface of YPD1. Contacts seen between the α1 helix of the response regulator and the four-helix bundle of the HPt protein in the YPD1/CheY theoretical complex are also found in the co-crystal structure of Spo0B/Spo0F. However, there are important differences between the two complexes.

First, Spo0B must dimerize to form the four-helix bundle. Spo0B is the only HPt protein thus far known to dimerize. Second, results from the yeast two-hybrid assay clearly showed residues from the αA helix of YPD1 to be involved in protein-protein interactions with SSK1-R2. There is no helix in the Spo0B dimer that corresponds to αA in YPD1. However, the structure of another HPt protein, ArcB, does contain a helix corresponding to that of αA in YPD1. Moreover, a sequence alignment of other HPt

domains suggests that these proteins have a corresponding αA helix. In contrast, the two helices in Spo0B, α1 and α2, are extended by several helical turns. The surface created by these extensions is mainly hydrophobic in nature, and as a result allows Spo0B to use a surface similar to that of YPD1 to bind response regulator domains. Third, interactions are seen between Spo0F and the C-terminal α/β domain of Spo0B. Out of the 22 residues that make contact with Spo0B on the surface of Spo0F, 15 make contact to the four helix bundle of Spo0B (Varughese, 2002; Zapf *et al.*, 2000). The remaining 7 residues make contact to the flanking α/β domain that is unique to the Spo0B structure. A sequence alignment of other HPt proteins revealed no other HPt protein containing this motif . This structural motif is similar to the response regulator-binding domain (e.g. CheA P2 domain) found near the four-helix bundle in histidine kinases (Varughese *et al.*, 1998). Therefore, it appears that Spo0B evolved from a histidine kinase to function as an HPt domain. Finally, a structural alignment of the two co-crystal complexes displays weak structural alignment between YPD1 and Spo0B at the protein-protein interface (Figure 6-2). Several hydrophobic residues on the surface of YPD1 were identified as being important for formation of an HPt protein-response regulator complex. Additionally, a sequence alignment of YPD1 with other monomeric HPt proteins revealed these surface residues are conserved in other HPt proteins (Porter *et al.*, 2003). However, a structural alignment of the two co-crystal complexes shows that while similar interactions occur between the proteins in both complexes the arrangement of secondary structure elements as well as absolute positions of residues at the protein-protein interface differs in the two complexes (Figure 6-2).

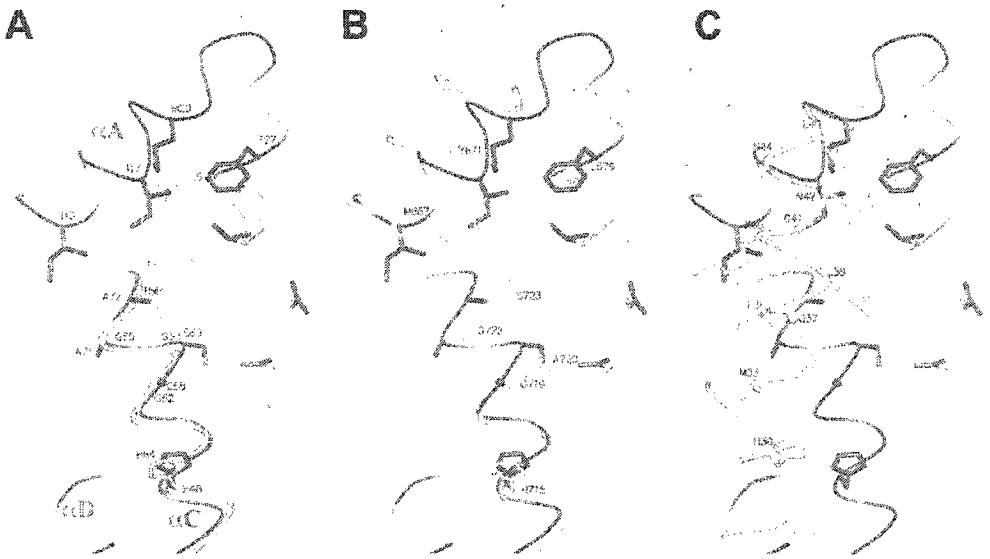

Figure 6-2
A. Alignment of YPD1 with CheA-P1. A structural alignment was performed between YPD1 (red) and the CheA-P1 domain (cyan) involved in chemotaxis in *E. coli*. The alignment highlights structurally conserved features in the response regulator binding site.
B. Alignment of YPD1 with ArcB^c. Another alignment was performed as above using ArcB^c (yellow) from *E. coli*.
C. Alignment of YPD1 with Spo0B. Response regulators in the two co-crystal structures were aligned and overlaid. The overlay of the HPt proteins reveals poor structural alignment between secondary structure elements of YPD1 and Spo0B.
(Figure from (Xu *et al.*, 2003))

The protein Spo0B is not a typical representative of the larger class of HPt proteins. The lack of an αA helix along with the fact that there is an additional response regulator binding interface makes it hard to justify the Spo0B/Spo0F complex as a typical model of HPt/response regulator domain protein-protein interactions. Nonetheless, this complex does display interactions that are consistent with the yeast two-hybrid assay. The hydrophobic patch located on the surface of Spo0B occupies an equivalent position to the patch on the surface of YPD1. This hydrophobic interaction may be a general binding characteristic of HPt proteins to response regulator domains with the speculation that specificity for cognate response regulators is determined by polar and charged residues located on the periphery of the hydrophobic patch.

6.2.3 Comparison of Yeast Two-Hybrid Results to *in vitro* Assays

Several *in vitro* methods for detecting protein-protein interactions were attempted with the aim of confirming the results obtained in the yeast two-hybrid screens. A complex between YPD1 and the phosphorylated SSK1-R2 domain was observed in native gel shift assays (Janiak-Spens *et al.*, 2000). However, using this method no complex could be observed between YPD1 and either SLN1-R1 or SKN7-R3. Nonetheless, one mutant from each of the four classifications in the yeast two-hybrid screen between YPD1 and SSK1-R2 were cloned into expression vectors, expressed and purified from an *E. coli* strain. Wild-type YPD1 or one of the YPD1 mutants from each interaction category were incubated in the presence of either phosphorylated or unphosphorylated SSK1-R2. The proteins were separated on a native polyacrylamide gel, the results were analyzed by Western blotting and the membrane was probed with anti-YPD1 or anti-SSK1-R2 antisera. Results from the assay show a detectable complex only in lanes containing wild-type YPD1 and the YPD1 mutant resulting in an enhanced interaction phenotype (I17A) (Figure 6-3). No interaction was observed between the severely disrupting mutant (E16A) or the moderately disrupting mutant (K67A). Furthermore, while a two-fold enhancement of interaction between YPD1 I17A and SSK1-R2 was observed in the yeast two-hybrid system, the relative amount of protein shifted in the native gel shift assay is unchanged. These results suggest that (i) the native gel shift assay is not sensitive enough to detect weak protein-protein interactions between YPD1 mutants and SSK1-R2, (ii) the assay is not quantitative, and (iii) small changes in affinity between YPD1 mutants and SSK1-R2 are unable to be detected in the native gel

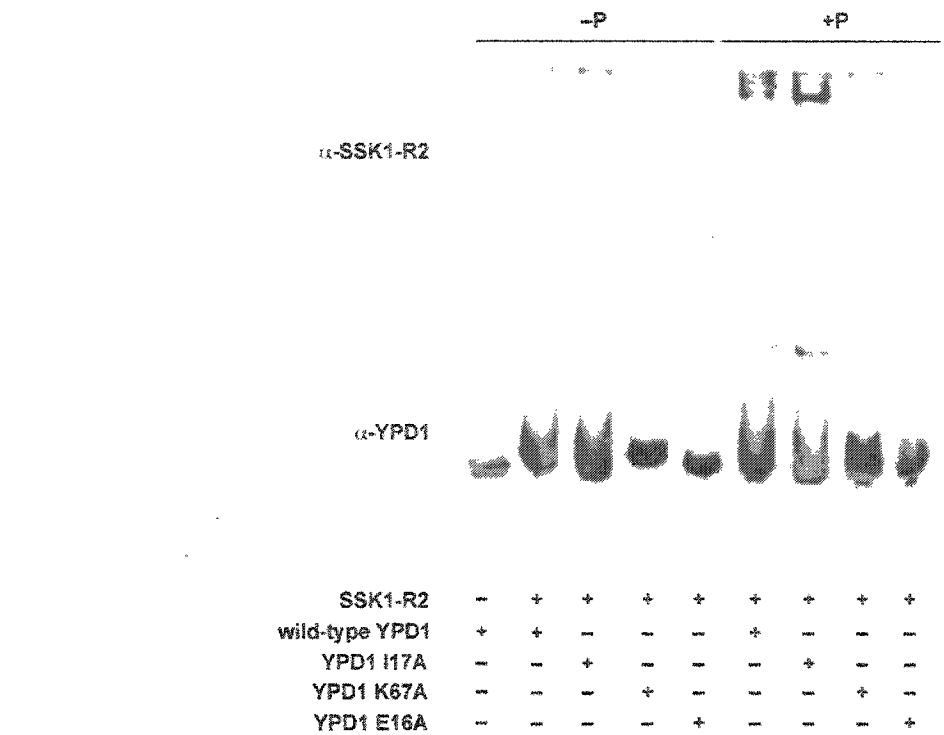

Figure 6-3

Native gel shift assay. A complex between YPD1 and SSK1-R2 is observed as a shift in mobility for both YPD1 and SSK1-R2. The labels –P and +P above the gels indicate the phosphorylated state of SSK1-R2 in the corresponding lanes. A complex is only observed between wild-type YPD1 or YPD1-I17A in the presence of phosphorylated SSK1-R2 (lanes 6 and 7).

shift assay. For these reasons the native gel assay was abandoned as an *in vitro* method to confirm the yeast two-hybrid results.

Protein-protein interactions between YPD1 and SSK1-R2 were also examined utilizing a bead-bound *in vitro* pull down assay. In this assay bead-bound GST-YPD1 and GST-YPD1 mutants were incubated with the regulatory domain of SSK1 in either a phosphorylated or an unphosphorylated state. The protein mixture was subjected to mild centrifugation to pellet bead-bound GST-YPD1 and the supernatant was removed to another tube. Samples were subjected to separation by SDS-PAGE. In this assay if SSK1-R2 interacts with YPD1 it will be found in the pellet, if no interaction occurs between the two proteins SSK1-R2 will only be found in the supernatant. Results from the assay were inconclusive due to the fact that in control experiments SSK1-R2 exhibits non-specific binding to the glutathione beads. Thus, the bead-bound *in vitro* pull down assay cannot be utilized as a means to confirm results from the yeast two-hybrid assay.

Currently another *in vitro* experimental method is being attempted in order to determine binding constants between YPD1 and the response regulators. Another member of the laboratory, Fabiola Janiak-Spens is looking at the kinetics of phosphoryl transfer between the SLN1-R1 domain and YPD1. Binding constants can be estimated between SLN1-R1 and wild-type YPD1 or YPD1 mutants by measuring the observed rate constants of the phosphoryl transfer step between SLN1-R1 and YPD1. Several YPD1 mutants were assayed in this manner, including a severely disrupting mutant (G68Q), several moderately disrupting mutants (K67A, R90A, and Q86A), and an enhanced binding mutant (Q34V). Kinetic parameters including V_{max}, the Michaelis constant, and overall forward rate were obtained (Table 6-1) and with the exception of Q34V show a

Table 6-1

Phosphoryl Transfer Rates and Michaelis Constants for Transfer Between Phospho-SLN1-R1 and Wild-Type and Mutant YPD1[a]

YPD1	V_{max} (s^{-1})	K_M (μM)	k (M^{-1} s^{-1})
Wild-type	43.1 ± 2.5	1.7 ± 0.3	25 x 10^6
K67A	33.1 ± 4.2	4.2 ± 1.5	7.9 x 10^6
R90A	11.1 ± 1.4	1.4 ± 0.6	7.9 x 10^6
Q86A	1.7 ± 0.3	1.4 ± 0.8	1.2 x 10^6
G68Q	0.003 ±	4 ±	750
Q34V	31.9 ± 8.1	1.4 ± 0.7	23 x 10^6

[a] Rates and constants were derived from time courses for reactions between phospho-SLN1-R1 (0.25 μM) and YPD1 (0.125 – 4 μM).

that there is a trend between classification of interaction observed in the yeast two-hybrid system and the overall rate of phosphotransfer. However, true binding constants could not be obtained between SLN1-R1 and YPD1 or YPD1 mutants due to the back transfer of phosphoryl groups from YPD1 to SLN1-R1.

6.2.4 Specificity of HPt Protein/Response Regulator Protein Interactions

In organisms that contain a multitude of two-component signaling systems it is imperative that cross-talk between these systems be avoided. Therefore, it is important to investigate how a particular HPt protein recognizes its cognate response regulator and activates it to produce the correct response. In order for specificity for a particular response regulator to occur there must be variations in the shapes and sequences of the

response regulators. Likewise, for cross-talk to be avoided between two-component signal transduction pathways, differences must also exist between histidine-containing phosphotransfer proteins. Complementarity between HPt proteins and response regulators must occur through affiliated changes in the sequence and shape of both proteins. While the sequence identity of response regulators is relatively low (20-30%), the similarity of the structures of response regulators is very high. Most variations in sequence identity (excluding the active site residues) occur on the surface of the molecule.

Two features distinguish the response regulator binding site on the surface of YPD1. A large hydrophobic patch located between H64 and the αA helix of YPD1 is the dominate feature of the binding site. In Chapters 3 and 4 yeast two-hybrid results showed that this hydrophobic patch represents the core of a response regulator binding site. Furthermore, the hydrophobic patch is a conserved feature among other HPt proteins from fungi, bacteria and plants. These hydrophobic residues on the four-helix bundle contact the α1 helix and the β5-α5 loop of the response regulator. We hypothesize that the hydrophobic patch is a general feature of all HPt proteins and provides insight into the general mechanism of interaction with response regulator domains.

Polar and charged residues surrounding the hydrophobic patch is a second feature of response regulator binding site. In the yeast two-hybrid assays, as well as the YPD1/SLN1-R1 co-crystal structure, interactions between YPD1 and the response regulators were detected between residues located just outside the hydrophobic patch on the surface of YPD1. However, a sequence alignment showed no conservation of these residues among other HPt domains. Therefore, we speculated that specificity for cognate

response regulators occurs through interactions surrounding the hydrophobic patch on the surface of HPt proteins (Porter *et al.*, 2003). These residues are located at the periphery of the hydrophobic core and contact less conserved active site loops (β1-α1, β3-α3, β4-α4) of the response regulator. Residues at the periphery of the hydrophobic core of YPD1 must allow for discrimination between response regulators by making the interactions with the correct response regulator favorable through shape, charge and hydrophobic complementarity of the protein surfaces. Analysis of the co-crystal structure of the YPD1/SLN1-R1 complex revealed that while there was a low percentage of total buried surface area in the complex (11.5%), there was a very high degree of surface complementarity. The degree of complementarity was near the average of proteins forming homodimers (Jones & Thornton, 1996). This suggests that while HPt/response regulator complexes are transient in nature, there is a high degree of specificity for between cognate protein pairs. This is consistent with the results of the two-hybrid system. Mutation of a single residue on the surface of YPD1 involved in making contact to a response regulator was enough to abolish the interaction altogether. It is apparent that response regulator binding is initiated through non-specific interactions at the hydrophobic core, but that discrimination is accomplished through non-conserved residues located at the periphery of the protein-protein interaction surface.

6.2.5 Conclusions

Results from the yeast two-hybrid system and interactions observed in the co-crystal structure of YPD1 and SLN1-R1 demonstrate that protein-protein interactions mainly occur between a response regulator and the four-helix bundle of an HPt protein.

The primary binding surface of the HPt domain is a hydrophobic patch located on the surface near the site of phosphorylation. In Chapter 3, a sequence alignment of HPt proteins was performed and revealed that the hydrophobic patch on the surface of YPD1 is a conserved feature among HPt proteins. However, due to poor sequence homology between the two proteins, Spo0B was not included in the sequence alignment. A comparison of the surface features of HPt proteins was performed using the structures of several HPt proteins that have been determined (CheA-P1, Spo0B, YPD1 and ArcB^c) (Matsushika & Mizuno, 1998b; Mourey *et al.*, 2001; Xu & West, 1999; Zapf *et al.*, 2000). The dimerization domain of the histidine kinase EnvZ was also included (Tomomori *et al.*, 1999). In each structure a hydrophobic patch is located on the surface of the four-helix bundle (Figure 6-4). However, the size and location of the patch varies slightly. The surfaces of the monomeric HPt domains (YPD1, ArcB^c and CheA-P1) show a single hydrophobic patch of a similar size, while Spo0B and EnvZ have smaller patches and that are distributed over the face of the four-helix bundle. The following facts suggest that YPD1 is a better model for monomeric HPt protein-response regulator interactions, while Spo0B is more suited as a model for dimeric HPt protein (or histidine kinase)-response regulator interactions: (i) the surface features of YPD1 mirrors those of other monomeric HPt domains with determined three-dimensional structures by both structural alignment and by surface comparison, (ii) sequence alignment between YPD1 and other monomeric HPt proteins reveals hydrophobic residues on the surface of YPD1 are conserved, (iii) poor sequence and structural alignment between YPD1 and Spo0B, and (iv) similar surface features exist between Spo0B and EnvZ.

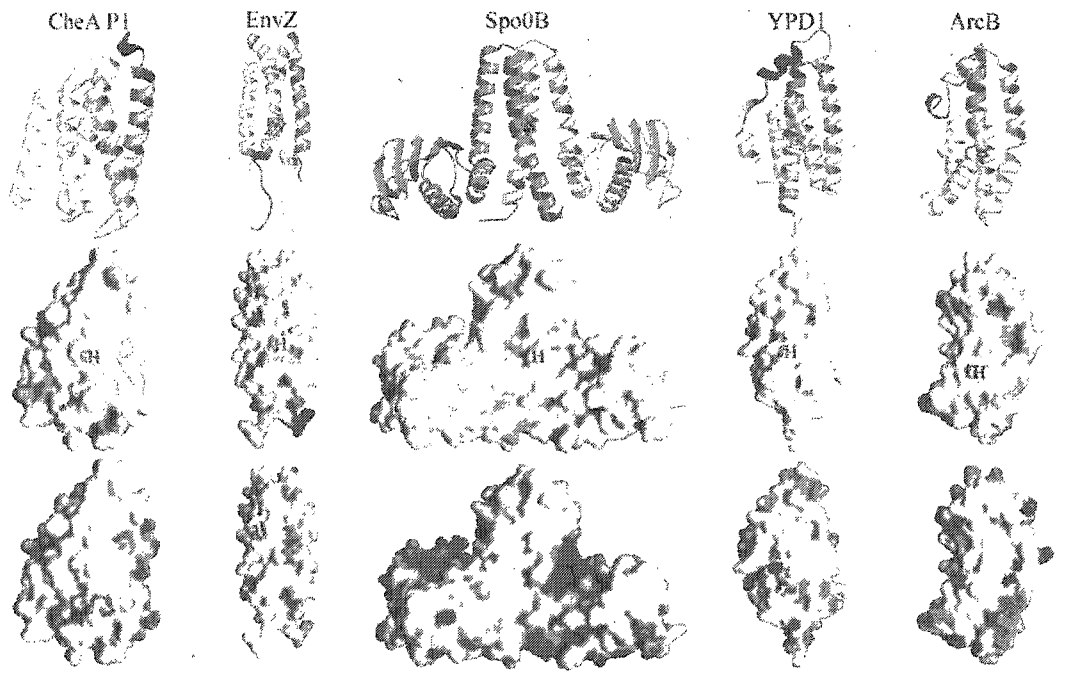

Figure 6-4
Surface Comparison of HPt Proteins. Molecular surface views of HPt proteins were created in order to compare surface features of these proteins. A ribbon diagram (top row) shows the underlying four-helix bundle for each of the surface maps. Locations and sizes of hydrophobic patches (grey) were compared amongst the HPt proteins (second row), as were the locations of charged residues (bottom row; negatively charged, red; positively charged, blue). The surfaces of three monomeric HPt proteins (CheA-P1, YPD1 and ArcB°), one dimeric HPt (Spo0B), and one dimeric histidine kinase (EnvZ) are compared in this figure.

A comparison of the yeast two-hybrid screens between YPD1 and each of the response regulators found in *S. cerevisiae* revealed ten residues on the surface of YPD1 that constitute the core response regulator binding surface. These residues originated from the αA, αB and αC helices and form a stripe of interactions between the site of phosphorylation and the αA helix of YPD1. Residues involved in specific interactions with a response regulator are located on either side of the stripe of core interactions.

Chapter 4 also revealed site-specific random mutations at the periphery of the hydrophobic patch of YPD1 to hydrophobic residues serve to enhance the binding between YPD1 and the response regulators. Mutation of Q34 to a more hydrophobic residue or a longer residue with hydrophobic character had a dramatic effect on the

binding of YPD1 with each of the response regulators. However, no trend was observed at a site (E58) located away from the hydrophobic patch. The results from the site-directed random mutagenesis with Q34 further demonstrated the importance of the hydrophobic patch on the surface of HPt for response regulator binding.

Results from the yeast two-hybrid assay were confirmed by the co-crystal structure of the YPD1/SLN1-R1 complex. Residues on the surface of YPD1 determined to be involved in protein-protein interactions with SLN1-R1 by yeast two-hybrid analysis were also observed in interactions in at least one of the two crystal forms of the co-crystal structure of the complex. The presence of two crystal forms suggests that multiple binding modes exist between YPD1 and SLN1-R1, and it is believed that the yeast two-hybrid results represent an average of the possible binding modes between the two proteins. Additionally, residues that constituted the core response regulator binding surface observed in Chapter 4 were found to make contact to α1 of SLN1-R1, while residues contributing to specific interactions with a response regulator were found to make contact to loops near the active site of the response regulator.

The co-crystal complex of YPD1 and SLN1-R1 also revealed a high level of surface complementarity between the two proteins. While the buried surface area of the complex is representative of transient protein-protein interactions, the level of complementarity at the protein-protein interface is more indicative of homodimers than of heterodimers.

In the previous chapters, protein-protein interactions between the histidine-containing phosphotransfer protein YPD1 and its cognate response regulator domains (SLN1-R1, SSK1-R2, and SLN7-R3) were examined. Through these studies, three

important features of the protein-protein interface have been determined: (i) a conserved hydrophobic patch is located on the surface of YPD1 and ten residues near this location represent the core response regulator binding surface, (ii) amino acid residues that flank this stripe of general response regulator interactions are involved in making specific contacts to one or more response regulators and may contribute to specificity of one response regulator over another, and (iii) a high level of surface complementarity between YPD1 and the response regulators exists that allows for these weakly interacting proteins to discriminate between response regulators.

References

Alberts, A. S., Bouquin, N., Johnston, L. H. & Treisman, R. (1998).Analysis of RhoA-binding proteins reveals an interaction domain conserved in heterotrimeric G protein β subunits and the yeast response regulator protein Skn7 *J. Biol. Chem.*, **273**: 8616-8622.

Albertyn, J., Hohmann, S. & Prior, B. A. (1994a).Characterization of the osmotic-stress response in *Saccharomyces cerevisiae*: osmotic stress and glucose repression regulate glycerol-3-phosphate dehydrogenase independently *Curr. Genet.*, **25**: 12-18.

Albertyn, J., Hohmann, S., Thevelein, J. M. & Prior, B. A. (1994b).*GPD1*, which encodes glycerol-3-phosphate dehydrogenase, is essential for growth under osmotic stress in *Saccharomyces cerevisiae*, and its expression is regulated by the high-osmolarity glycerol response pathway *Mol. Cell. Biol.*, **14**: 4135-4144.

Alex, L. A., Borkovich, K. A. & Simon, M. I. (1996).Hyphal development in *Neurospora crassa*: Involvement of a two-component histidine kinase *Proc. Natl. Acad. Sci. (USA)*, **93**: 3416-3421.

Baikalov, I., Schröder, I., Kaczor-Grzeskowiak, M., Grzeskowiak, K., Gunsalus, R. P. & Dickerson, R. E. (1996).Structure of the *Escherichia coli* response regulator NarL *Biochemistry*, **35**: 11053-11061.

Barford, D. (1991).Molecular mechanisms for the control of enzymatic activity by protein phosphorylation. *Biochem Biophys Acta*, **1133**: 55-62.

Barrett, J. F., Goldschmidt, R. M., Lawrence, L. E., Foleno, B., Chen, R., Demers, J. P., Johnson, S., Kanojia, R., Fernandez, J., Bernstein, J., Licata, L., Donetz, A., Huang, S., Hlasta, D. J., Macielag, M. J., Ohemeng, K., Frechette, R., Frosco, M. B., Klaubert, D. H., Whiteley, J. M., Wang, L. & Hoch, J. A. (1998).Antibacterial agents that inhibit two-component signal transduction systems *Proc. Natl. Acad. Sci. (USA)*, **95**: 5317-5322.

Barrett, J. F. & Hoch, J. A. (1998).Two-component signal transduction as a target for microbial anti-infective therapy *Antimicrob. Agents Chemother.*, **42**: 1529-1536.

Bartel, P. L. & Fields, S., Eds. (1997). The yeast two-hybrid system. New York: Oxford University Press.

Bellsolell, L., Prieto, J., Serrano, L. & Coll, M. (1994).Magnesium binding to the bacterial chemotaxis protein CheY results in large conformational changes involving its functional surface *J. Mol. Biol.*, **238**: 489-495.

Bilwes, A. M., Alex, L. A., Crane, B. R. & Simon, M. I. (1999).Structure of CheA, a signal-transducing histidine kinase *Cell*, **96**: 131-141.

Bilwes, A. M., Quezada, C. M. & Croal, L. R., Crane, B.R., Simon, M.I. (2001).Nucleotide Binding by the HIstidine Kinase Chea *Nat. Struct. Biol.*, **8**: 353-360.

Birck, C., Mourey, L., Gouet, P., Fabry, B., Schumacher, J., Rousseau, P., Kahn, D. & Samama, J.-P. (1999).Conformational changes induced by phosphorylation of the FixJ receiver domain *Structure*, **7**: 1505-1515.

Blair, D. F. (1995).How bacteria sense and swim *Annu. Rev. Microbiol.*, **49**: 489-522.

Blomberg, A. & Adler, L. (1989).Roles of glycerol and glycerol-3-phosphate dehydrogenase (NAD^+) in acquired osmotolerance of *Saccharomyces cerevisiae J. Bacteriol.*, **171**: 1087-1092.

Brandstatter, I. & Kleber, J. J. (1998).Two genes with similarity to bacterial response regulators are rapidly and specifically induced by cytokinin in *Arabidopsis Plant Cell*, **10**: 1009-1019.

Brewster, J. L. & Gustin, M. C. (1994).Positioning of cell growth and division after osmotic stress requires a MAP kinase pathway *Yeast*, **10**: 425-439.

Brown, J. L., Bussey, H. & Stewart, R. C. (1994).Yeast Skn7p functions in a eukaryotic two-component regulatory pathway *EMBO J.*, **13**: 5186-5194.

Brown, J. L., North, S. & Bussey, H. (1993).*SKN7*, a yeast multicopy suppressor of a mutation affecting cell wall β-glucan assembly, encodes a product with domains homologous to prokaryotic two-component regulators and to heat shock transcription factors *J. Bacteriol.*, **175**: 6908-6915.

Burke, D., Dawson, D. & Stearns, T. (2000). Methods in yeast genetics, edited, pp. 103-105: Cold Spring Harbor Press.

Cardenas, M. E., Sanfridson, A., Cutler, N. S. & Heitman, J. (1998).Signal-transduction cascades as targets for therapeutic intervention by natural products *Trends Biotech.*, **16**: 427-433.

Carter, C. W., Jr. & Sweet, R. M., Eds. (1997). Macromolecular Crystallography, Part A. Vol. 276. Methods in Enzymology. Edited by M. I. Simon. San Diego: Academic Press.

Chang, C. (1996).The ethylene signal transduction pathway in *Arabidopsis*: an emerging paradigm? *Trends Biochem. Sci.*, **21**: 129-133.

Chang, C., Kwok, S. F., Bleecker, A. B. & Meyerowitz, E. M. (1993).*Arabidopsis* ethylene-response gene *ETR1*: similarity of product to two-component regulators *Science*, **262**: 539-544.

Chang, W.-T., Thomason, P. A., Gross, J. D. & Newell, P. C. (1998).Evidence that the RdeA protein is a component of a multistep phosphorelay modulating rate of development in *Dictyostelium EMBO J.*, **17**: 2809-2816.

Chien, C.-T., Bartel, P. L., Sternglanz, R. & Fields, S. (1991).The two-hybrid system: a method to identify and clone genes for proteins that interact with a protein of interest *Proc. Natl. Acad. Sci. (USA)*, **88**: 9578-9582.

Chooback, L. & West, A. H. (2003).Co-crystallization of the yeast phosphorelay protein YPD1 with the SLN1 response regulator domain and preliminary X-ray diffraction analysis *Acta Cryst.*, **D**: *In press*.

Chothia, C. & Janin, J. (1975).Principles of protein-protein recognition *Nature*, **256**: 705-708.

Cobb, M. H. & Goldsmith, E. J. (1995).How MAP kinases are regulated *J. Biol. Chem.*, **270**: 14843-14846.

Colosimo, A., Xu, Z., Novelli, G., Dallapiccola, B. & Gruenert, D. C. (1999).Simple version of "megaprimer" PCR for site-directed mutagenesis *BioTech.*, **26**: 870-873.

Crews, C. M. & Erickson, R. L. (1993).Extracellular signals and reversible protein phosphorylation: what to Mek of it all *Cell*, **74**: 215-217.

Davis, R. J. (1993).The mitogen-activated protein kinase signal transduction pathway *J. Biol. Chem.*, **268**: 14553-14556.

DeLano, W. L. (2002). *The PyMOL molecular graphics system*, DeLano Scientific, San Carlos, CA.

Djordjevic, S., Goudreau, P. N., Xu, Q., Stock, A. M. & West, A. H. (1998).Structural basis for methylesterase CheB regulation by a phosphorylation-activated domain *Proc. Natl. Acad. Sci. (USA)*, **95**: 1381-1386.

Djordjevic, S. & Stock, A. M. (1998).Structural analysis of bacterial chemotaxis proteins: components of a dynamic signaling system *J. Struct. Biol.*, **124**: 189-200.

Dutta, R., Qin, L. & Inouye, M. (1999).Histidine kinases: diversity of domain organization *Mol. Microbiol.*, **34**: 633-640.

Ekici, A. B., Park, O. S., Fuchs, C. & Rautenstrauss, B. (1997).One-tube, two-stage PCR-directed *in vitro* mutagenesis using megaprimers *Elsevier Trends Journals Technical Tips Online*.

Estojak, J., Brent, R. & Golemis, E. A. (1995).Correlation of two-hybrid affinity data with in vitro measurements *Mol. Cell. Biol.*, **15**: 5820-5829.

Eustice, D. C., Feldman, P. A., Colberg-Poley, A. M., Buckery, R. M. & Neubauer, R. H. (1991).A sensitive method for the detection of β-galactosidase in transfected mammalian cells *BioTech.*, **11**: 739-742.

Fabret, C. & Hoch, J. A. (1998).A two-component signal transduction system essential for growth of *Bacillus subtilis*: implications for anti-infective therapy *J. Bacteriol.*, **180**: 6375-6383.

Falke, J. J., Bass, R. B., Butler, S. L., Chervitz, S. A. & Danielson, M. A. (1997).The two-component signaling pathway of bacterial chemotaxis: A molecular view of signal transduction by receptors, kinases, and adaptation enzymes *Annu. Rev. Cell Dev. Biol.*, **13**: 457-512.

Ferrigno, P., Posas, F., Koepp, D., Saito, H. & Silver, P. A. (1998).Regulated nucleo/cytoplasmic exchange of HOG1 MAPK requires the importin β homologs NMD5 and XPO1 *EMBO J.*, **17**: 5606-5614.

Fields, S. & Song, O. (1989).A novel genetic system to detect protein-protein interactions *Nature*, **340**: 245-246.

Fields, S. & Sternglanz, R. (1994).The two-hybrid system: an assay for protein-protein interactions *Trends Genet.*, **10**: 286-292.

Fukuda, M., Gotoh, I., Adachi, M., Gotoh, Y. & Nishida, E. (1997).A novel regulatory mechanism in the mitogen-activated protein (MAP) kinase cascade *J. Biol. Chem.*, **272**: 32642-32648.

Gouet, P., Chinardet, N., Welch, M., Guillet, V., Cabantous, S., Birck, C., Mourey, L. & Samama, J.-P. (2001).Further insights into the mechanism of function of the response regulator CheY from crystallographic studies of the CheY-$CheA_{124-257}$ complex *Acta Cryst.*, **D57**: 44-51.

Grebe, T. W. & Stock, J. B. (1999).The histidine protein kinase superfamily *Adv. Micro. Physiol.*, **41**: 139-227.

Guan, K.-L. (1994).The mitogen activated protein kinase signal transduction pathway: from the cell surface to the nucleus *Cell. Signal.*, **6**: 581-589.

Hilliard, J. J., Goldschmidt, R. M., Licata, L., Baum, E. Z. & Bush, K. (1999).Multiple mechanisms of action for inhibitors of histidine protein kinases from bacterial two-component systems *Antimicrob. Agents Chemother.*, **43**: 1693-1699.

Hlasta, D. J., Demers, J. P., Foleno, B. D., Fraga-Spano, S. A., Guan, J., Hilliard, J. J., Macielag, M. J., Ohemeng, K. A., Sheppard, C. M., Sui, Z., Webb, G. C., Weidner-Wells, M. A., Werblood, H. & Barrett, J. F. (1998).Novel inhibitors of bacterial two-component systems with Gram positive antibacterial activity: pharmacophore identification based on the screening hit closantel *Bioorg. Med. Chem. Lett.*, **8**: 1923-1928.

Ho, Y., Gruhler, A., Heilbut, A., Bader, G. D., Moore, L., Adams, S.-L., Millar, A., Taylor, P., Bennett, K., Boutilier, K., Yang, L., Wolting, C., Donaldson, I., Schandorff, S., Shewnarane, J., Vo, M., Taggart, J., Goudreault, M., Muskat, B., Alfarano, C., Dewar, D., Lin, Z., Michalickova, K., Willems, A. R., Sassi, H., Nielsen, P. A., Rasmussen, K. J., Andersen, J. R., Johansen, L. E., Hansen, L. H., Jespersen, H., Podtelejnikov, A., Nielsen, E., Crawford, J., Poulsen, V., Sorensen, B. D., Matthiesen, J., Hendrickson, R. C., Gleeson, F., Pawson, T., Moran, M. F., Durocher, D., Mann, M., Hogue, C. W. V., Figeys, D. & Tyers, M. (2002).Systematic identification of protein complexes in *Saccharomyces cerevisiae* by mass spectometry *Nature*, **415**: 180-183.

Hoch, J. A. (2000).Two-component and phosphorelay signal transduction *Curr. Opin. Microbiol.*, **3**: 165-170.

Hoch, J. A. & Silhavy, T. J., Eds. (1995). Two-component signal transduction. Washington, D.C.: American Society for Microbiology Press.

Hua, J., Chang, C., Sun, Q. & Meyerowitz, E. M. (1995).Ethylene insensitivity conferred by *Arabidopsis ERS* gene *Science*, **269**: 1712-1714.

Imamura, A., Hanaki, N., Nakamura, A., Suzuki, T., Taniguchi, M., Kiba, T., Ueguchi, C., Sugiyama, T. & Mizuno, T. (1999).Compilation and characterization of Arabidopsis thaliana response regulators implicated in His-Asp phosphorelay signal transduction *Plant Cell Physiol.*, **40**: 733-742.

Janiak-Spens, F., Sparling, D. P. & West, A. H. (2000).Novel role for an HPt domain in stabilizing the phosphorylated state of a response regulator domain *J. Bacteriol.*, **182**: 6673-6678.

Janiak-Spens, F., Sparling, J. M., Gurfinkel, M. & West, A. H. (1999).Differential stabilities of phosphorylated response regulator domains reflect functional roles of the yeast osmoregulatory SLN1 and SSK1 proteins *J. Bacteriol.*, **181**: 411-417.

Janiak-Spens, F. & West, A. H. (2000).Functional roles of conserved amino acid residues surrounding the phosphorylatable histidine of the yeast phosphorelay protein YPD1 *Mol. Microbiol.*, **37**: 136-144.

Jiang, P., Atkinson, M. R., Srisawat, C., Sun, Q. & Ninfa, A. J. (2000).Functional dissection of the dimerization and enzymatic activities of *Escherichia coli* nitrogen regulator II an their regulation by the PII protein *Biochemistry*, **39**: 13433-13449.

Jones, S., Marin, A. & Thornton, J. M. (2000).Protein domain interfaces: characterization and comparison with oligomeric protein interfaces *Prot. Eng.*, **13**: 77-82.

Jones, S. & Thornton, J. M. (1996).Principles of protein-protein interactions *Proc. Natl. Acad. Sci. (USA)*, **93**: 13-20.

Kakimoto, T. (1996).CKI1, a histidine kinase homolog implicated in cytokinin signal transduction *Science*, **274**: 982-985.

Kato, M., Mizuno, T., Shimizu, T. & Hakoshima, T. (1997).Insights into multistep phosphorelay from the crystal structure of the C-terminal HPt domain of ArcB *Cell*, **88**: 717-723.

Kato, M., Mizuno, T., Shimizu, T. & Hakoshima, T. (1999).Refined structure of the histidine-containing phosphotransfer (HPt) domain of the anaerobic sensor kinase ArcB from *Escherichia coli* at 1.57 Å resolution *Acta Cryst.*, **D55**: 1842-1849.

Ketela, T., Brown, J. L., Stewart, R. C. & Bussey, H. (1998).Yeast Skn7p activity is modulated by the Sln1p-Ypd1p osmosensor and contributes to regulation of the HOG1 pathway *Mol. Gen. Genet.*, **259**: 372-378.

Keyse, S. M. (2000).Protein phosphatases and the regulation of mitogen-activated protein kinase signaling *Curr. Opin. Cell Biol.*, **12**: 186-192.

Knowles, J. R. (1980).Enzyme-catalyzed phosphoryl transfer reactions *Annu. Rev. Biochem.*, **49**: 877-919.

Kofoid, E. C. & Parkinson, J. S. (1988).Transmitter and receiver modules in bacterial signaling proteins *Proc. Natl. Acad. Sci. USA*, **85**: 4981-4985.

Kyte, J. & Doolittle, R. (1982).A Simple Model for Displaying the Hydrophobic Character of a Protein *J. Mol Biol*, **157**: 105-132.

Larsen, T. A., Olson, A. J. & Goodsell, D. S. (1998).Morphology of protein-protein interfaces *Structure*, **6**: 421-427.

Laskowski, R. A. (1995).SURFNET: A program for visualizing molecular surfaces, cavities, and intermolecular interactions *J. Mol. Graph.*, **13**: 323-330.

Laskowski, R. A., MacArthur, M. W., Moss, D. S. & Thornton, J. M. (1993).PROCHECK: a program to check the stereochemical quality of protein structures *J. Appl. Cryst.*, **26**: 283-291.

Lee, P.-J. & Stock, A. M. (1996).Characterization of the genes and proteins of a two-component system from the hyperthermophilic bacterium *Thermotoga maritima J. Bacteriol.*, **178**: 5579-5585.

Li, S., Ault, A., Malone, C. L., Raitt, D., Dean, S., Johnston, L. H., Deschenes, R. J. & Fassler, J. S. (1998).The yeast histidine protein kinase, Sln1p, mediates phosphotransfer to two response regulators, Ssk1p and Skn7p *EMBO J.*, **17**: 6952-6962.

Li, S., Dean, S., Li, Z., Horecka, J., Deschenes, R. J. & Fassler, J. S. (2002).The eukaryotic two-component histidine kinase Sln1p regulates OCH1 via the transcription factor, Skn7p *Mol. Biol. Cell*, **13**: 412-424.

Lukat, G. S. & Stock, J. B. (1993).Response regulation in bacterial chemotaxis *J. Cell. Biochem.*, **51**: 41-46.

Madhani, H. D. & Fink, G. R. (1998).The riddle of MAP kinase signaling specificity *Trends Genet.*, **14**: 151-155.

Madhusudan, James, Z., Whiteley, J. M., Hoch, J. A., Xuong, N. H. & Varughese, K. I. (1996).Crystal structure of a phosphatase-resistant mutant of sporulation response regulator Spo0F from *Bacillus subtilis Structure*, **4**: 679-690.

Maeda, T., Wurgler-Murphy, S. M. & Saito, H. (1994).A two-component system that regulates an osmosensing MAP kinase cascade in yeast *Nature*, **369**: 242-245.

Mager, W. H. & Varela, J. C. S. (1993).Osmostress response of the yeast *Saccharomyces Mol. Microbiol.*, **10**: 253-258.

Maher, B. A. (2002).A tale of two-hybrid *The Scientist*: 38-39.

Matsushika, A. & Mizuno, T. (1998a).Mutational analysis of the histidine-containing phosphotransfer (HPt) signaling domain of the ArcB sensor in *Escherichia coli Biosci. Biotechnol. Biochem.*, **62**: 2236-2238.

Matsushika, A. & Mizuno, T. (1998b).The structure and function of the histidine-containing phosphotransfer (HPt) signaling domain of the *Escherichia coli* ArcB sensor *J. Biochem.*, **124**: 440-445.

McEvoy, M. M., Muhandiram, D. R., Kay, L. E. & Dahlquist, F. W. (1996).Structure and dynamics of a CheY-binding domain of the chemotaxis kinase CheA determined by nuclear magnetic resonance spectroscopy *Biochemistry*, **35**: 5633-5640.

Mizuno, T. (1997).Compilation of all genes encoding two-component phosphotransfer signal transducers in the genome of *Escherichia coli DNA Res.*, **4**: 161-168.

Morgan, B. A., Banks, G. R., Toone, W. M., Raitt, D., Kuge, S. & Johnston, L. H. (1997).The Skn7 response regulator controls gene expression in the oxidative stress response of the budding yeast *Saccharomyces cerevisiae EMBO J.*, **16**: 1035-1044.

Morgan, B. A., Bouquin, N., Merrill, G. F. & Johnston, L. H. (1995).A yeast transcription factor bypassing the requirement for SBF and DSC1/MBF in budding yeast has homology to bacterial signal transduction proteins *EMBO J.*, **14**: 5679-5689.

Mourey, L., Da Re, S., Pédelacq, J.-D., Tolstykh, T., Faurie, C., Guillet, V., Stock, J. B. & Samama, J.-P. (2001).Crystal structure of the CheA histidine phosphotransfer domain that mediates response regulator phosphorylation in bacterial chemotaxis *J. Biol. Chem.*, **276**: 31074-31082.

Nicholls, A., Sharp, K. A. & Honig, B. (1991).Protein folding and association: insights from the interfacial and thermodynamic properties of hydrocarbons *Proteins: Str. Funct. Genet.*, **11**: 281-296.

Nishida, E. & Gotoh, Y. (1993).The MAP kinase cascade is essential for diverse signal transduction pathways *Trends Biochem. Sci.*, **18**: 128-131.

Nooren, I. M. A. & Thornton, J. M. (2003).Structural characterisation and functional significance of transient protein-protein interactions *J. Mol. Biol.*, **325**: 991-1018.

Ofran, Y. & Rost, B. (2003).Analysing six types of protein-protein interfaces *J. Mol. Biol.*, **325**: 377-387.

Ota, I. M. & Varshavsky, A. (1992).A gene encoding a putative tyrosine phosphatase suppresses lethality of an N-end rule-dependent mutant *Proc. Natl. Acad. Sci. (USA)*, **89**: 2355-2359.

Ota, I. M. & Varshavsky, A. (1993).A yeast protein similar to bacterial two-component regulators *Science*, **262**: 566-569.

Pao, G. M., Tam, R., Lipschitz, L. S. & Saier, M. H., Jr. (1994).Response regulators: structure, function and evolution *Res. Microbiol.*, **145**: 356-361.

Papworth, C., Bauer, J. C., Braman, J. & Wright, D. A. (1996).Site-directed mutagenesis in one day with >80% efficiency *Strategies (Stratagene)*, **9**: 3-4.

Parkinson, J. S. & Kofoid, E. C. (1992).Communication modules in bacterial signaling proteins *Annu. Rev. Genet.*, **26**: 71-112.

Pawson, T. & Nash, P. (2000).Protein-protein interactions define specificity in signal transduction *Genes Dev.*, **14**: 1027-1047.

Pirrung, M. C. (1999).Histidine kinases and two-component signal transduction systems *Chem. & Biol.*, **6**: R167-R175.

Porter, S. W., Xu, Q. & West, A. H. (2003).Ssk1p response regulator binding surface on histidine-containing phosphotransfer protein Ypd1p *Euk. Cell*, **2**: 27-33.

Posas, F. & Saito, H. (1997).Osmotic activation of the HOG MAPK pathway via Ste11p MAPKKK: Scaffold role of Pbs2p MAPKK *Science*, **276**: 1702-1705.

Posas, F. & Saito, H. (1998).Activation of the yeast SSK2 MAP kinase kinase kinase by the SSK1 two-component response regulator *EMBO J.*, **17**: 1385-1394.

Posas, F., Witten, E. A. & Saito, H. (1998).Requirement of STE50 for osmostress-induced activation of the STE11 mitogen-activated protein kinase kinase kinase in the high-osmolarity glycerol response pathway *Mol. Cell. Biol.*, **18**: 5788-5796.

Posas, F., Wurgler-Murphy, S. M., Maeda, T., Witten, E. A., Thai, T. C. & Saito, H. (1996).Yeast HOG1 MAP kinase cascade is regulated by a multistep phosphorelay mechanism in the SLN1-YPD1-SSK1 "two-component" osmosensor *Cell*, **86**: 865-875.

Qin, L., cai, S., Zhu, Y. & Inouye, M. (2003).Cysteine-scanning analysis of the dimerization domain of EnvZ, an osmosensing histidine kinase *J. Bacteriol.*, **185**: 3429-3435.

Robinson, L. L. & Brasch, M. A. (1998).Identification of interacting proteins with the ProQuest two-hybrid system *Focus*, **20**: 19-23.

Robinson, M. J. & Cobb, M. H. (1997).Mitogen-activated protein kinase pathways *Curr. Opin. Cell Biol.*, **9**: 180-186.

Robinson, V. L., Buckler, D. R. & Stock, A. M. (2000).A tale of two components: a novel kinase and a regulatory switch *Nat. Struct. Biol.*, **7**: 626-633.

Robinson, V. L., Wu, T. & Stock, A. M. (2003).Structural analysis of the domain interface in DrrB, a response regulator of the OmpR/PhoB subfamily *J. Bacteriol.*, **185**: 4186-4194.

Roychoudhury, S., Zielinski, N. A., Ninfa, A. J., Allen, N. E., Jungheim, L. N., Nicas, T. I. & Chakrabarty, A. M. (1993).Inhibitors of two-component signal transduction systems: inhibition of alginate gene activation in *Pseudomonas aeruginosa Proc. Natl. Acad. Sci. (USA)*, **90**: 965-969.

Rudolf, J., Tolliday, N., Schmitt, C., Schuster, S. C. & Oesterhelt, D. (1995).Phosphorylation in halobacterial signal transduction *EMBO J.*, **14**: 4249-4257.

Sakai, H., Honma, T., Aoyama, T., Sato, S., Kato, T., Tabata, S. & Oka, A. (2001).ARR1, a transcription factor for genes immediately responsive to cytokinins *Science*, **294**: 1519-1521.

Sakai, H., Hua, J., Chen, Q. G., Chang, C., Medrano, L. J., Bleecker, A. B. & Meyerowitz, E. M. (1998).ETR2 is an ETR1-like gene involved in ethylene signaling in *Arabidopsis Proc. Natl. Acad. Sci. (USA)*, **95**: 5812-5817.

Schaeffer, H. J. & Weber, M. J. (1999).Mitogen-activated protein kinases: Specific messages from ubiquitous messengers *Mol. Cell. Biol.*, **19**: 2435-2444.

Schüller, C., Brewster, J. L., Alexander, M. R., Gustin, M. C. & Ruis, H. (1994).The HOG pathway controls osmotic regulation of transcription via the stress response element (STRE) of the *Saccharomyces cerevisiae CTT1* gene *EMBO J.*, **13**: 4382-4389.

Schuster, S. C., Noegel, A. A., Oehme, F., Gerisch, G. & Simon, M. I. (1996).The hybrid histidine kinase DokA is part of the osmotic response system of *Dictyostelium EMBO J.*, **15**: 3880-3889.

Seger, R. & Krebs, E. G. (1995).The MAPK signaling cascade *FASEB J.*, **9**: 726-735.

Serebriiskii, I. G. & Golemis, E. A. (2000).Uses of *lacZ* to study gene function: Evaluation of β-galactosidase assays employed in the yeast two-hybrid system *Anal. Biochem.*, **285**: 1-15.

Serebriiskii, I. G., Khazak, V. & Golemis, E. A. (2001).Redefinition of the yeast two-hybrid system in dialogue with changing priorities in biological research *BioTech.*, **30**: 634-655.

Shieh, J.-C., Wilkinson, M. G., Buck, V., Morgan, B. A., Makino, K. & Millar, J. B. A. (1997).The Mcs4 response regulator coordinately controls the stress-activated Wak1-Wis1-Sty1 MAP kinase pathway and fission yeast cell cycle *Genes & Dev.*, **11**: 1008-1022.

Song, H. K., Lee, J. Y., Lee, M. G., Min, J. M. K., Yang, J. K. & Suh, S. W. (1999).Insights into eukaryotic multistep phosphorelay signal transduction revealed by the crystal structure of Ypd1p from *Saccharomyces cerevisiae J. Mol. Biol.*, **293**: 753-761.

Stock, A. M., Martinez-Hackert, E., Rasmussen, B. F., West, A. H., Stock, J. B., Ringe, D. & Petsko, G. A. (1993).Structure of the Mg^{2+}-bound form of CheY and mechanism of phosphoryl transfer in bacterial chemotaxis *Biochemistry*, **32**: 13375-13380.

Stock, A. M. & Mowbray, S. L. (1995).Bacterial chemotaxis: a field in motion *Curr. Opin. in Struct. Biol.*, **5**: 744-751.

Stock, A. M., Robinson, V. L. & Goudreau, P. N. (2000).Two-component signal transduction *Annu. Rev. Biochem.*, **69**: 183-215.

Stock, A. M. & West, A. H. (2002). Response regulator proteins and their interactions with histidine protein kinases. In Histidine kinases in signal transduction, edited by R. Dutta, pp. 237-271, New York: Academic Press.

Stock, J. & Da Re, S. (2000).Signal transduction: Response regulators on and off *Curr. Biol.*, **10**: R420-R424.

Stock, J. B., Surette, M. G., Levit, M. & Park, P. (1995). Two-component signal transduction systems: Structure-function relationships and mechanisms of catalysis. In Two-component signal transduction, edited by T. J. Silhavy, pp. 25-51, Washington, D.C.: American Society for Microbiology.

Swanson, R. V., Alex, L. A. & Simon, M. I. (1994).Histidine and aspartate phosphorylation: two-component systems and the limits of homology *Trends Biochem. Sci.*, **19**: 485-490.

Swanson, R. V., Sanna, M. G. & Simon, M. I. (1996).Thermostable chemotaxis proteins from the hyperthermophilic bacterium *Thermotoga maritima J. Bacteriol.*, **178**: 484-489.

Tanaka, T., Saha, S. K., Tomomori, C., Ishima, R., Liu, D., Tong, K. I., Park, H., Dutta, R., Qin, L., Swindells, M. B., Yamazaki, T., Ono, A. M., Kainosho, M., Inouye, M. & Ikura, M. (1998).NMR structure of the histidine kinase domain of the *E. coli* osmosensor EnvZ *Nature*, **396**: 88-92.

Tomomori, C., Tanaka, T., Dutta, R., Park, H., Saha, S. K., Zhu, Y., Ishima, R., Liu, D., Tong, K. I., Kurokawa, H., Qian, H., Inouye, M. & Ikura, M. (1999).Solution structure of the homodimeric core domain of *Escherichia coli* histidine kinase EnvZ *Nat. Struct. Biol.*, **6**: 729-734.

Towbin, H., Staehelin, T. & Gordon, J. (1979).Electrophoretic Transfer of Proteins From Polyacrylamide Gels to Nitrocellulose Sheets: Proceedure and Some Applications. *PNAS*, **76**: 4350-4354.

Varughese, K. I. (2002).Molecular recognition of bacterial phosphorelay proteins *Curr. Opin. Microbiol.*, **5**: 142-148.

Varughese, K. I., Madhusudan, Zhou, X. Z., Whiteley, J. M. & Hoch, J. A. (1998).Formation of a novel four-helix bundle and molecular recognition sites by dimerization of a response regulator phosphotransferase *Mol. Cell*, **2**: 485-493.

Vidal, M., Brachmann, R. K., Fattaey, A., Harlow, E. & Boeke, J. D. (1996a).Reverse two-hybrid and one-hybrid systems to detect dissociation of protein-protein and DNA-protein interactions *Proc. Natl. Acad. Sci. (USA)*, **93**: 10315-10320.

Vidal, M., Braun, P., Chen, E., Boeke, J. D. & Harlow, E. (1996b).Genetic characterization of a mammalian protein-protein interaction domain by using a yeast reverse two-hybrid system *Proc. Natl. Acad. Sci. (USA)*, **93**: 10321-10326.

Volkman, B. F., Nohaile, M. J., Amy, N. K., Kustu, S. & Wemmer, D. E. (1995).Three-dimensional solution structure of the N-terminal receiver domain of NTRC *Biochemistry*, **34**: 1413-1424.

Volz, K. & Matsumura, P. (1991).Crystal structure of *Escherichia coli* CheY refined at 1.7-Å resolution *J. Biol. Chem.*, **266**: 15511-15519.

Wallace, A. C., Laskowski, R. A. & Thornton, J. M. (1995).LIGPLOT: a program to generate schematic diagrams of protein-ligand interactions *Prot. Eng.*, **8**: 127-134.

Wang, N., Shaulsky, G., Escalante, R. & Loomis, W. F. (1996).A two-component histidine kinase gene that functions in *Dictyostelium* development *EMBO J.*, **15**: 3890-3898.

Welch, M., Chinardet, N., Mourey, L., Birck, C. & Samama, J.-P. (1998).Structure of the CheY-binding domain of histidine kinase CheA in complex with CheY *Nat. Struct. Biol.*, **5**: 25-29.

Wells, J. A. (1991).Systematic mutational analyses of protein-protein interfaces *Methods Enzymol.*, **202**: 390-411.

West, A. H. & Stock, A. M. (2001).Histidine kinases and response regulator proteins in two-component signaling systems *Trends Biochem. Sci.*, **26**: 369-376.

Westheimer, F. H. (1987).Why nature choses phosphates? *Science*, **235**: 1173-1178.

White, M. A. (1996).The yeast two-hybrid system: forward and reverse *Proc. Natl. Acad. Sci. (USA)*, **93**: 10001-10003.

Wilkinson, J. Q., Lanahan, M. B., Yen, H.-C., Giovannoni, J. J. & Klee, H. J. (1995).An ethylene-inducible component of signal transduction encoded by *Never-ripe Science*, **270**: 1807-1809.

Witters, L. A. (1990).Protein phosphorylation and dephosphorylation. *Cur. Cell Bio.*, **2**: 212-220.

Wurgler-Murphy, S. M., Maeda, T., Witten, E. A. & Saito, H. (1997).Regulation of the *Saccharomyces cerevisiae HOG1* mitogen-activated protein kinase by the *PTP2* and *PTP3* protein tyrosine phosphatases *Mol. Cell. Biol.*, **17**: 1289-1297.

Xu, Q., Nguyen, V. & West, A. H. (1999).Purification, crystallization, and preliminary X-ray diffraction analysis of the yeast phosphorelay protein YPD1 *Acta Cryst.*, **D55**: 291-293.

Xu, Q., Porter, S. W. & West, A. W. (2003).The Yeast YPD1/SLN1-R1 Complex: Insights into Molecular Recognition in Two-Component Signalling Systems *Structure*, **11**: 1569-1581.

Xu, Q. & West, A. H. (1999).Conservation of structure and function among histidine-containing phosphotransfer (HPt) domains as revealed by the crystal structure of YPD1 *J. Mol. Biol.*, **292**: 1039-1050.

Yaku, H. & Mizuno, T. (1997).The membrane-located osmosensory kinase, EnvZ, that contains a leucine zipper-like motif functions as a dimer in *Escherichia coli FEBS Lett.*, **417**: 409-413.

Zapf, J., Sen, U., Madhusudan, Hoch, J. A. & Varughese, K. I. (2000).A transient interaction between two phosphorelay proteins trapped in a crystal lattice reveals the mechanism of molecular recognition and phosphotransfer in signal transduction *Structure*, **8**: 851-862.

Zhou, H., Lowry, D. F., Swanson, R. V., Simon, M. I. & Dahlquist, F. W. (1995).NMR studies of the phosphotransfer domain of the histidine kinase CheA from *Escherichia coli*: assignments, secondary structure, general fold, and backbone dynamics *Biochemistry*, **34**: 13858-13870.

Zinda, M. J. & Singleton, C. K. (1998).The hybrid histidine kinase *dhkB* regulates spore germination in *Dictyostelium discoideum Dev. Biol.*, **196**: 171-183.